# DEVELOPMENT AND CHARACTERIZATION OF A NEXT GENERATION, FIELD-FREE ATMOSPHERIC PRESSURE PHOTOIONIZATION (APPI) SOURCE FOR LIQUID CHROMATOGRAPHY - MASS SPECTROMETRY

by

Ross David McCulloch

B.Sc., The University of Waterloo, 2002
M.Sc., The University of Waterloo, 2005

A THESIS SUBMITTED IN PARTIAL FULFILLMENT OF
THE REQUIREMENTS FOR THE DEGREE OF
DOCTOR OF PHILOSOPHY

in

The Faculty of Graduate Studies
(Chemistry)

THE UNIVERSITY OF BRITISH COLUMBIA
(Vancouver)

April 2013

# Abstract

A prototype next-generation, atmospheric pressure photoionization (APPI) source for LC-MS applications has been developed. The device was fabricated through modification of a TurboV ion source. The device incorporates a stainless steel source block and a photoionization lamp mounted to a heated nebulizer. Sample transfer conduits were machined within the source block creating a “flowing reaction chamber” in which ion-molecule reactions, critical to APPI performance, proceed. A potential applied to the source block, provides a field-free environment within. An additional “flight tube” mounted to the outlet of the source block extends the length of the field-free region.

The design of the prototype device mirrors the configuration exploited within early, field-free APPI sources. The preliminary goal of this research project was to use the prototype device to compare the relative performance of field-free sources with open-geometry APPI sources. These devices provide no extended field-free region. All ion-molecule reactions proceed within an electrical field, altering the processes of ion formation and transmission. To our knowledge, this was the first comprehensive, head-to-head evaluation of the two APPI configurations, upon a current MS platform.

Factors affecting field-free APPI performance were characterized, leading to a more complete understanding of source optimization. Through an empirical evaluation, the prototype field-free source was found to routinely provide superior performance relative to current open-geometry designs, at times providing order-of-magnitude sensitivity advantages. Significant improvements are tied to the provision of the extended field-free region, enabling efficient analyte ion formation, while enhancing overall ion transmission.

The performance of the prototype device was compared to ESI and APCI for the analysis of clinically relevant analytes using high throughput, rapid screening LC/MS workflows. The prototype source was routinely found to provide the greatest sensitivity for the analysis of neutral steroids, including vitamin D, while displaying reduced susceptibility to matrix effects - particularly relative to ESI. This observation was confirmed using a robust linear regression method to build statistical confidence within the results. It was also determined that nebulizer temperature and gas flow rate

significantly alter the extent of matrix suppression, realizing new parameters which may impact APPI method optimization.

# Preface

The majority of the research described within this dissertation and the entirety of the writing was completed by the author, Ross McCulloch. The contributions of supervisors, collaborators and any who contributed to the results are described in detail below.

Contributions of others:

Chapter 2: A prototype device was developed based upon the collaborative assistance of Research Associate, Damon Robb. The TurboV source housing modified in the development of the prototype device was kindly donated by Thomas Clark. Many of the prototype device components were constructed with the assistance of the staff of the UBC machine shop staff.

Chapter 3: Some analytes including neutral steroids, vitamin D metabolites and PAHs; as well as serum and plasma matrices were provided by AB/Sciex. AB/Sciex also generously provided access to various MS instruments and ion sources necessary to perform many of the platform and source comparison experiments. Adam Latawiec of AB/Sciex performed sample preparation for several of the performance comparison experiments.

Chapter 4: Several of the neutral steroid analytes were again provided by AB/Sciex.

**Publications arising from work presented in the dissertation:**

1. McCulloch, R. D., Robb, D. B., & Blades, M. W. (2008). A dopant introduction device for atmospheric pressure photoionization with liquid chromatography/mass spectrometry. *Rapid Communications in Mass Spectrometry*, *22*, 3549-3554.

The research described in Appendix B is the basis for this publication.

# Table of Contents

# List of Tables

# List of Figures

# List of Symbols and Abbreviations

| | |
|---|---|
| ACN | acetonitrile |
| APCI | atmospheric pressure chemical ionization |
| API | atmospheric pressure interface |
| APPI | atmospheric pressure photoionization |
| CE | charge exchange |
| CE | collision energy |
| CLIA | chemiluminescent immunoassay |
| CI | chemical ionization |
| cf-FAB | continuous flow fast atom bombardment |
| CPBA | competitive protein binding assay |
| CSA | cross sectional area |
| CXP | collision cell exit potential |
| D | diffusion coefficient |
| DC | direct current |
| DI | deionized |
| DLI | direct liquid introduction |
| DMSO | dimethyl sulfoxide |
| DNA | deoxyribonucleic acid |
| DP | declustering potential |
| EI | electron impact |
| EIA | enzyme immunoassay |
| EP | entrance potential |
| ESI | electrospray ionization |
| EU | European Union |
| FAB | fast atom bombardment |
| ff-APPI | field-free APPI |
| FIA | flow injection analysis |
| GC | gas chromatography |

| | |
|---|---|
| GS1 | nebulizer gas |
| GS2 | auxiliary gas or lamp gas |
| h | Planck’s constant |
| HPLC | high performance liquid chromatography |
| HV | high voltage |
| ID | internal diameter |
| IE | ionization energy |
| IPA | isopropanol |
| $k_1$ | ion recombination rate constant |
| $k_2$ | ion formation rate constant |
| $k_{PT}$ | proton transfer rate constant |
| L | field-free length |
| LC | liquid chromatography |
| LLE | liquid-liquid extraction |
| LPM | litres per minute |
| MALDI | matrix assisted laser desorption ionization |
| MCA | multiple channel acquisition |
| ME | matrix effect |
| MRM | multiple reaction monitoring |
| $m_{RLR}$ | robust linear regression slope |
| MS | mass spectrometry |
| MW | molecular weight |
| M/W | methanol/water |
| m/z | mass to charge ratio |
| n | ion current density |
| ν | frequency |
| $N_m$ | concentration of analyte neutrals |
| OD | outside diameter |
| OEM | original equipment manufacturer |
| PA | proton affinity |
| PAH | polycyclic aromatic hydrocarbon |

| | |
|---|---|
| PCI | post column infusion |
| PEEK | polyether ether ketone |
| PID | photoionization detector |
| PI | photoionization |
| PT | proton transfer |
| Q0 | first RF only quadrupole |
| Q1 | first mass filtering quadrupole |
| Q3 | second mass filtering quadrupole |
| RIA | radioimmunoassay |
| RF | radio frequency |
| RLR | robust linear regression |
| RSD | relative standard deviation |
| RT | retention time |
| $R^2$ | correlation factor |
| $\sigma$ | standard deviation |
| SPE | solid phase extraction |
| S/S | stainless steel |
| t | time |
| $t_d$ | diffusion lifetime |
| TEM | nebulizer temperature |
| $t_r$ | recombination lifetime |
| THF | tetrahydrofuran |
| TIC | total ion chromatogram |
| UHPLC | ultra high performance liquid chromatography |
| US | United States |
| UV | ultraviolet |
| XIC | extracted ion chromatogram |

# Acknowledgements

I offer my sincere gratitude to the faculty, staff and my fellow graduate students at the University of British Columbia, who have all contributed to guide and inspire my research.

I owe particular thanks to Dr. Damon Robb, whose collaborative assistance has been an immeasurable driving force behind my research. This thesis would not have been possible without your guidance and support.

Special appreciation also must be extended to Dr. Michael Blades, my supervising professor, for his support and world perspective. I view him as a professional mentor for my continued career endeavors.

I am also grateful for the financial support provided by the Natural Sciences and Engineering Research Council of Canada.

I would like to extend special thanks of course to my parents, Don and Elaine, who have provided me with unconditional support throughout my years of education. Even when faced with their son leaving home to venture across the country, they provided me unwavering encouragement.

Finally I thank Melissa – My greatest love, supporter and inspiration.

To my family

# Chapter 1. Introduction

This dissertation will describe the development and relative performance of a new field-free Atmospheric Pressure Photoionization (APPI) source intended to address a broad range of LC-MS applications. We foresee the new prototype APPI source to have many potential uses throughout the field of analytical mass spectrometry ranging from the clinical life sciences, to drug discovery, to the analysis of petroleum and environmental significant sample types. This research project focused mainly upon the growing clinical LC-MS industry, serving as a particularly interesting and relevant area of application, however, this is just one small area an improved APPI source design is expected to present a significant advantage.

The clinical analysis of biological fluids for diagnostic health screening, toxicology and therapeutic drug monitoring among other analytical applications is a relatively young, rapidly expanding field of research. Mass spectrometry represents an enormous global industry that is continually evolving to fulfill the need for faster, highly sensitive and selective clinical assays. In the future, the requirement for reduced samples analysis times and increasingly lower limits of detection will continue to drive the field of mass spectrometry to develop new technologies as the needs of the pharmaceutical and life science industries will in all likelihood never be satisfied.

The rapid development of liquid chromatography – mass spectrometry technologies over the last two decades has been in large part a response to the demands of the drug discovery industry,[1] however, the clinical field has rapidly emerged as a significant driving influence.[2] Despite considerable advancement on the technical end of LC-MS development, a number of technical limitations persist. The LC-MS technique may in principle be broken into a number of key functional elements as described in Figure 1-1. Advances in chromatography have led toward narrower diameter columns and smaller particle diameters

providing improved resolution, separation efficiency and throughput. Accordingly, mass analyzers have adapted to provide faster scan rates and improved transmission efficiencies allowing for lower detection limits and higher selectivity. The bridge between these two technologies, however, the ion source, could be considered the primary factor limiting technique performance. Although a number of commonplace ionization methods exist there is still debate as to which ion source is the most suitable for accurate, high throughput clinical analyses.

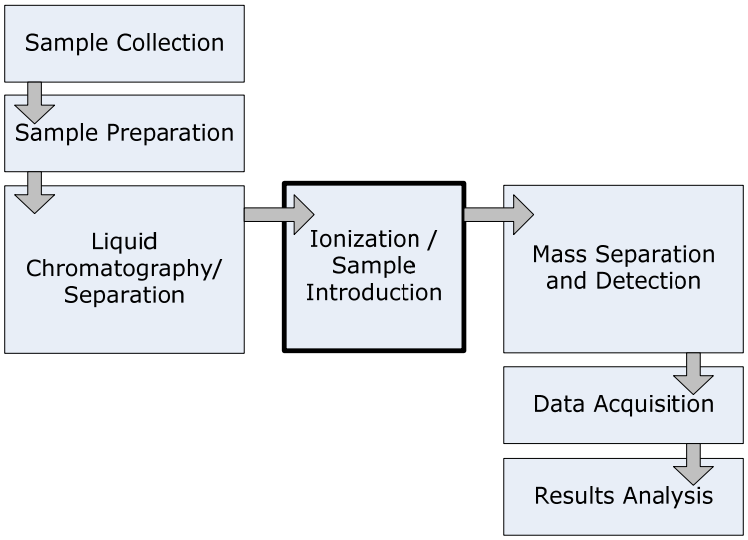


**Figure 1-1. Block flow diagram demonstrating steps critical to a clinical LC-MS workflow**

This thesis will present a thorough evaluation of atmospheric pressure photoionization (APPI), as a universal candidate for LC-MS applications. The following will discuss the design of a prototype field-free APPI source intended to improve ionization and transmission efficiency relative to other commercially available photoionization sources. The performance of this prototype APPI source will be characterized relative to other atmospheric pressure ion sources, utilizing a range of relevant clinical analytes. Finally the performance of this new design will be evaluated as a prospective technique for high throughput assays involving real biological matrices.

## 1.1. Liquid Chromatography – Mass Spectrometry (LC-MS)

The marriage between the physical separation abilities of liquid chromatography with mass analysis capabilities of mass spectrometry has made LC-MS the method of choice for many bio-analyses, supplanting alternative methods such as immunoassays or conventional HPLC techniques. LC-MS has fast become the ideal technique for analyzing an extensive range of biological samples, among them plasma, serum, saliva and urine, each requiring both high sensitivity, along with discrete selectivity. In order to facilitate the union of liquid chromatography with mass spectrometry one must recognize the complex nature of introducing a dirty heterogeneous liquid sample into the gas-phase, ionizing its analyte components and finally transferring them efficiently from the atmospheric pressure lab environment into the ultra-low pressure vacuum of the mass analyzer. This subject represents an intense, on-going focus of analytical research for over the past half century.[3]

## 1.2. The Atmospheric Pressure Interface

Early MS designs relied heavily upon ionization methods such as electron impact (EI), chemical ionization (CI) and/or fast atom bombardment (FAB) among other techniques. Although useful and historically invaluable, these techniques were subject to significant limitations. Analyses were constrained to highly volatile, non-labile compounds of low molecular weight, and require that the ionization processes occur within the vacuum environment of the mass analyzer. In order to expand the range of compounds amenable to analysis by mass spectrometry, it was desirable to analyze the liquid effluent of a high flow chromatograph. Early successful attempts to interface a continuous solvent stream with a vacuum environment include direct liquid introduction (DLI), continuous flow fast atom bombardment (cf-FAB), and moving belt/wire devices. Each of these methods

possessed limitations as well, however, including significant carryover issues and poor sensitivity as a consequence of limited flow rates or flow splitting.

This brings us to the modern era where the atmospheric pressure ionization (API) interface has emerged as the most widely adopted method for combining liquid chromatography with tandem mass spectrometry. The API interface has allowed LC-MS/MS to become the workhorse of the modern clinical laboratory.[4] As its name suggests, ions are produced from a vapourized liquid stream at atmospheric pressure. A small subset of eluent vapour containing a mixture of analyte ions, neutral solvent complexes and matrix elements is directed toward the mass analyzer. Compounds and clusters possessing a charge may be sampled through a restricted orifice or sampling capillary. Utilizing a series of skimmers, focusing elements and differential pumping stages, a high vacuum region can be maintained within the mass analyzer while providing uninterrupted sampling from the ion source at atmospheric pressure. An electric potential difference between the ionization region and the MS interface is generally necessary to preferentially guide ions toward the entrance orifice. Most often a counter flow of curtain or drying gas (frequently nitrogen) is introduced prior to the sampling orifice in order to inhibit the flow of neutral compounds (unionized solvent, source gases and matrix components) into the MS analyzer. Use of curtain gas reduces the potential for the contamination of the ion guide elements within the MS vacuum region.

### 1.3. Ionization at Atmospheric Pressure

Undisputedly, the two most oft employed atmospheric pressure ionization methods for LC-MS applications are electrospray ionization (ESI) and atmospheric pressure chemical ionization (APCI). These two techniques may be considered the staple ionization methods for modern clinical LC-MS/MS workflow.[5,6] In terms of the range of amenable compounds, these techniques are deemed to be rather complimentary - ESI being useful for large, highly polar

analytes and APCI being better suited for the analysis of less polar, small molecules. As a result, these two methods are often combined into a single dual mode ion source allowing for the analysis of an extensive range of compounds with a variety of physical properties. Alternative options exist however; ionization methods such as Atmospheric Pressure Photoionization (APPI) and Matrix Assisted Laser Desorption Ionization (MALDI) have carved their own niches as viable candidates when ESI and APCI fail to provide the performance required for specific applications. The following will be a brief discussion surrounding the various commercially available API source options.

### 1.3.1. Electrospray Ionization (ESI)

Electrospray as an ion source for mass spectrometry will soon turn 45 years old. The technique was first described by Dole et al. in 1968 as means for producing a charged spray of polystyrene in methanol for analysis.[7] It is Fenn et al. (1984), however, who are credited with adapting the technique to interface mass spectrometry and providing the first in-depth exploration into the elementary function and potential of the technique.[8] ESI is today not only the most utilized LC-MS ionization source, but as such may also be considered the most widely understood method in terms of its underlying fundamentals, capabilities and limitations. The mechanisms and early application of ESI have been considered extensively in reviews by Gaskell (1994)[9] and Bruins (1998)[10] and later in more detail by Kabarle (2009),[11] Wilm (2011),[12] and Crotti (2011).[13] Additional thorough reference materials can be found throughout the literature.[14,15] In that there is no shortage of background reading on this subject, the presentation of ESI theory herein will be limited to a somewhat high level discussion.

Electrospray ionization uses an electrified capillary (or needle) to produce a fine spray from a continuously supplied solvent stream, often the effluent of a liquid chromatograph as demonstrated in figure 1-2a. The sampling interface of the mass spectrometer acts as a counter electrode towards which charged species

are drawn. The nebulization process is typically assisted using a high velocity gas flow, with the aim of producing a fine spray of solvents droplets containing the analyte of interest, sample matrix materials, and often a variety of additive modifiers. As the charged solvent droplets travel toward the MS interface evaporation processes occur until ultimately individual charged molecules or clusters are released into the atmospheric pressure source environment as gas-phase ions (figure 1-2b). The mechanisms surrounding the ESI process are slowly becoming more understood and are now attributed to either ion evaporation[16] or charged residue models.[7] These processes will be considered in detail later within the discussion.

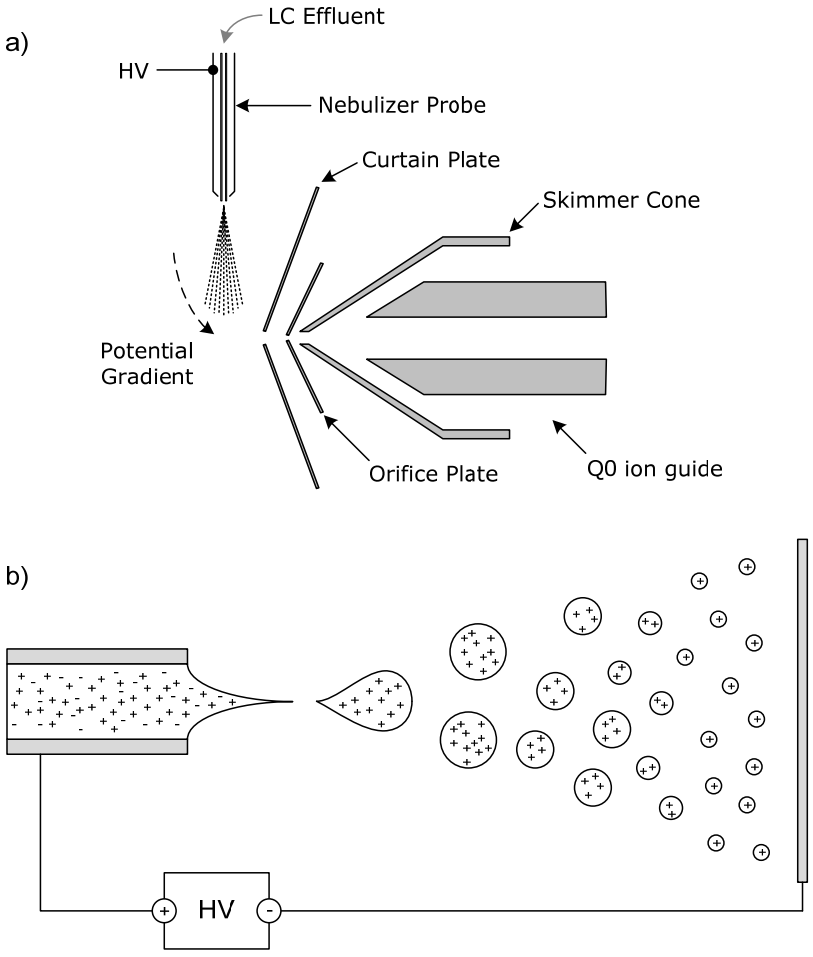


**Figure 1-2. a) Schematic representation of an electrospray Ionization source. b) Simplified electrospray process demonstrating the release of charged ions from solution to the gas-phase.**

The electrospray ionization mechanism is somewhat unique to other techniques in that analyte species must be present within solution in a pre-charged state. This means that ESI lends itself effectively to the analysis of either ionic compounds or polar analytes containing suitable acidic or basic functionalities with which to adopt a charge through either protonation / deprotonation or the adduction of an ionic constituent (such as $Na^+$, $K^+$ $NH_3^+$, $Cl^-$ or $Br^-$, however, numerous other adducts are commonly reported[17]). Multiple charging (typically $[M+nH]^{n+}$) is common for larger molecules leading conveniently to a reduced mass to charged ratio (m/z) making the analysis of macromolecules accessible to mass analyzer with a limited mass range. There are a number of drawbacks to ESI, however, including limited dynamic range, and poor efficiency for most non-polar analytes, as well as for workflows incorporating involatile solvents or matrices. ESI is also known to be quite susceptible to matrix ionization suppression, the mechanisms for which will be addressed in some detail later within the discussion.

### 1.3.2. Atmospheric Pressure Chemical Ionization (APCI)

Atmospheric Pressure Chemical Ionization (APCI) currently has widespread acceptance as an alternative ionization technique to ESI, expanding the range of compounds amenable to LC-MS analysis to neutral compounds of limited polarity. A functional schematic for a modern APCI source is provided in figure 1-3. In APCI, the effluent of an LC is sprayed under pneumatic assistance from a narrow capillary into a heated nebulizer, consisting of a glass or ceramic tube maintained at temperatures at or above $400^oC$. Solvent droplets containing the analyte, as well as other matrix components, rapidly desolvate to produce neutral gas-phase molecules. A corona discharge is then used to indirectly ionize the analyte through a series of gas-phase ion-molecule reactions involving primary reagent nitrogen ions and intermediate solvent ion clusters.

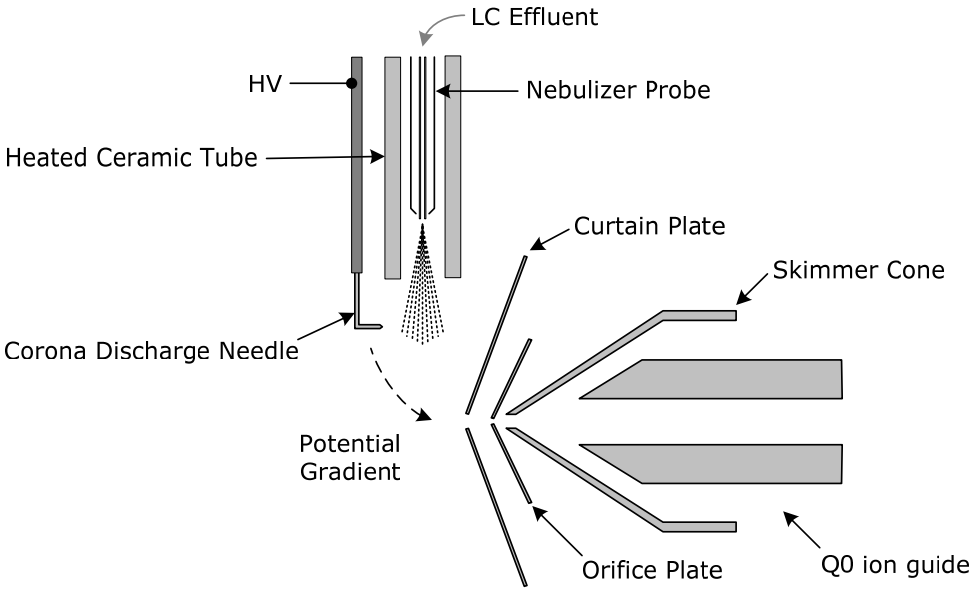


**Figure 1-3. Schematic representation of an Atmospheric Pressure Chemical Ionization (APCI) source.**

APCI is considered to be a less-soft ionization technique when compared to ESI, meaning considerable ion fragmentation is often observed. The high temperature environment tends to limits APCI to the analysis of smaller molecules that are not appreciably thermally labile. Since the ionization pathways in APCI take place within the gas-phase through ion-molecule reactions, rather than through solution phase chemistry as in ESI sources, the ionization of neutral molecules of limited polarity becomes possible. This has positioned APCI as a complimentary technique to ESI. The two methods are often paired in combined dual mode devices, integrating both methods within a single ion source. APCI is also known to have minimal susceptibility to matrix ion suppression, identified earlier as a noteworthy limitation of ESI.

Few review articles cover the general breadth of APCI applications and its fundamentals,[18] however, general articles and texts reviewing atmospheric pressure ionization tend to provide an understanding of the field in some detail.[2,19] Carroll et al. were among the first to demonstrate an atmospheric

pressure CI source based upon corona discharge – similar to modern APCI devices.[20] An early description of the gas-phase, ion–molecule chemistry applicable to CI sources was presented by Good et al. (1970).[21] This model is now considered to be the established mechanism for reagent ion generation in CI and can be extended largely to APCI as well.

### 1.3.3. Alternative Commonplace Ionization Sources

A number of alternative commercially available ion sources have been introduced with the aim to overcome the limitations of conventional ESI and APCI. Matrix Assisted Laser Desorption Ionization (MALDI) is perhaps the most widely accepted of these, although it is not typically operated at atmospheric pressure and usually not in direct tandem with liquid chromatography. MALDI provides a suitable method for ionizing complex macro- molecules like DNA, proteins, polymers and sugars. An inherently soft ionization method, MALDI is able to efficiently ionize fragile biomolecules, while preserving the basic molecular structure from fragmentation. Numerous review articles discuss the mechanisms and range of application suitable for MALDI, a testament to the relative impact of the technique on the field of bioanalysis.[22-24]

Alternatively, Nanospray, a “scaled-down” version of ESI, has been developed to satisfy the desire to analyze small sample volumes, by providing a high ion transmission efficiency relative to conventional ESI.[25] Nanospray sources are routinely used to characterize proteins and peptides and are suitable for low flow nano-bore LC based methods. Neither Nanospray nor MALDI provide much advantage for traditional clinical analyses and herein will reside outside the focus of this discussion.

### 1.3.4. Atmospheric Pressure Photoionization (APPI)

Since the development and characterization of a new Atmospheric Pressure Photoionization (APPI) source is the focus of this dissertation, a thorough discussion into its history, fundamentals, applications and potential will be presented. An understanding of the accepted principles and ionization mechanisms governing APPI performance should be considered critical to the production of an improved device design. As will be identified, a lack of fundamental understanding in the past has led to the now exclusive manufacture of commercially available APPI sources that falls short of performance expectations. Consequently, there has been a general lack of widespread acceptance for the technique as a result of poor overall sensitivity, save for a restricted range of highly non-polar analytes that ESI and APCI simply fail to ionize. Photoionization is viewed as a novel technique suitable for analyzing a limited, niche range of compounds rather than as a universal, highly sensitive ionization method.

#### 1.3.4.1. Fundamental Operating Principles of Atmospheric Pressure Photoionization

Although several APPI source designs exist, each functions under similar operating principles. These principles have been summarized extensively throughout the literature with several detailed reviews providing insight into APPI mechanisms and applications.[26-29] In general, the APPI process can be broken down into several critical steps for discussion, namely: vapourization, primary ionization, analyte ionization through ion-molecule reactions and finally ion transmission into the mass analyzer. For reference a basic APPI block diagram and schematic representative of many APPI sources are provided in figure 1-4.

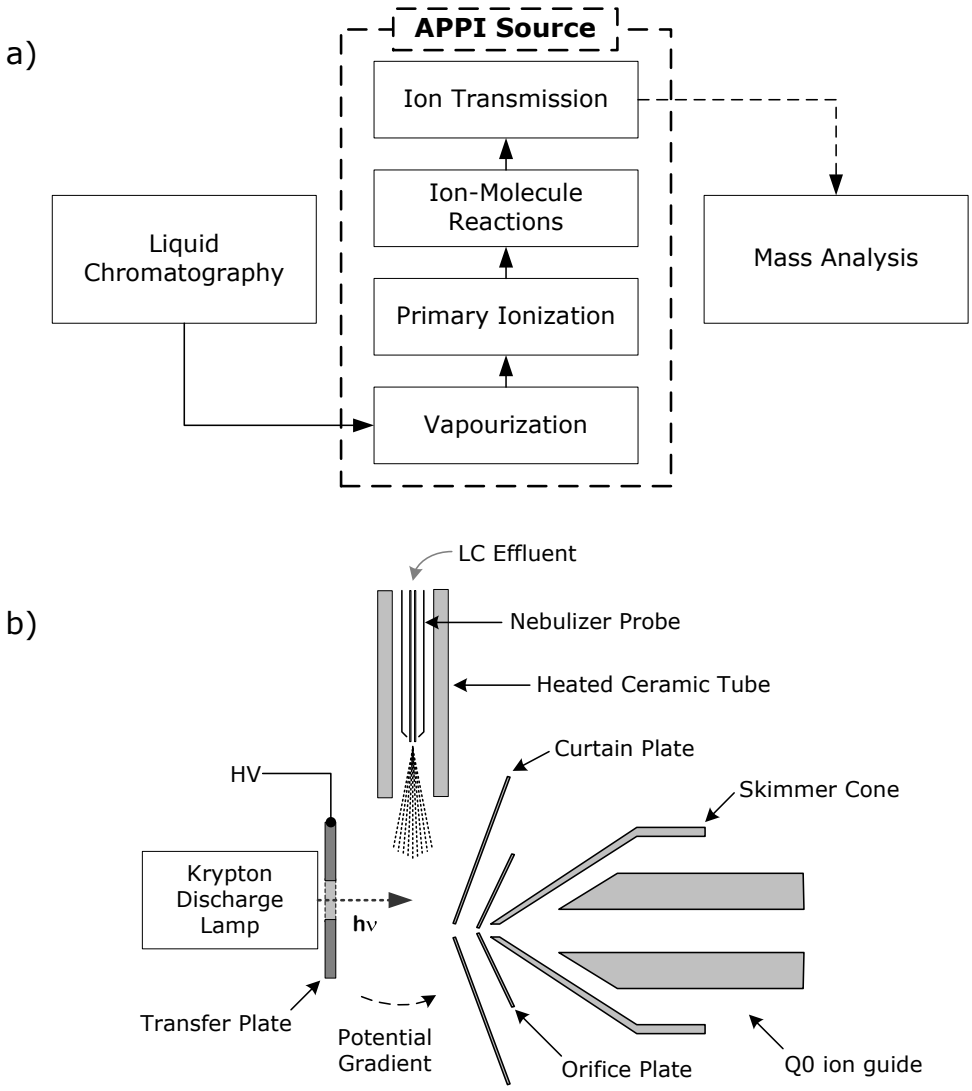


**Figure 1-4. a) Block diagram demonstrating processes relevant to Atmospheric Pressure Photoionization sources. b) Schematic diagram for a Photospray™ source, representative of many commercially available APPI sources.**

a) Vapourization

Like APCI, ionization in APPI is the result of a critical series of indirect ion-molecule reactions within the gas-phase. There is therefore a requirement that the liquid effluent of a chromatograph be efficiently vapourized with a heated nebulizer. A fine capillary is used to spray a liquid stream under the assistance of a high velocity gas flow within a heated ceramic or glass tube. Aerosol solvent droplets rapidly desolvate to produce a heterogeneous cloud containing source

gases (air, $N_2$, etc.), LC solvents, additives, analytes, and other matrix components.

b) Primary Ionization

Primary photoionization occurs when the nebulized plume is irradiated using a Krypton VUV-discharge lamp with radiant energies of 10.0 and 10.6 eV (at 123.6 nm and 116.5 nm respectively). If a component of the vapour has an ionization energy below that of the photon source ($IE_M < h\nu$), ionization may occur as represented by equation 1.

(1) $M + h\nu \rightarrow M^{\bullet+} + e^-$

If M is the analyte of interest, then equation 1 describes a direct photoionization pathway. Ionization of the analyte directly is considered to be a statistically unlikely process given the relatively low number density of the analyte with respect to the predominant photon absorbing solvent cloud. Most common reverse phase solvents such as methanol, acetonitrile and water have ionization energies slightly above that of the light source ($IE_s > h\nu$). As a result, photon absorption can lead to the production of excited state species, however, no direct solvent photoionization should occur. Consequently, analyte ion current derived through direct photon absorption and subsequent photoionization is expected to be negligible due mostly to limited photon flux. Instead, APPI sources are universally required to employ an easily ionizeable additive or dopant to facilitate the generation of primary reagent ions given by equation 2. Photoionized dopant radicals serve as intermediate reagent ions used to deliver charge to the analyte (see section c).

(2) $D + h\nu \rightarrow D^{\bullet+} + e^-$

Common dopant candidates include toluene, acetone, anisole and chloro- or bromobenzene. A variety of common dopants in addition to various common LC

solvents are listed in Table 1-1,[30,31] including reported ionization energies and proton affinities. An ideal dopant candidate must have an ionization energy below that of the photon source in order to facilitate primary ionization ($IE_D < h\nu$). A dopant flow rate set to 5-10% of the total solvent flow is frequently adopted to attain maximum analyte signal under common high-flow reverse phase LC conditions.[32] If sufficiently miscible under selected LC conditions (solvent, pressure, temperature), a dopant may be added directly to the mobile phases post-column. Alternatively, the dopant can be vapourized independently and introduced along with the nebulizer gas. In select circumstances (typically normal phase separations) the LC solvents themselves can include an easily photoionizable component such as IPA, DMSO, THF or hexane. In these instances the mobile phase itself will fulfill the role of the dopant reagent ion supply.

**Table 1-1. Ionization energies and proton affinities relevant to APPI**

| Compound | MW / g.mol$^{-1}$ | IE / eV[a] | PA / kJ.mol$^{-1}$ [b] | Miscible [c] |
|---|---|---|---|---|
| Anisole | 108.14 | 8.20 | 839.6 | L |
| Toluene | 92.14 | 8.83 | 784.0 | L |
| Bromobenzene | 157.00 | 9.00 | 754.1 | L |
| Chlorobenzene | 112.56 | 9.07 | 753.1 | L |
| Dimethyl sulfoxide | 78.13 | 9.10 | 884.4 | S |
| Tetrahydrofuran | 72.11 | 9.40 | 822.1 | S |
| Acetone | 58.08 | 9.70 | 812.0 | S |
| Hexane | 86.18 | 10.13 | 672.8 | N |
| Isopropanol | 60.10 | 10.17 | 793.0 | S |
| Methanol | 32.04 | 10.84 | 754.3 | S |
| Acetonitrile | 41.05 | 12.20 | 779.2 | S |
| Water | 18.02 | 12.62 | 691.0 | S |

*a* - All ionization enegeries obtained from reference [30]
*b* - All proton affinities obtained from reference [30] with the exception of hexane; see [31]
*c* - In $H_20$ at 25$^{o}$C; S - soluble, L - low solubility, N - not soluble
Solvents listed below dashed line are not photoionized by Kr discharge lamp

c) Ion-molecule Reactions

i) Charge exchange ionization

Photoionized dopant molecules represent a supply of reagent ions that may take part in secondary ion-molecule reactions, ultimately imparting a charge upon the analyte. In positive ion MS mode the analyte can be charged through one of two pathways: charge exchange or proton transfer. The former mechanism is described by equation 3. Charge exchange, CE, is viable when the ionization energy of the analyte is less than the recombination energy of the dopant reagent ion ($IE_M < IE_D$).

(3) $D^{\bullet+} + M \rightarrow D + M^{\bullet+}$ *(charge exchange)*

CE is extremely useful for the analysis of highly non-polar analytes, permitting the efficient formation of $M^{\bullet+}$ ions. This is particularly important for analytes that are not able to protonate or readily form alkali adducts. The ability to exploit the CE mechanism sets APPI apart from ESI and APCI, which predominantly produce $[M+H]^+$ or $[M+Na]^+$ quasi-molecular ions rendering them unsuitable for the ionization of most non-polar analytes.

ii) Proton transfer ionization

The proton transfer, PT, mechanism is a somewhat more involved pathway that requires a closer look at the interaction between the dopant reagent ions and the accompanying solvent vapour. Under reverse conditions a gross excess of polar organic phase (either methanol or acetonitrile) is generally provided. In these circumstances the solvent, S, may react (often to completion) with the pre-ionized dopant reagent supply. The result is the formation of acidic protonated solvent clusters as described by equation 4.

(4) $D^{\bullet+} + nS \rightarrow S_nH^+ + (D\text{-}H)^{\bullet}$ *(Solvent cluster formation)*

Here, n, is the co-ordination number of solvent molecules within a cluster. The value of n, determining the size of a cluster, is affected heavily by the solvent flow rate, as well as source temperature. At higher flow rates the range of solvent cluster co-ordination values generally increases, producing clusters that are stabilized through solvation and display decreased acidity. The forward rate of cluster formation is expected to be a very fast, collision-limited process since the source is operated at atmospheric pressure in the presence of an excess of solvent vapour.[20] The most profound consequence of cluster ion formation is an inevitable decrease in the dopant reagent ion population, resulting in a diminished ability to perform CE ionization. A benefit to solvent cluster ion formation, however, is the production of a sufficiently acidic reagent ion supply suitable for taking part in proton transfer reactions with the analyte, as described in equation 5.

(5) $S_nH^+ + M \rightarrow MH^+ (S)_m + (n\text{-}m)S$ *(Proton transfer ionization)*

PT may occur provided an analyte exhibits higher gas-phase basicity than that of the reagent ion cluster. The early developers of APPI did not anticipate the proton transfer pathway, however, it provides a fortuitous method for ionizing a wide range of polar compounds provided the analyte possesses a suitable proton affinity. The ability to ionize both polar analytes by proton transfer and non-polar analytes through charge exchange positions APPI as the most universal soft ionization source available today.

iii) PI in negative MS mode

APPI is also suitable for MS workflows in negative ion modes through a number of ionization mechanisms such as electron capture/transfer, halide attachment and proton abstraction. Negative ion pathways were not utilized under the scope of this thesis and will not be discussed in much detail going forward. Historically,

however, and from the standpoint of providing insight into furthering source design, some description of these mechanisms is instructional. A thorough survey of the accepted negative ion APPI mechanisms and their applications is available within the literature.[33-36]

In summary, oxygen, which is always present within APPI sources, possesses a relatively high electron affinity allowing it to rapidly scavenge photoelectrons produced through primary dopant ionization (see eq. 2). The formation of a superoxide radical ion can be described by equation 6 below.

(6) $O_2 + e^- \rightarrow O_2^{\bullet -}$ *(Superoxide formation)*

The superoxide radical anion may act as a reagent ion in negative ion modes. It is often the most basic species produced within the APPI source and is readily capable of abstracting a proton from many analytes (equation 7).

(7) $M + O_2^{\bullet -} \rightarrow HO_2^{\bullet} + (M\text{-}H)^-$ *(Proton abstraction)*

Alternatively, if the analyte itself has a suitably high electron affinity it may be able to scavenge photoelectrons directly on it own or through abduction of an electron from the superoxide radical as described in equations 8 and 9 respectively.

(8) $M + e^- \rightarrow M^{\bullet -}$ *(Direct electron capture)*

(9) $M + O_2^{\bullet -} \rightarrow M^{\bullet -} + O_2$ *(Electron transfer)*

When utilizing LC methods employing halogenated solvents such as chloroform or dichloromethane, a dissociative electron capture mechanism has been reported.[34-39] Halogenated solvents are able to scavenge photoelectrons and subsequently produce a dissociated solvent radical and free halogen anion

(equation 10). The analyte may then adduct the charged halogen to create a stabilized ion through anion attachment as describe in equation 11. Ross et al. (2010) demonstrated that employing a halogenated additive like 1,4-dibromobutane may also result in anion attachment for non-polar environmental samples, producing favourable results over conventional dopant-only APPI methods.[40]

(10) $S + e^- \rightarrow (S\text{-}X)^\bullet + X^-$ *(Electron capture – halide dissociation)*

(11) $M + X^- \rightarrow (M+X)^-$ *(Halide attachment)*

In summary, there are a wide range of channels available to APPI sources through which analyte ionization may take place. With the exception of the largely inefficient direct PI pathway, each mechanism requires the use of a dopant to generate intermediate reagent ions. Employing dopants in APPI is now considered to be standard operating procedure. Dopant use may provide sensitivity enhancement over several orders of magnitude greater than direct photoionization alone. As a result, a full understanding of dopant and ion-molecule chemistry is critical to the design of an optimized source design. For example, the formation of reagent ions ($D^{\bullet+}$, $S_nH^+$, $O_2^{\bullet-}$) is thought to be the result of fast exothermic reactions that are collision-limited. Thus, provided that dopant, solvent, and/or oxygen are each provided in excess, the reagent ion population should reach a stable equilibrium within a few microseconds. The subsequent ion-analyte interactions may then proceed and may continue to advance during passage through the ion source. What is implied here is that the provision of extended reaction time could be directly related to analyte ion production, providing kinetic or geometric factors through which the APPI source design may be refined.

d) Ion Transmission

Another feature that distinguishes APPI from both ESI and APCI is that a large electric potential is not needed to facilitate the ionization process. ESI of course requires that the spray probe be held at high potential (4-5 kV), while APCI utilizes a high voltage corona discharge. In both devices the field created in the open space between the high potential ion source elements and the MS interface is used to guide ions toward the mass analyzer. The inclusion of a large electric field unfortunately complicates the addition of ion focusing elements intended to improve ion transmission. In all modern APPI designs, however, the mechanism of ionization does not require such a field. Instead, ion mobility toward the MS orifice must be induced using an additional bias potential (transfer voltage) applied to the surrounding source elements. The bias voltage is independently controllable and may be adjusted without impacting the ionization process - this may enable the ability to tailor the electric field thereby optimizing ion transfer. Although the potential benefits gained through ion focusing in APPI sources have never been established, the prospect of improved ion transmission may in the future provide APPI with an additional advantage over other source options.

#### 1.3.4.2. Historical Development of Photoionization at Atmospheric Pressure

Prior to the introduction of APPI, the photoionization detector (PID) had been a longstanding tool in gas chromatography,[41-46] however, only a few applications demonstrated an extension of the technique to a continuous liquid stream.[47-50] Of these devices, none were intended to interface directly with mass spectrometry. It is now just over one decade since Bruins et al (2000)[51] and Syage et al. (2000)[52] simultaneously, yet independently introduced photoionization sources, extending LC-MS assays to non-polar and moderately-polar analytes. Both devices contained fundamental similarities as well as differences, however, both functioned under the mechanisms and principles described above. In common,

early devices utilized single photon ionization, using a vacuum-ultraviolet Krypton discharge lamp to generate analyte ions from a vapourized LC effluent. In contrast, both sources utilize ion transmission fields differently, dramatically affecting the ionization process, resulting spectra and the overall analyte ionization efficiency. A description of the development path for these two designs leading to a full account of all modern commercially available photoionization sources will be presented below.

#### 1.3.4.2.1. Closed-geometry Field-free APPI Sources

Since the commercial introduction of APPI, two distinct device designs have been developed: an open-geometry source and a closed-geometry, field-free design. The historical development of these two designs is relevant to this dissertation as the development path for each speaks directly toward the motivation for this research project.

Around the year 2000, Bruins and Robb[51] first described an APPI source design incorporating a solid stainless steel source block as demonstrated in figure 1-5. A conduit passing through the source block provides passage for the nebulized LC effluent, while a second perpendicular side channel is used to introduce photons from a conventional, orthogonally mounted Krypton PI discharge lamp. Dopant vapour passing through the area irradiated by the discharge lamp is photoionized and may then participate in ion-molecule reactions with the analyte. These reactions proceed during transit through an extended flight tube, leading to analyte ion formation. A bias voltage is applied to the source elements and flight tube, creating a field within the open space between the source block and MS curtain plate. This field is required to guide ions toward the MS interface. While within the source block and flight tube region, ions experience a field-free environment. Consequently, during transit both positive and negatively charge ions co-exist and may re-combine freely until they are finally separated upon entering the field region. Total ion current within field-free region is expected to

continuously diminish as a result of the recombination of oppositely charged species at a rate proportional to the square of the available current density.[53] The recombination process is thought to be the dominant ion loss process within field-free sources and must be considered as a critical factor affecting source design.

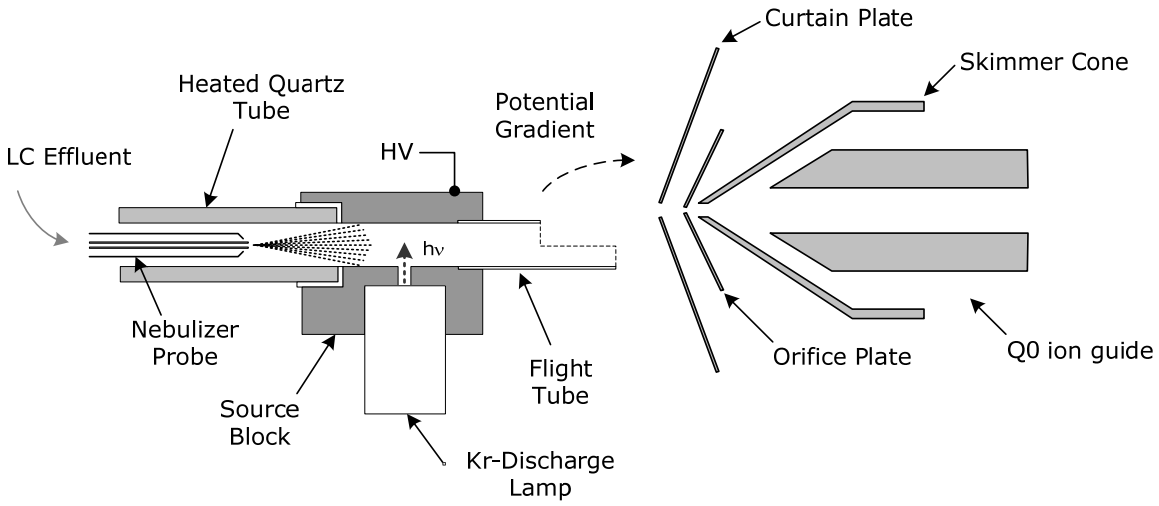


**Figure 1-5. Schematic representation of a first-generation, closed-geometry, field-free Atmospheric Pressure Photoionization source.**

MDS Sciex commercialized the first closed-geometry, field-free APPI source under the name Photospray for use on early series API 3000 and QStar mass analyzer. Photospray sources were manufactured using a modified housing and heated nebulizer utilized in early APCI sources, with the ion path of the source set co-linear to the MS ion path. Photospray sources received immediate praise, allowing for improved detection limits over APCI and ESI for a number of compounds including non-polar environmental compounds like PAHs[51,54,55] and clinically significant applications like the analysis of testosterone in biological fluids.[5151,56,57]

#### 1.3.4.2.2. Open-geometry APPI Sources

In 2000, a second APPI source utilizing an open-geometry design was described and commercialized by Syagen Technology under the name Photomate.[52] A functional schematic that can describe many Syagen open-geometry APPI

sources is given in figure 1-6a. No source block is incorporated within this design and likewise, no field-free region is provided. Primary ionization takes place within the open environment in front of a discharge lamp mounted in close proximity to the MS sampling orifice. A heated nebulizer is used to vapourize a liquid stream, this time mounted orthogonal to the MS ion path. As vapourized dopant passes through the region irradiated by the lamp, primary photoionization and secondary ion-molecule reactions proceed. A bias field potential is required to drive charged species toward the MS sampling orifice, while neutrals are removed by an exhaust system. The field created between the transfer plate and MS interface provides near-immediate separation of oppositely charged species, limiting ion recombination losses. Rapid charge separation offers the ostensible advantage of increased total ion current delivery, however, this does not take into account the process of charge transfer from primary reagent ions to the analyte. Here, reagent ions and analyte neutrals only co-reside within the ionization region for a short period before the ions are quickly swept toward the mass analyzer - potentially restricting analyte ion formation.

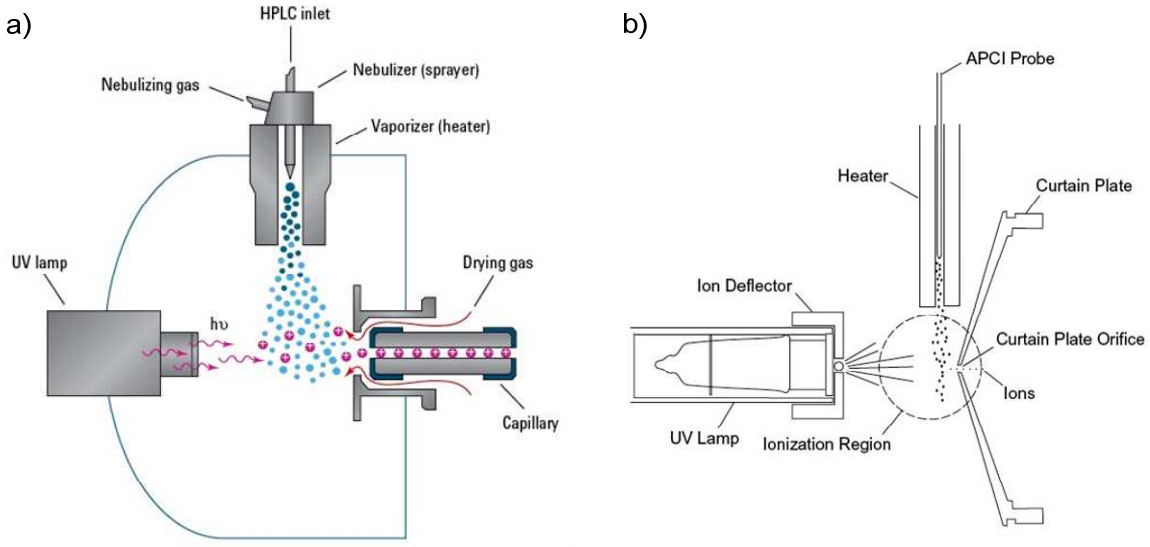


**Figure 1-6. Functional schematic representations for a) open-geometry Agilent Photomate sources and b) open-geometry Photospray sources.**

In order to improve upon their open-geometry design, Syage et al. incorporated a proprietary high energy RF Krypton discharge lamp. The motivation was to

enhance primary ionization efficiency through improved radiant output of the source. To the author's knowledge, the overall improvement attained through use of a more powerful lamp has yet to be established, however, theory dictates that an increase in lamp current or dopant flow rate will always lead to enhanced primary ionization.[58] However, it should also be noted that increased lamp power has only been shown to have minimal impact on the resultant analyte ionization efficiency, despite an observed increase in total ion current.[53] This brute force attempt to boost APPI sensitivity would appear to be somewhat shortsighted, as it does not take into account the critical importance of the various ion-molecule reaction pathways discussed above.

Syagen Technology is now the largest producer of exclusively open-geometry APPI sources, providing OEM devices for a range of MS manufacturers including but not limited to Agilent Technologies, Thermo Scientific and Waters. Continuing the same direction, in 2004 AB/Sciex also opted to produce an open-geometry Photospray source design to mirror the development path of modern TurboV sources built for use on 4000 series mass analyzers (figure 1-6b). These sources take advantage of a well-engineered heated nebulizer,[59] orthogonal spray geometry and an entrained exhaust system for reduced carryover. The modern Photospray no longer incorporates a source block or any provision for an extended field-free region. Coincidentally, many of the benefits provided by the first-generation field-free APPI sources over ESI and APCI appear to have been lost during this transition. This observation was supported by Jacobs et al. (2004), reporting that the sensitivity gains provided by first generation APPI sources over APCI were lost when similar methods were transferred to the modern open-geometry Photospray sources, at least for the analysis of testosterone.[60] Today, all modern commercially available APPI sources have adopted an open-geometry platform.

#### 1.3.4.3. Current Application of Atmospheric Pressure Photoionization

Despite the lack of overwhelming, universal acceptance for the technique, APPI sources are not without their applications. APPI is currently recognized as a niche device for its ability to ionize non-polar analytes particularly well, specifically those not appreciably ionized by ESI or APCI. APPI sources are also reputedly less susceptible to matrix ionization suppression than ESI in particular,[27] thus APPI has some usefulness for the analysis of very complex biological or environmental samples.

Areas in which APPI has found particular acceptance include the analysis of pharmaceuticals,[61-81] steroids,[51,56,57,82-115] lipids,[116-131] environmental contaminants such as PAHs,[54,55,132-154] flame-retardants,[155-168] herbicides/fungicides/pesticides, [169-178] fullerenes,[179-185] crude/petroleum products, [186-210] polymers, [211-219] dyes,[220-223] , explosives,[224] sugars, [225] dissolved organic matter, [226,227] and peptides. [228,229] Modifications made to the APPI source design leading to an improved understanding of its functioning and limitations will inevitably increase the number of suitable applications and ultimately technique acceptance.

## 1.4. Scope of Research

This research project began with an evaluation of the relative performance of a modern open geometry APPI source versus the first-generation, closed-geometry APPI source design. To the author's knowledge, no direct head-to-head evaluation of the two designs has been completed on a single MS platform. The goal was to identify the root cause of the reduced relative sensitivity reported by Jacobs et al. when first evaluating the performance of open-geometry Photospray sources.[60]

This dissertation will discuss the development of an in-house built, field-free APPI source, fabricated using the housing of a modified commercially available TurboV ion source. This allowed for a direct comparison of the two geometric platforms permitting use of identical photoionization lamps, heated nebulizers, exhaust systems and mass analyzers. Early results will show that significant performance enhancement could be recognized through careful consideration of parameters affecting primary ionization, ion-molecule reactions and ion transmission.

The prototype, field-free APPI source design was then thoroughly evaluated against other common API sources including, ESI, APCI and a commercially available Photospray source for a range of compounds of clinical and environmental importance. This evaluation was then expanded to characterize the relative impact of matrix effects brought upon through the analysis “real” samples with complex biological matrices.

# Chapter 2. Development of a Prototype, Field-free APPI Source

In this chapter the design, fabrication and characterization of a prototype, field-free APPI source will be discussed. This body of research was motivated by the desire to evaluate the relative performance of open- and closed-geometry APPI source designs on a common MS platform. A performance comparison was completed through the head-to-head analysis of a variety of standard compounds under various source conditions and geometric parameters.

## 2.1. Background Theory

### *Field-free geometry APPI sources*

There is much that can be learned from past LC-MS ion source development that may be applied to the creation of an improved APPI source design. The first generation closed-geometry Photospray source was not the first field-free ionization sources utilized for LC-MS applications. For instance, radioactive Nickel-63 chemical ionization sources also require no electric fields or high voltages in order to produce ions. Analogous to closed-geometry APPI, oppositely charged ions within these sources are allowed to recombine freely prior to MS sampling. The early literature describing $^{63}$Ni-foil source fundamentals can provide great insight into the impact of source geometry on ion generation and loss processes.

In 1974, Carroll et al. elegantly described an atmospheric pressure interface centered around a radioactive Nickel-63 foil ion source.[230] This device exploited a cylinder of thin $^{63}$Ni-foil to produce a source of electrons utilized in the formation of primary reagent ions within what was referred to as a “continuous sampling …

reaction chamber". In the absence of external fields, the kinetics of a series of ion-molecule reactions parallel to those of modern APCI and APPI sources were considered. Carroll presented that the change in ion density within a field-free source could be described by:

$$\frac{dn}{dt} = -k_1 n^2 + k_2 P \tag{12}$$

where n is the ion current density, $k_1$ is the ion recombination rate constant and the term $k_2P$ denotes the rate of ion production, where $k_2$ represents the overall forward rate constant for ion production and P is the product of the absolute concentrations of reactant species. Under steady state conditions, the rate of change in ion current approaches zero and the relationship simplifies to:

$$n = \left( \frac{k_2 P}{k_1} \right)^{1/2} \tag{13}$$

Implied here is that under typical operating conditions the number density of ions within the source will depend on the equilibrium between ion formation and recombination processes. Additionally, the rate of ion recombination is also expected to scale with the square of the total number density of available charge carriers. Carroll went further to consider the potential loss of ions through diffusion toward the walls of the reaction chamber. Within their model, the impact of diffusion as a loss process was determined to be around the same order as expected through recombination losses. Utilizing equation 14 and 15, the expected ion lifetimes as a function of diffusion and recombination losses within first-generation field-free APPI sources can also be calculated.

$$t_d = \frac{1}{D}\left( \frac{L}{\pi} \right)^2 \tag{14}$$

$$t_r = \frac{1}{k_1 n} \tag{15}$$

Assuming a diffusion coefficient, D, of 0.1 cm/sec (assumed for ion sources at atmospheric pressure[230]) and a reaction chamber radius, L, of 0.35 cm a diffusion lifetime, $t_d$, on the order of 100 ms is expected. Conversely, utilizing $10^{-6}$ $cm^3/s$ as a typical recombination rate constant[231] and a primary ion current density of $4x10^9$ ions•$cm^{-3}$ estimated for a field-free APPI source,[53] a recombination lifetime of 250 μs is estimated. Assuming the ballpark accuracy of these values, ion recombination should be the dominant loss process for ion sources similar to the first-generation, field-free APPI source. Compared to early $^{63}$Ni source designs, field-free APPI devices have a much larger active volume and considerably higher primary ion current. As a result, the effects of diffusive losses are likely to present an insignificant impact, where as ion recombination losses are expected to be far more prominent.

Taking a closer look at equation 12, specifically for the generation of analyte ions, the term $k_2P$ represents the rate of ion formation. In principle P can be expanded to represent a reaction mechanism specific to APPI represented by the product of the reagent ion concentration, $n_r$ and the total concentration of analyte neutrals within the source, $N_M$. Using the proton transfer mechanism as a starting point, the steady-state equation governing analyte ion formation can be represented by:

$$\frac{dn_{MH}}{dt} = -k_1 n_- n_{MH} + k_{PT} n_r N_m = 0 \tag{16}$$

where $n_{MH}$ is the number density of analyte ions, $n_-$ is the number density of negative charge carriers, and $k_{PT}$ is the forward rate constant for the proton transfer reaction.[53] Under ideal conditions the population of reagent ions ($n_r$) will approach the concentration of negative charge carriers ($n_-$) and both terms may

be eliminated. We may also assume the concentration of neutral analyte molecules will remain abundant relative to the population that is ultimately protonated. (Strictly speaking, the population of reagent ions, negative charge carriers and analyte neutrals may become exhausted under some conditions, implying there are limits to which these equations apply, based upon the approximations made above). Simplification and re-arrangement of equation 16 yields:

$$n_{MH} = \frac{k_{PT} N_M}{k_1} \tag{17}$$

This relationship predicts that number density of analyte ions will depend only upon the ratio between the ion formation and loss constants; and the total concentration of analyte neutrals. Absent now from this equation is reagent ion concentration. Worthy of note, the primary reagent ion concentration will always increase with increased the dopant flow or lamp power, however, from equation 17, the production of analyte ions should be independent of reagent concentration, provided it remains in excess, a hallmark of recombination-limited ion sources.[58] The rate constants for both charge transfer and proton transfer mechanisms are expected to range from $10^{-10}$ to $10^{-9}$ $cm^3/s$.[230] Siegel and Fite assumed a recombination rate constant of $10^{-6}$ $cm^3/s$ for a comparable field-free $^{63}Ni$ β-ray source, yielding an estimated $10^{-3}$ ratio between ion production and recombination rate constants.[232] From here, the anticipated analyte ions concentration may be estimated, however, ultimately analyte sensitivity will be not only dependent upon the accuracy of the assumed rate constants, but also upon the efficiency of ion transmission. In the end, the transfer of ions from the atmospheric pressure source environment through the MS interface may also be a contributing factor that limits analyte sensitivity.

The space charge repulsion has the ability to limit ion transmission through the interface of a mass spectrometer.[233] Space charge limitations result from the

repulsion of like-charged ions when confined within an external electric field. At high density, like-charges within close proximity will repel one another, altering their respective trajectories. In the case of an ion beam akin to that produced by the field-free APPI source block, space charge repulsion could result in beam de-focusing, particularly within the confined region of the MS sampling orifice. The effects of space charge, limiting transfer efficiency, are known to be determined by the overall charge density, ion velocity, particle mass and field strength.[234] Space charge limitations in mass spectrometry are widely associated with ion trap instruments, where ions are collected and stored for an extended period within a trapping field.[235] More relevantly, however, these effects have been identified as the driving force limiting ion transfer efficiency in ESI and APCI sources.[233] With regards to the field-free source, we hypothesize that a reduction in total ion current through lengthening of the ion reaction zone region, while maintaining a high concentration of analyte ions could improve overall transmission and thus analyte sensitivity. It is unclear to this point, however, the degree to which space charge limits throttle ion transfer in field-free APPI sources. We expect the effect to vary significantly instrument-to-instrument and that it should be considered an important factor impacting ion source design.

*The case of open geometry APPI sources*

The analyte ionization mechanisms at play for open-geometry sources are governed by a slightly modified set of parameters. Since no field-free region is provided within these sources, we expect that there will be a near-instantaneous separation of opposite charges within the vicinity of the primary ionization region. Ions with a like-charge to the voltage applied to the transfer plate will be repelled and toward the MS sampling orifice. Oppositely charged species will be drawn toward the transfer plate and quickly grounded, limiting the role of charge recombination. (Similar to the field-free source, ion diffusion losses are assumed to be an insignificant contributor to ion loss processes.) Consequently, we expect that ion recombination within open-geometry sources may be considered

negligible; in-turn the total ion currents delivered should also be significantly higher than observed for field-free sources. It is anticipated that analyte ions will be produced through the same critical ion-molecule reaction pathways that governing field-free APPI sources. In open-geometry sources, primary ionization occurs in the direct vicinity of the sampling interface (a length of only 3-5 mm). The total reaction time is then limited to the short period that reagent ions and analyte neutral molecules co-reside within the primary ionization region, and as a result, the progression of ion-molecule reactions may be restricted.

From a theoretical standpoint considering only first principles it is difficult to discern which ion source configuration will provide the best overall analyte sensitivity. Open-geometry sources are less restricted by recombination losses, however, given elevated total ion currents, the effects of space charge repulsion, limiting ion transmission are expected to be a more dominant factor than experienced by the field-free devices. It is also unknown if the limited reaction time provided within open-geometry sources will limit ion-molecule reactivity and the initial production of analyte ions. The primary focus of this chapter will be to verify through an empirical comparison which source configuration provides the best overall performance. To our knowledge a thorough head-to-head evaluation of the two APPI source designs has never been completed upon a single, modern MS platform.

## 2.2. Methods and Materials

### 2.2.1. Prototype Source Design

The first Photospray source developed by MDS Sciex was based upon a closed-geometry field-free design incorporating a stainless steel ion source block. A photo of an early prototype field-free APPI source developed by Robb and Bruins is provided in figure 2-1a.[51] This device was later used as the basis for the first-generation Photospray source design. These devices were intended to interface

with API 3000 and QStar series mass analyzers and were manufactured through the modification of a co-linear APCI source housing. The next generation of now modern platform API instruments utilizing a 4000 series MS interface required a redesign of all ion sources, including both the hybrid ESI/APCI and APPI sources. The current open-geometry Photospray design emerged as shown in figure 2-1b.

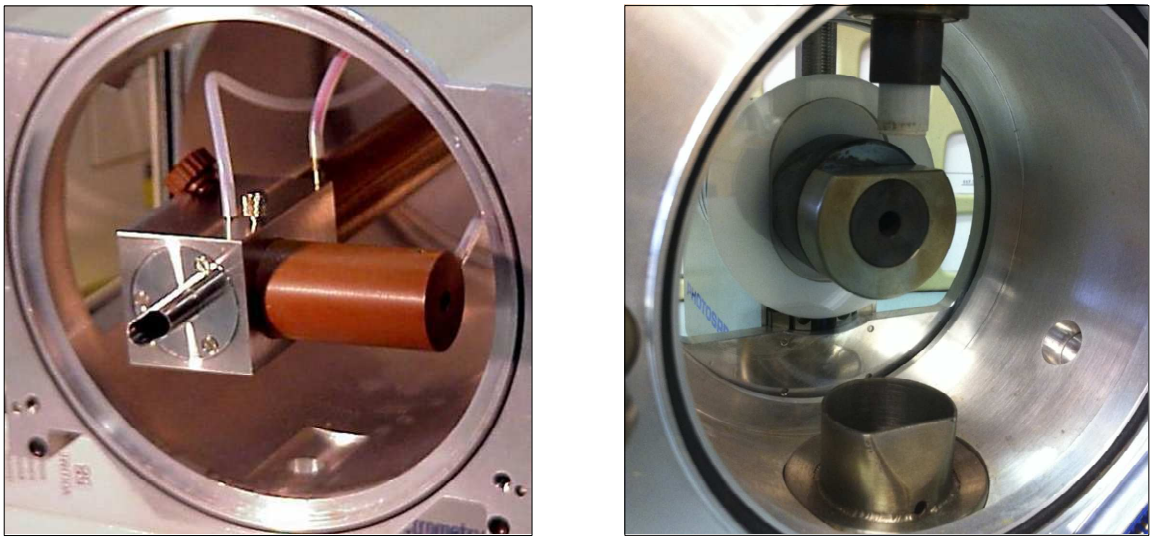

**Figure 2-1. a) Photo of first generation, closed geometry field-free Photospray source, designed for use on MDS/Sciex 3000 series and QStar mass spectrometers. b) Photo of a current open-geometry Photospray source designed for use on 4000 series API mass spectrometers.**

In order to establish a realistic comparison of the two APPI configurations, a stainless steel source block was machined in-house (University of British Columbia, BC, Canada) and mounted within a modified TurboV source housing. A photo and cross-sectional schematic of the new source block are provided in figure 2-2. The source block was engineered to mirror the dimensions and functionality of the first-generation source block as closely as possible. A 7-mm diameter conduit was provided for sample and ion transport. A second channel 3-mm in diameter was included orthogonally to the sample transport conduit allowing photons to irradiate the vapourized solvent plume. A third 1-mm diameter conduit was provided orthogonally to the photon channel to provide a means for introducing a flow of nitrogen lamp gas. Lamp gas is required to keep

the photon conduit clear of solvent and dopant vapour ensuring that both photon absorption and dopant ionization occur only within the sample transport conduit. Lamp gas was provided and regulated by an external source of high purity nitrogen boil. Nitrogen gas is assumed to be transparent to incident photons and should not directly affect photon flux.

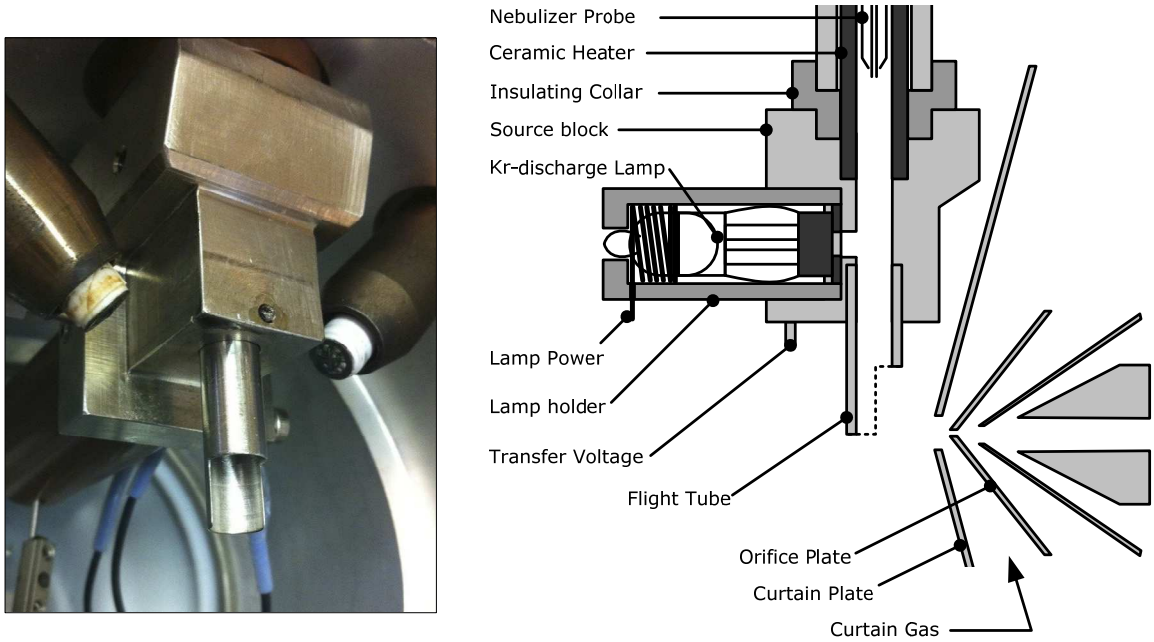


**Figure 2-2 a) Photo of the prototype closed-geometry, field-free APPI source built using a modified orthogonal Turbo V source housing, for use on 4000 series API mass spectrometers. b) Schematic diagram for the field-free APPI source.**

Modern TurboV ion sources are equipped for both ESI and APCI functionality. The prototype APPI source requires the use of the APCI heated nebulizer and sample nebulizing probe. As a result, the mass analyzer and control software identified the prototype source as an APCI heated nebulizer. The heated nebulizer and sample probe were operated as designed without modification. The APCI corona discharge needle was removed to accommodate the installation of the source block. Minor modifications were also made to the source housing in order to permit the application of external electrical and lamp gas provisions.

The source block was mounted directly to the output of the ceramic heated nebulizer using a custom machined Vespel adapting ring. The ring permitted electrical isolation of the source block allowing for the application of an additional offset transfer voltage, required to transmit ions into the mass analyzer. Offset Transfer voltage was provided using an external Stanford Research (Sunnyvale, CA) PS350 programmable DC high voltage supply. The dimensions of the source block were selected to accommodate positional adjustment in the x- (vertical) and y-axis (horizontal) directions. The source block position along the z axis (co-linear to the MS ion flight path) was fixed and could not be adjusted under the current design.

A Cathodeon Ltd. (Cambridge, England) PKS 100, Krypton photoionization discharge lamp was mounted to the source block using a custom machined Vespel lamp holder, held in place by two set screws. The lamp was mounted in a fixed position and was not independently adjustable in any direction (This differs from the modern open-geometry source configuration which allows for lamp position adjustment vertically). The PI lamp was operated in a continuous DC output mode, powered by a custom built HV power supply (Electrical Services, University of British Columbia, BC, Canada). Operating current was restricted to ~ 0.8 mA for all experiments, providing a constant source of photons at two wavelengths (123.6 nm and 116.5 nm) with radiant energies of 10.0 and 10.6 eV. The custom HV power supply could accommodate lamp operation up to a maximum current of 2.0 mA, however, a restricted setting was selected in order to increase lamp lifetime.

In the current design a removable stainless steel “flight tube” was mounted to the base of the ion source block providing an *extended field-free region*. The solvent plume and ions must travel the length of the flight tube before entering the open source environment. Flight tubes may be substituted interchangeably for tubes of varying dimensions in order to alter the length or restrictive geometry of the field free reaction region. The end of the flight tube was machined asymmetrically

with the intention of inducing an element of ion focusing to the ion transmission field that extends between the flight tube and the MS curtain plate. The shape of this end cut was arrived at intuitively rather than empirically and its contribution to ion transmission has not yet been characterized.

### 2.2.2. Instrumentation

All experiments were performed on an Applied Biosystems/MDS Sciex (Concord, ON, Canada) API 3200 triple quadrupole mass spectrometer. Source comparison experiments were conducted using a prototype Photospray source – functionally identical to commercially available APPI sources. Syagen Technologies provided an additional prototype Photomate APPI source including a proprietary high intensity Krypton discharge lamp and integrated RF power supply. Transfer voltage for the Photomate source was applied using an additional external Stanford Research (Sunnyvale, CA) PS350 programmable DC HV supply.

Flow injection experiments were performed using an integrated switching valve with a 10-μL sample loop. All analyses were carried out in Multiple Reaction Monitoring (MRM) mode with a scan time of 200 ms and a dwell time of 5 ms. MRM transitions for reserpine $[M+H]^+$ - 609 → 195, testosterone $[M+H]^+$ - 289 → 109, estradiol $[M-H_2O+H]^+$ - 255 → 159, progesterone $[M+H]^+$ - 315 → 97, cortisone - 361 → 163, acridine $[M+H]^+$ - 180.2 → 152.0 and fluoranthene $[M]^+$ - 202.2 → 152.2 were utilized. Optimized MS parameters (those independent of ion source performance) were maintained for all experiments.

Where applicable, HPLC grade methanol or a 50:50 mixture of methanol/DI water was infused without additives at 200 μL/min using a Harvard Apparatus (Holliston, MA) syringe pump, while toluene dopant was also infused at 20 μL/min using a second integrated syringe pump unless otherwise specified. Mobile phase and dopant streams were combined using a T-union prior to

entering the heated nebulizer probe. No evidence of immiscibility between the mobile phase and toluene dopant was observed under the MS operating conditions provided in Table 2-1. For steady-state analyte infusion experiments, a third external syringe pump was used to deliver samples through an additional T-union placed in-line with the mobile phase flow.

**Table 2-1. Performance evaluation: Optimized source conditions**

| Parameter | Prototype Source | PhotosprayTM |
|---|---|---|
| Transfer voltage | 1600 V | 700 V |
| Nebulizer temp | 300 $^{o}$C | 350 $^{o}$C |
| Nebulizer gas | 30 psi | 35 psi |
| Lamp gas | 0.3 L/min | 30 psi |
| Lamp current | 0.7 mA | n/a |
| Toluene dopant | 20 μL/min | 20 μL/min |
| Mobile Phase (MeOH) | 200 μL/min | 200 μL/min |
| Solvent additives | none | none |

### 2.2.3. Chemicals

Reserpine, fluoranthene, acridine, testosterone, estradiol, progesterone and cortisone were purchased from Sigma (St. Louis, MO), all as dry solids at no less than 97% purity. HPLC grade methanol and toluene were obtained from Fisher Scientific (Fair Lawn, NJ). Reserpine, fluoranthene, acridine solids were dissolved individually in pure methanol to produce 4.0, 1.0 and 1.0 mM stock solutions respectively. Each stock solution was further diluted in methanol to produce 0.4, 0.1 and 0.1 μM standard solutions. Testosterone, estradiol, progesterone and cortisone stock solutions were prepared by dissolving dried solids individually in methanol to produce 1-mg/mL standard samples. The standards were further diluted to 1-μg /mL in methanol. Additional dilutions were made as required. All chemicals were used as purchased without further purification.

All ion current measurements were performed using a model 427 current amplifier from Kiethley Instruments (Cleveland, OH) and a model TDS 340A digital oscilloscope from Tektronix (Wilsonville, OR). Ion current was collected for 50 seconds (average of 1000 samples) with a gain of $10^6$ V/A and a rise time of 300 ms unless otherwise stated. Additional passive low pass filtering was utilized at 10 Hz for all analyses. Current measurements were made by directly connecting the curtain and/or orifice plates to virtual ground through the current amplifier using a custom built BNC wiring harness. Voltage biases were applied to subsequent interface elements to ensure total ion collects using a custom variable voltage power supply. Normal interface voltages were supplied as needed in order to facilitate standard MS operation and ion transmission.

The measurement of ion current transmission beyond the orifice plate was performed using a modified skimmer cone and Q0 current collection cup. A factory skimmer cone was modified to accept a custom PEEK insulating sleeve permitting electrical isolation from the MS chassis. A BNC lead connection was made to the insulated skimmer cone through a modified positional locating pin. The lead was fed through a hermetic fitting in the chassis of the MS in order to facilitate the uninterrupted functioning of the MS vacuum system. A custom current collecting Faraday cup was mounted within QO and used to verify that all current passing through orifice plate was collected on the skimmer cone. The faraday cup was connected to the skimmer cone using a removable branched electrical connection. The faraday cup was removed from QO for all other measurements and standard MS functionality was verified.

## 2.3. Results and Discussion

### 2.3.1. Prototype Source Characterization

Prior to a formal evaluation of source performance, an investigation was completed into the source parameters affecting optimization of the prototype

APPI source using the infusion and flow injection of various standards. Gas flow rates, voltages and vapourizer temperature were independently optimized to provide maximum signal and stability under fixed solvent and analyte conditions (Table 2-1). Flow injection experiments were performed at a methanol flow rate of 200 μL/min to represent volumes suitable for conventional LC-MS methods.

#### 2.3.1.1. Nebulizer (GS1) and Lamp Gas Flow Rates

An optimized lamp gas flow rate of 0.3 L/min was routinely identified for the prototype source, across all experiments (data not shown). The peak analyte signal was observed at a sharp, localized lamp gas flow rate. Without a lamp gas, no analyte signal was observed, presumably the result of complete absorption of incident radiation within the photon introduction conduit. The signal also quickly diminished upon transition to higher gas flow rates, likely in response to the turbulent disruption of the laminar flow of the sample vapour plume. Verifying lamp gas optimization should be considered critical when optimizing any APPI-LC-MS method.

The optimization of the nebulizer gas flow rate (GS1) was somewhat more complicated. Increased nebulizer gas flow will have an effect on the surface temperature and average temperature across the cross-section of heated nebulizer. Vapourizer temperature is known to have a critical impact on the formation of reagent ions, protonated solvent clustering and subsequent ion-molecules interactions involving the analyte. Additionally, the nebulizer gas flow rate relates directly to the concentration, velocity and thus residence time of ions within the extended-field free ionization region. The nebulizer gas flow rate was generally optimized toward lower values, allowing for increased ion-molecule reactivity, while maximizing the gas-phase analyte neutral concentration. Below a minimum threshold of around 20 psi, analyte signal rapidly diminished, presumably the result of inefficient vapourization.

#### 2.3.1.2. Curtain Gas

The provision of a continuous flow of nitrogen curtain or drying gas, counter current to the ion path through the MS interface, is required to ensure that neutral compounds are not permitted to enter the sampling orifice. Ionized compounds under the influence of an external potential field are able to penetrate the curtain gas and may be sampled by the mass analyzer. Inevitably, the flow of curtain gas will also disrupt the transmission of ions to some determinable extent.

Figure 2-3 demonstrates the effect of curtain gas flow on the signals obtained from the infusion of a testosterone standard. Ion transmission was found to optimize at 10 psi, the minimum value permitted by the MS software interface. This translates to a mass flow rate of approximately 1.5 LPM (measured upstream from the curtain plate) – a portion of which will be drawn into the MS orifice, with the remainder passing through the curtain plate orifice. The signal was observed to drop steeply with increased curtain gas flow.

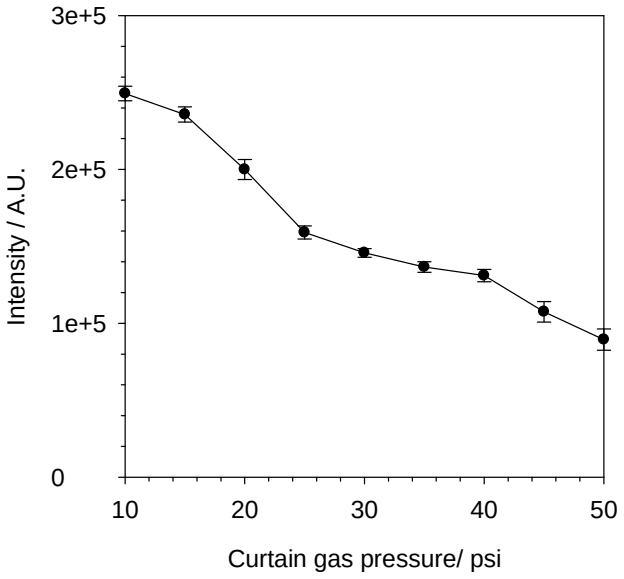


**Figure 2-3. Signal response obtained for the infusion of a 1 μg/mL testosterone standard as a function of curtain gas pressure for the field-free APPI source.**

The MS instrument manufacturer recommends a minimum 20 psi operating pressure which was shown to result in a roughly 20% decrease in ion

transmission with respect to the optimal value. This trade off appears reasonable provided that contamination of the MS interface is averted, however, the effects may vary for analyzers that utilize a larger orifice diameters or vacuum pumping capacity. It should be noted that the effect of curtain gas upon signals obtained using alternative sources such as ESI and APCI were much less severe (data not shown), in contrast to the APPI source. The exact cause for the significant discrepancy between ion sources is unknown; however, we speculate that it may result from an increased dependence on ion focusing within APPI sources.

#### 2.3.1.3. Heated Nebulizer Temperature

Maximum analyte signal was routinely obtained at nebulizer temperatures optimized 50-75$^{o}$C lower than empirically determined for the open-geometry Photospray source. This may be attributed to changes in gas flow dynamics as a result of the closed-geometry ion source block confining the nebulized solvent plume, decreasing heat exchange between the ceramic nebulizer, the sample and the ambient source environment. Figure 2-4 presents temperature measurements obtained with a thermocouple comparing the open-geometry and field-free APPI sources. Temperatures measured at both the outside surface of the nebulizer tower and at the outlet of the heated nebulizer are in excellent agreement between the open- and the field-free source designs. However, temperatures measured directly in front of the PI lamp, within the primary ionization regions for both sources, differ significantly. As a relevant example, at an instrument set point of 300$^{o}$C the temperature in the ionization region of the closed geometry source was measured to be 210$^{o}$C, compared to 112$^{o}$C for the open geometry source. The full implications of reduced nebulizer temperature requirements have yet to be evaluated, however, it could lead to reduced fragmentation and thus improved performance for the analysis of thermally labile compounds.

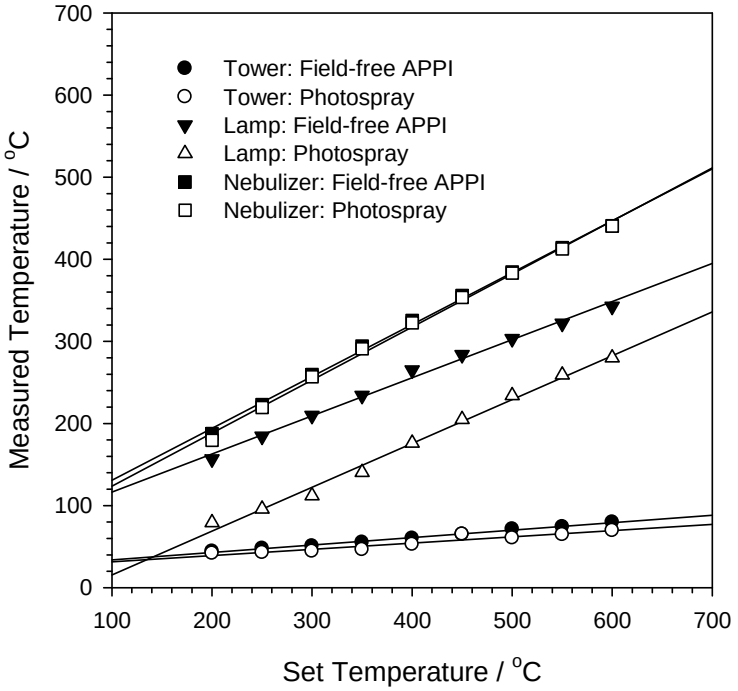


**Figure 2-4. In-source temperature measurements obtained as a function of set point temperature for both the Photospray and field-free APPI sources at various locations.**

### 2.3.1.4. Source Block Positioning and Transfer Voltage

Nebulizer and source block positioning was shown to be critical to the performance of the new source geometry, more so than observed for the open-geometry source. Ion transport from the source block into the sampling orifice requires application of an ion transfer voltage consistent with all APPI source designs. As ions exit the field-free region with a trajectory orthogonal to the MS ion flight path they are re-directed by the applied field spanning between the tongue of the transport tube and the curtain plate, focusing them ideally toward the orifice. The field strength required to most efficiently transmit ions was dependent on both the vertical position of the nebulizer relative to the orifice (Figure 2-5a) and the ion velocity as its exits the field-free region. Ion velocity at this point can be tied to the total laminar mass flow of gas exiting the transport tube. Efficient ion transfer from the field-free region to the MS orifice is thus

dependent on a vector sum of an ion's momentum in both the vertical (dependent on the nebulizer gas flow rate) and axial (dependent on its mobility within the transfer field) directions.

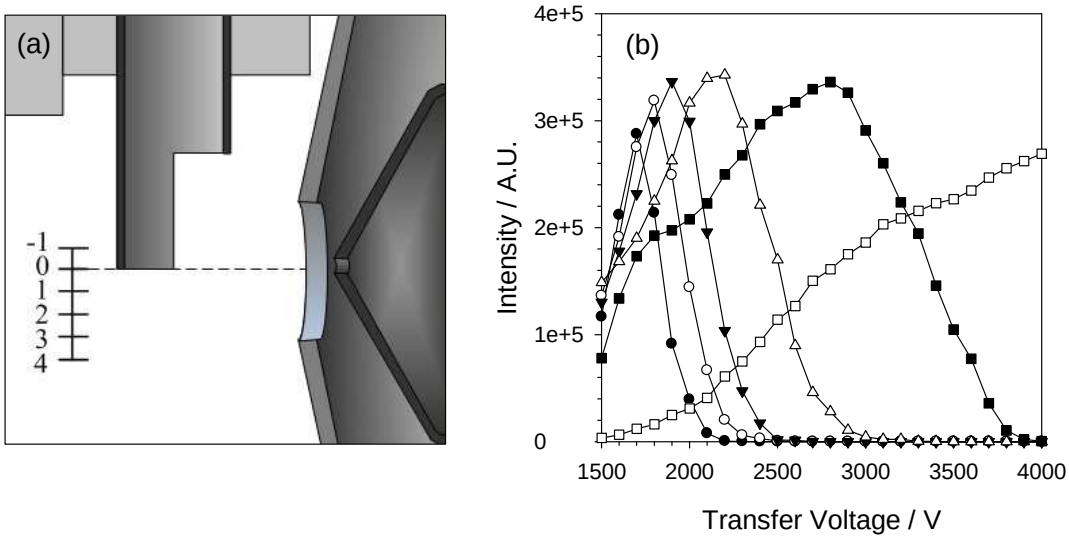


**Figure 2-5. Schematic depiction of source block position relative to the MS sampling orifice. b) XIC signal intensity for the flow injection of a 0.1 µM reserpine standard as a function of applied ion transfer voltage, at various source block vertical positions with a fixed volumetric flow rate. (●) -1 mm, (○) 0 mm, (▼) 1 mm, (△) 2 mm, (■) 3 mm, (□) 4 mm.**

No optimal vertical nebulizer position was identified but instead ion transmission was optimized through simultaneous adjustment of both nebulizer gas flow and transfer voltage at a variety of positions, the results of which are shown in Figure 2-5b. Maintaining a fixed volumetric flow rate, optimal signal was obtained at increasingly higher transfer voltages as the nebulizer was lowered relative to the sampling orifice. No single vertical position was found to demonstrate enhanced sensitivity. This observation was used to simplify source tuning as the vertical position was fixed for a given gas flow rate, with only adjustment of the field strength required.

As expected, horizontal nebulizer positioning was simplified due to the inherent symmetry of the ion flight path. Centering the nebulizer relative to the orifice axis was shown to provide optimal results for all experiment suggesting that this parameter could remain fixed in future designs (data not shown). It should also

be noted that there was no significant mass dependence observed with respect to optimal source positioning or transfer voltage requirements over the limited range of analytes tested.

#### 2.3.1.5. The Measurement of Ion Current

Table 2-2 summarizes the total ion current transfer efficiency for the closed-geometry APPI source. Ion current measurements demonstrating the transmission efficiency of the source for the infusion of only dopant, as well as the combined infusion of dopant and reverse phase LC solvents are provided. Current measurements were made at several locations, utilizing the curtain plate, orifice plate and skimmer cone as ion collecting electrodes, enabling the determination of the TIC generated and ultimately transferred into the mass analyzer. The factors affecting primary ionization within a custom-built photoionization detector have been previously considered by Robb et al. (2006)[58] Their device was designed to explore the factors affecting the generation of primary reagent ions within field-free APPI sources similar to the current closed-geometry design - also utilizing a standard DC krypton photoionization lamp. Parameters including lamp operating current, as well as both solvent and dopant flow rates were thoroughly characterized. Under dopant only conditions similar to those utilized during this study, the primary ion current measured in the direct vicinity of the photoionization lamp was determined to be on the order of 1 μA. This value is representative of the initial production of photoion current within the device, limiting the effects of time dependent ion loss processes. We take this figure to be roughly similar to the primary ion current expected within the proximity of the photoionization region of the prototype closed-geometry source.

*Dopant only case*

As shown in Table 2-2, for the dopant only case, the ion current ultimately collected at the MS curtain plate was measured to be around 11 nA, roughly 100 fold lower than the assumed primary ion current reported by Robb. The cause of

the large disparity is attributed to the effects of charge recombination that persist during transit through the extended field-free flight tube region. Ion current will continue to decrease until oppositely charged ions are finally separated at the outlet of the flight tube. In a study prior to their early characterization experiments, Robb et al. measured a TIC of 13 nA produced at the curtain plate of the first-generation, field-free APPI source under similar conditions.[53] This value is in close agreement with our measurements indicating that both early and current closed-geometry source designs generate roughly comparable overall ion production efficiencies. Table 2-2 also shows that under dopant only conditions, the amount of ion current that was able to penetrate the curtain gas and pass through the curtain plate aperture before finally striking the MS orifice plate was roughly 60% of TIC measured to exit the field-free region; the remaining 40% was lost to detection, presumably impacting the curtain plate.

*Dopant with combined solvent flow*

To verify the effect of solvent flow on the TIC, an additional supply of mobile phase solvents was introduced, providing typical conditions relevant to a real LC-MS workflow. Table 2-2 demonstrates that ion current measured at the curtain plate was reduced from 11 nA to around 7 nA upon the infusion of an additional solvent flow comprised of a 50:50 methanol/water mixture at a flow rate of 200 μL/min. The resulting loss of total ion current may be attributed to various proposed mechanisms,[58] however, for our purposes it is sufficient to conclude that a reduction in TIC is expected to coincide with an increase in solvent flow. At any rate, 7 nA represents the starting point from which ion current may be considered in terms of transmission efficiency under a set of reasonable LC-MS solvent conditions. An ion current of roughly 4 nA was measured at the orifice plate under conditions including the infusion of an additional LC solvent stream. This represents an approximately 40% reduction in TIC transferred through the curtain plate – similar to the dopant only example.

**Table 2-2. Transmission of ion current with the field-free APPI source**

| Electrode | Measured Current / nA | % Curtain ion currrent |
|---|---|---|
| Primary ionization[a] | 1000 | - |
| *Dopant only* | | |
| Curtain Plate | 11.3 | 100.0% |
| Orifice plate | 6.5 | 57.5% |
| *Dopant + mobile phase*[b] | | |
| Curtain plate | 7.3 | 100.0% |
| Orifice plate | 4.2 | 58.1% |
| Skimmer + Q0 | 0.6 | 8.2% |
| Skimmer | 0.5 | 6.7% |

*a - primary ion current assumed from reference [58]*
*b - 50:50 methanol/water + 0.05% formic acid at 200 μL/min*

Finally, the efficiency of ion transmission through the 250-micron diameter orifice plate nozzle was determined. The TIC passing through the orifice plate and striking the skimmer cone coupled to the faraday cup was measured to be about 0.6 nA - roughly 8% of the TIC exiting the source block. Without the faraday cup in place the current collected on the skimmer alone fell slightly to 0.5 nA. This infers that although imperfect, ion collection upon the skimmer cone alone is at least reasonably representative of the current transmitted through the orifice, even when an ion stopping bias voltage is not provided down stream within QO.

Although the reduction in ion transmission through the orifice nozzle does represent a substantial loss, the overall efficiency does appear at face value to be an improvement over the efficiency reported for an ESI source. Utilizing a mass analyzer with an even larger, 300-micron orifice diameter, Zook and Bruins reported that the primary ion current produced by their ESI source was around 50 nA[236] - derived from the infusion of a quaternary ammonium salt standard (50 μM at solution at 5 μL/min). Roughly 90% of the ion current, leaving the ESI nebulizer probe, was determined to arrive at the curtain plate in this system. Since charge recombination is not expected to be a significant factor within ESI sources, the efficiency of transport through the open source environment should presumably be quite high. In light of the divergent nature of the electrospray ion

trajectory, however, only around 1% of that current was measured to pass through the curtain plate, striking the grounded orifice plate. No explicit ion focusing elements are typically incorporated within standard ESI sources. A further order-of-magnitude was lost during transit through the orifice plate, ultimately arriving at the skimmer cone, within the analyzer vacuum region. Finally, only about 12 pA of ion current was passed through the skimmer to the first quadrupole ion guides. Transmission efficiency will be dependent on many parameters related to the design of the mass analyzer, however, suffice to say, roughly 10 fold more ion current was detected within the vacuum environment for the orthogonal, field-free APPI source relative to their ESI based system under realistic operating conditions. The take away message from this assessment is simply that ion current produced within the closed-geometry APPI source and ultimately transferred into the mass analyzer is at least comparable if not superior to what may be expected for a typical ESI-MS system. It remains to be seen, however, the degree to which the optimization of ion source geometry may further affect transmission efficiency for the closed-geometry source.

From here we are left to postulate the root cause for the observed ion transmission loss through the curtain and orifice plates. We propose that space charge limitations may play a role in the restriction of ion transmission. Alternatively, we may also propose that ion transmission could be limited simply by inefficient ion focusing and may be in-turn improved through the geometric optimization of source block and flight tube. These possibilities will be addressed in further detail within the source characterization section.

### 2.3.2. Head-to-head Performance Evaluation

#### 2.3.2.1. Open-geometry Photospray Source Comparison

The prototype source takes advantage of ion-molecule reaction chemistry identical to the commercial Photospray source. As a result, full-scan spectra

obtained through direct infusion of dopant, solvent and various analyte standards consistently presented identical spectral background species differing only by enhanced ion currents and varying relative ion intensities (data not shown). The magnitude of enhancement toward analyte sensitivity was verified by flow injection analysis. The relative performance for both sources using single component injections of reserpine, acridine and fluoranthene standards was determined. Figure 2-6 presents XIC traces obtained using both sources for 4 consecutive injections of a reserpine standard, demonstrating reproducibility and dramatic sensitivity enhancement. The closed-geometry source was shown to significantly out perform the commercial Photospray system by factors of 22, 13 and 6 times for each analyte respectively. This improvement was reproducible on a day-to-day basis, however, may vary based upon the selection of user optimizable parameters. As such, these values can be used to gauge the potential for order-of-magnitude scale improvement rather than adopted as figures-of-merit. The root of this enhancement is believed to be derived from the inclusion of an extended field-free reaction zone within the closed-geometry source design.

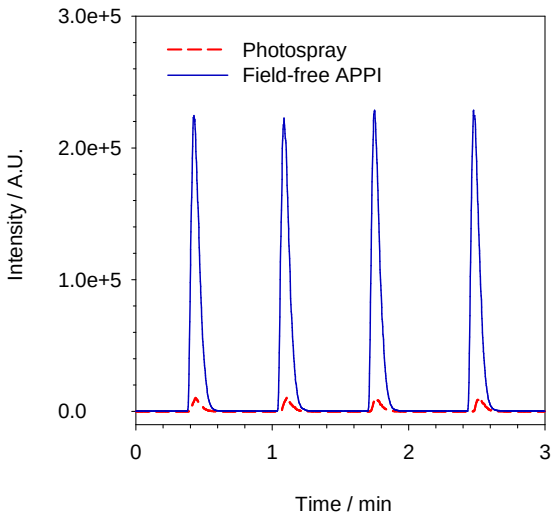


**Figure 2-6 XIC signal intensities obtained for 4 consecutive 10 µL injections of reserpine standard. Results compare the response for the Photospray source relative to the field-free APPI source.**

The ion-molecule reaction region within the open-geometry source is limited to the vertical distance between the top of the irradiation conduit and the sampling orifice - a distance of roughly 3-5 mm. All transfer of charge from dopant reagent ions to the analyte must occur during transit through this region prior to sampling at the MS orifice. Both the primary ionization of dopant and formation of protonated ion clusters are known to be very fast reactions at atmospheric pressure, attaining equilibrium within a few microseconds. The reagent ion population quickly reaches an equilibrium state within the vicinity of the region irradiated by the discharge lamp. The step limiting overall efficiency in this scenario becomes the transfer of a proton or charge from a reagent ion species to the analyte. Since the reagent ion population is assumed to remain in excess for a limited transmission length, the time provided for reactions to proceed between reagent ions and analyte neutrals ultimately limits analyte ionization efficiency.

For the prototype closed-geometry source configuration described thus far, the combined ion source block and transfer tube flight path extends the reaction zone by approximately 25 mm relative to the open geometry source. Within this region ion loss processes persist, however, the population of analyte ions is allowed to reach an equilibrium state. The results demonstrate that enhanced sensitivity for a particular analyte may be directly tied to the provision of an extended field-free reaction region; however, the underlying mechanisms behind this effect are still unclear.

#### 2.3.2.2. Comparison with a Prototype Photomate Source

The performance comparison study was extended to include an additional prototype Photomate APPI source. Although never commercially manufactured, Syagen Technologies developed a prototype open-geometry source intended for use on 4000 series AB Sciex mass analyzers. The device, pictured in figure 2-7, exploited a modified TurboV ion source housing, facilitating the use of the same

heated nebulizer and sample probe included for APCI applications. A proprietary, high radiant output, Krypton discharge lamp was utilized in this design, including an external RF power supply module. The manufacturer included a high output light source with the intention of increasing primary ionization efficiency through enhanced photon flux. We hypothesize that this may pay dividends for ionization through the direct photoionization mechanism, however, according to theory this is little different than increasing primary ionization through increasing the dopant flow rate.

**Figure 2-7. Photo of prototype open-geometry Photomate source, designed for use on MDS/Sciex 4000 series mass spectrometers.**

Figure 2-8 provides MRM XIC traces demonstrating the relative sensitivity obtained for the Photospray, Photomate and prototype closed-geometry APPI sources, for cortisone and progesterone single component standards introduced by flow injection. As anticipated, the relative performance of the Photospray and Photomate sources were determined to be very similar, given their analogous geometries and functionality. Although the Photomate device was only a prototype design and no assurances can be made that the device was fully optimized, we saw no evidence to suggest that the inclusion of a high output RF photon source provides any significant advantage over standard DC Krypton discharge photoionization lamps. The closed-geometry source on the other

hand, was found to provide significantly higher analyte sensitivity than either the Photospray or Photomate sources, presumably resulting from the provision of an extended field-free reaction region.

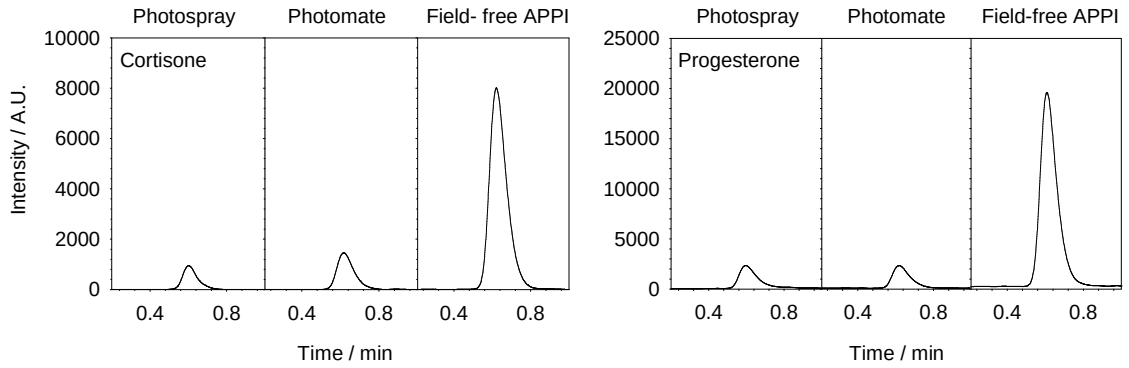


**Figure 2-8. XIC signals obtained for the flow injection of 10 ng/mL Cortisone (left) and Progesterone (right) standards demonstrating the head-to-head performance of the prototype Photomate source relative to both the commercial Photospray and prototype field-free APPI sources.**

Figure 2-9 provides ion current measurements, obtained as a function of toluene dopant flow rate, with the additional continuous infusion of a 50:50 methanol/water make up flow at 200 μL/min. Ion current was measured using a wiring harness connecting both the curtain and orifice plates directly to virtual ground through the current amplifier, in order to ensure efficient total ion collection. Figure 2-9a demonstrates the affect of the increased lamp power provided by the Photomate source; at a dopant flow rate of 20 μL/min, nearly 50 and 150 times more total ion current was generated relative to the Photospray and field-free APPI sources respectively. The obvious curvature displayed in the Photomate data indicates that ion recombination loss processes become a significant factor at such elevated ion currents, regardless of the near-immediate charge separation provided within the primary ionization region open-geometry source designs. Figure 2-9b presents the same data scaled to focus on the results obtained for the Photospray and close-geometry sources. The Photospray data demonstrates a nearly linear increase in TIC with dopant flow rate indicating that the effects of recombination have been drastically reduced

within this design, at least under some constrained LC-MS conditions. The curvature displayed in the results obtained for the closed-geometry source approaches an asymptotic limit, demonstrating that charge recombination is in fact a significant factor for the field-free design. Overall, the field-free source was determined to deliver roughly 1/3 the total ion current produced by open-geometry Photospray source.

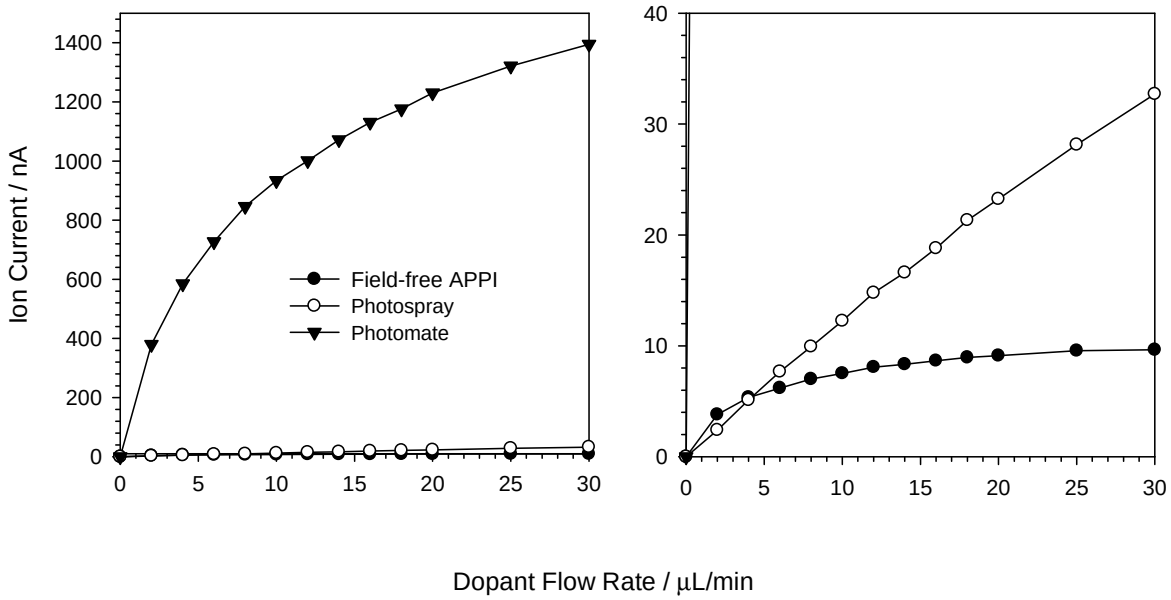


**Figure 2-9. Ion current data collected for the Photomate, Photospray and field-free APPI sources as a function of toluene dopant flow rate. b) Scale adjusted to isolate ion current data obtained for the Photospray and field-free APPI sources.**

In spite of a reduced total ion current output, analytical results have clearly demonstrated that analyte sensitivity remains enhanced given the provision of a field-free reaction zone. Under the same conditions, it is interesting to note that transmitted total ion currents of 0.8 and 2.0 nA were measured to reach the orifice plate for the Photospray and field-free sources respectively (data not shown). This result suggests that regardless of the elevated TIC demonstrated by the open-geometry source, the field-free geometry is in fact more effective at transferring the ion current through the curtain plate. We may presume this to be the result of improved ion focusing, however, there is also the possibility that the

effects of space charge repulsion within the field-free source are suppressed by reducing the total ion current generated.

Figure 2-10a explores the effect of dopant flow rate on the ion current collected separately at both the curtain and orifice plates, for the field-free source. Both trends are indicative of a scenario where charge recombination is likely the dominant factor limiting ion current, leading to an increasingly regressive slope with increased primary ionization. The data for the current collected at the orifice plate, however, is shown to reach an asymptotic limit while the curtain plate ion current continues to rise, although with a diminishing returns.

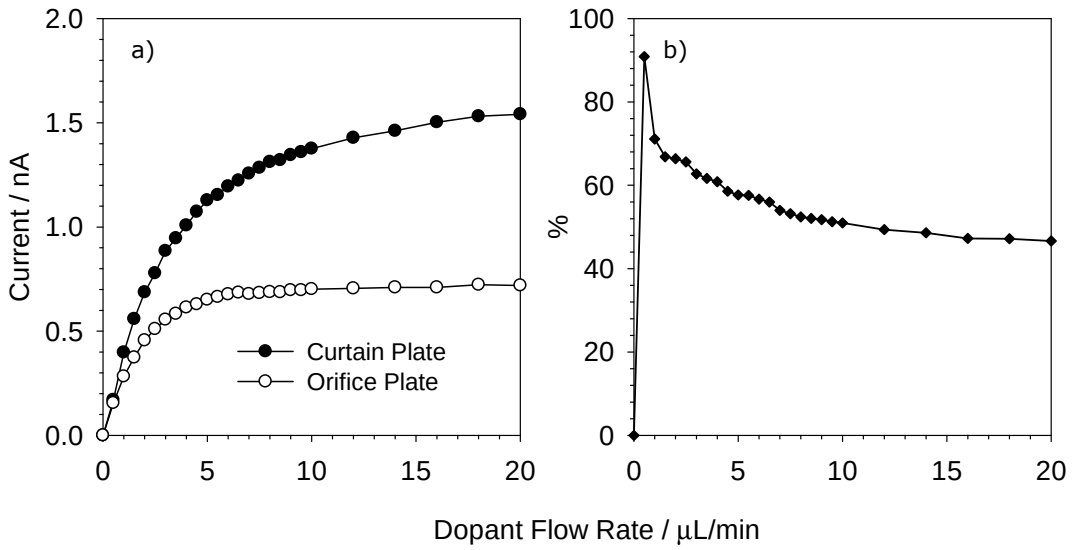


**Figure 2-10. a) Ion current data collected upon the curtain plate and orifice plates as a function of toluene dopant flow rate. b) Orifice plate ion current transmission displayed as a fraction of the total ion current reaching the curtain plate, as a function of dopant flow rate. Methanol mobile phase supplied at 200 µL/min.**

Figure 2-10b displays the percentage of ion current measured at the orifice plate as a fraction of the ion current measured at the curtain plate. The results suggest that the efficiency of ion transfer through the curtain plate decreases with increased initial ion current. Assuming an even distribution of charge across the ionization transfer conduit, we may take this as evidence to suggest that space charge repulsion may be a contributing factor to the limit observed upon ion

transmission through the curtain plate. Should ion focusing alone be responsible for transmission efficiency, we would expect the relative transmission to the curtain and orifice plates to scale proportionally.

To summarize, we have yet to fully explore the role of space charge limitations on the transmission of ion current through the curtain or orifice plates, and as such we concede that only the first step has been taken toward a complete understanding of ion transfer efficiency. Much would be gained from a thorough inspection of all parameters governing ion transmission limitations. All that can truly be concluded at this point is that increased ion current does not translate directly to increased sensitivity for a particular analyte.

### 2.3.3. Addressing Source Geometry

#### 2.3.3.1. Length of the Extended Field-free Region

We now extend our investigation to look deeper at the effect of the extended field-free region on attainable sensitivity for three alternative length transport tubes. Figure 2-11 compares XIC traces obtained for the flow injection for a range of compounds, using flight transport tubes 15, 20 and 25-mm in length. The vertical placement of the heated nebulizer was correspondingly adjusted to maintain a consistent flight tube exit position relative to the MS sampling orifice. This ensured an identical ion transport field was preserved between configurations resulting in an effective change in only the length of the field-free region and therefore reaction time. Signals for reserpine and acridine, ionized through proton transfer, exhibited an average of approximately 20% improvement in sensitivity for every 5 mm increase in transport length, establishing a clear trend demonstrating sensitivity enhancement through increased ion transit time. The existing source housing would not permit clearance for flight tubes longer than 25-mm, however, additional linear improvement is expected should the source be again re-engineered to accommodate a longer field-free flight transport

region. Practical limits to sensitivity for analytes ionized through proton transfer are at this point unknown, provided an excess population of reagent ions is maintained.

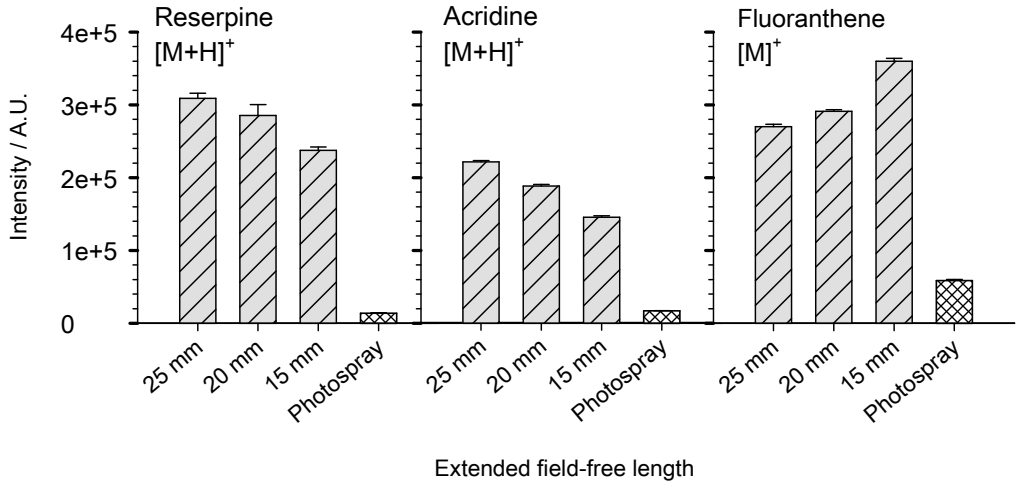


**Figure 2-11. XIC signal intensities obtained as a function of flight tube length for 3 standard analytes introduced through flow injection. Toluene dopant was supplied a 20 μL/min for each trial.**

Conversely, the results for non-polar fluoranthene, ionized through charge exchange, exhibited the opposite trend with sensitivity steadily decreasing as the transport region was lengthened. We believe this reverse trend to be connected to the ionization chemistry involved with use of toluene as a dopant for charge exchange in the presence of organic reverse phase solvents (i.e. methanol or acetonitrile). Toluene photoions have been shown to react, often to completion, in the presence of excess methanol, losing all charge to the formation of protonated solvent clusters. The result is a significant depletion in the population of dopant reagent ions available to participate in the charge exchange pathway. We propose this causes an imbalance in the competition between the rate of analyte ion production and charge recombination resulting in a net loss of analyte ion current as transit length is increased. It is expected that use of alternatively established dopant candidates such as chlorobenzene, bromobenzene or anisole would provide a stable population of dopant reagent ions, even in the presence of methanol or acetonitrile.[142,237] Providing an excess supply of dopant reagent

ions should result in a reversal of the observed trend for the fluoranthene charge exchange mechanism, once again leading to improved sensitivity as the field-free reaction region is extended. This hypothesis was confirmed through a series of follow-up experiments - the details of which fall outside the realm of source comparison and are instead located in appendix A. To date, toluene is the most commonly utilized dopant for APPI applications. It is instructive to recognize that careful selection of a suitable dopant for each application is critical when optimizing an APPI method.

Moving forward, the effect of flight tube length on the total ion current produced by the field-free source was considered. Figure 2-12 provides ion current data measured at the curtain plate for source block configurations utilizing a variety of flight tube lengths, at three dopant flow rates. The results demonstrate a clear non-linear decrease in ion current production with increased reaction time - coinciding well with theory governing the rate of ion recombination expected for a field-free source environment. Further, the observed trend is expected to continue if extended to even longer flight tubes provided that no other loss processes become significant. The current data fits a second order power trend with excellent agreement, displaying an $R^2$ correlation factor of no less than 0.998 for the range of dopant flow rates tested.

Figure 2-12b presents the isolated case for a 20-µL/min dopant flow rate, representative of a typical LC-MS workflow. Here, ion current was measured to drop roughly 50% while moving from a 15-mm tube to a 25-mm tube. Forecasting through regression, the TIC is expected to diminish asymptotically approaching zero current as the collision frequency decreases with the shrinking population of charge carriers.

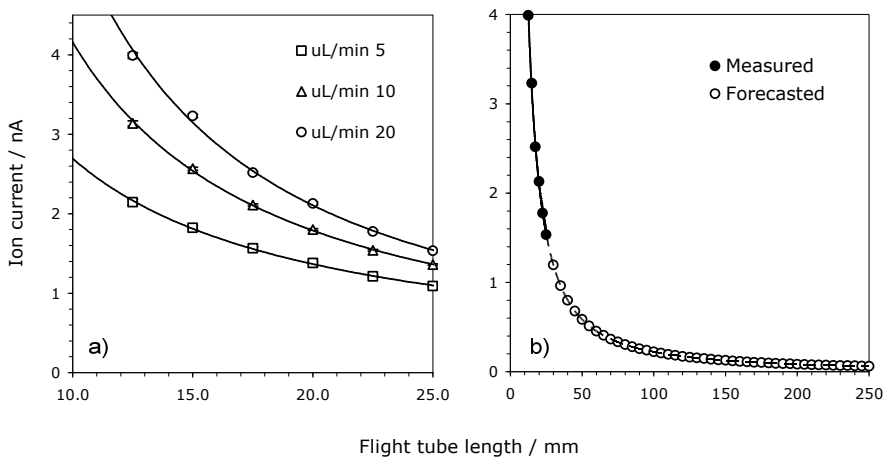


**Figure 2-12. a) Ion current data collected at the curtain plate, demonstrating the effect of flight tube length upon total ion current transmission. b) Extension of the ion current data collected (at 20 μL/min) to forecast or predict the total ion current anticipated for increasingly longer flight tubes.**

If we can conclude that analyte ion production is expected to increase linearly by 20% with every 5-mm increase in the length of the reaction zone, then we may infer that in order to double sensitivity, a flight tube length of roughly 50 mm would be required - provided that the reagent ion current remains in excess. Our predictions suggest that the TIC should decrease by roughly an additional 60% moving from a 25 to a 50 mm flight tube, yielding approximately 0.5 nA of current. At this level we may assume that suitable population of reagent ions is maintained.

In a more dramatic prediction, a flight tube length of 250 mm would be required to generate an order-of-magnitude scale increase in analyte ion yield over the present configuration. At this length, sub 60 pA of total ion current is expected. Reagent ions represent a fraction of the total ion current, thus it is possible that the concentration of reagent ion species will no longer be available in excess. The population of reagent ions provided for proton transfer reactions includes predominantly protonated solvent clusters ($S_nH^+$) ranging in concentration, co-ordination and acidity. At this time, determining the relative concentrations of all proton transfer reagent species present within the source is a difficult task. Most solvent clusters are dissociated within the MS interface and are therefore lost to

detection, complicating characterization. Additionally, as the transit length increases and the ion density decreases, the contribution of ion diffusion losses to the reaction conduit walls may become a significant factor. In the absence of an accurate measure of the total reagent ion current, and only a limited understanding of the loss processes involved, evaluating the benefits of increasingly longer flight tube length is best left to future empirical evaluation.

#### 2.3.3.2. Tapered Flight Tube Diameter

The use of tapered, conical shaped flight tubes was also explored as a means to further enhance ion transmission efficiency. The goal was to evaluate performance while adapting a series of flight tubes with increasingly restricted cross-sectional areas (CSA), designed with the intention of confining the effluent of the flight tube to a reduced profile, thereby closely matching the diameter of the curtain plate orifice. Several conical shaped flight tubes, pictured in figure 2-13a, were manufactured in house. The conical tubes were designed to restrict the CSA of the exit profile to 1/2, 1/3 and 1/4 the CSA of an un-altered flight tube with straight walls. The total length of the flight tubes and the shape of the end-cut profile were maintained to provide the closest possible comparison to the original, straight-walled flight tube design. A schematic of the restricted profile flight tube is provided in figure 2-13b.

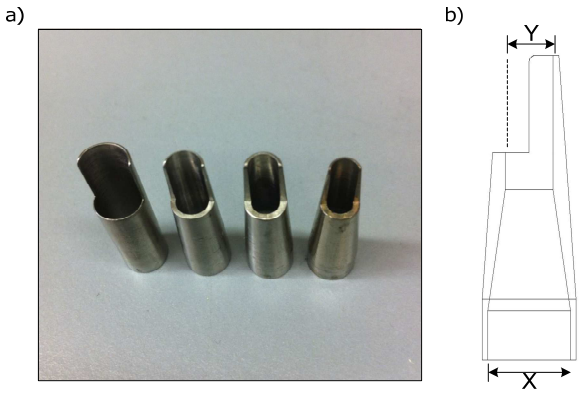


**Figure 2-13. a) Photo of the straight walled flight tube (left) with 3 tapered flight tubes presenting increasingly restricted cross sectional areas. b) Schematic for a tapered flight tube demonstrating a reduction from diameter "X" to diameter "Y".**

Figure 2-14 provides XIC signals obtained for the flow injection of a testosterone standard using each of the restricted flight tubes. Sensitivity was established to increase steadily yet modestly, with decreased flight tube diameter. The best results were obtained for the flight tube with the greatest restriction, providing roughly 50% improved ion transmission over the straight-walled flight tube profile. Limits to enhanced sensitivity through decreased flight tube profile have yet to be established

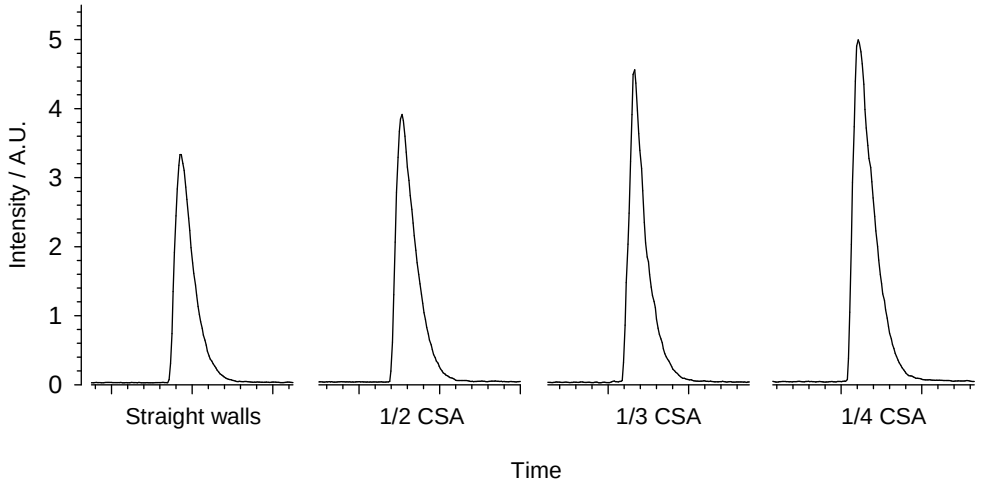


**Figure 2-14. XIC signals obtained for the flow injection of a 10 ng/mL testosterone standard, using flight tubes of increasingly restricted cross sectional area (CSA).**

The exact mechanisms contributing to the observed enhancement in analyte sensitivity have yet to be established. In a separate preliminary study, total ion current reaching both the curtain and orifice plates was observed to diminish with decreased flight tube cross sectional area (data not shown). This would suggest that improved analyte sensitivity may not be the result of enhanced ion focusing, but rather another mechanism entirely. Future efforts could continue to explore the role of space charge limitations upon ion transmission through the curtain and orifice plates as function of the flight tube CSA. Regardless, the results indicate that further performance improvement may be attainable through continued re-design of the ion source block and flight tube geometry.

## 2.4. Conclusions

This chapter provided an introduction to an orthogonal geometry, field-free APPI source that draws heavily upon design principles presented by early generation co-linear sources, however, also builds upon many of the advantages afforded by modern, open-geometry ion sources. The new ion source incorporates a closed-geometry stainless steel source block intended to enhance sensitivity through the provision of an extended field-free region. This allows for more efficient exploitation of the dopant reagent chemistry now considered critical to APPI performance.

The device was characterized and its performance further evaluated through head-to-head comparison with a modern, commercially available Photospray source, as well as a prototype open-geometry Photomate source. To our knowledge this has been the first comprehensive evaluation of the relative capabilities of both open- and closed APPI design geometries on a modern MS platform. The closed-geometry, field-free source design was demonstrated to out-perform both of the established open-geometry sources, at times providing order-of-magnitude scale improvement in sensitivity. Although this study was limited to a comparison against only two APPI sources, we have no reason to believe that comparable results would not be recognized against all modern open-geometry sources, lacking an extended field-free reaction region.

A cursory examination of the effect of design geometry on source performance has demonstrated that significant enhancement to sensitivity may still be attainable through continued refinement of the source block geometry. This presents an obvious avenue for continued research as we have yet to establish true limits to technique performance based on the optimization of primary reagent ion generation, ion-molecule reaction chemistry and ion transmission efficiency. The next step in this line of research was to evaluate the new source design against the performance of other common ion sources such as ESI and APCI.

This was accomplished through the analysis of real-samples of current interest to the clinical field, including samples containing complex biological or environmental matrices.

# Chapter 3. Evaluating Source Performance Relative to ESI and APCI Through the Analysis of Clinically and Environmentally Relevant Sample Types

In the previous chapter we demonstrated an advantage provided by the closed-geometry, field-free APPI source design over the open-geometry APPI sources commercially available today. Due largely to poor overall performance, modern open-geometry APPI sources often offer little to no advantage over the alternative ionization methods. As a result, the widespread acceptance of photoionization has been limited and clinical LC-MS methods rely heavily upon ESI and APCI instead. This chapter will continue to evaluate the performance of the closed-geometry APPI source design relative to these alternative ionization methods, using practical LC-MS workflows to establish the potential of the technique.

## 3.1. Introduction

As discussed previously, modern APPI has been adopted for the analysis of an extensive range of compound classes for a variety of reasons. The greatest sensitivity advantage appears to be for the analysis of low polarity compounds including PAHs, pesticides and flame-retardants, however, the analysis of oil and petroleum samples is perhaps the fastest growing area of application. Although in some instances a limited sensitivity advantage may be provided, a decreased susceptibility to matrix ion suppression has positioned APPI as a candidate for the analysis of clinically and environmentally important samples. Such applications include the screening of complex biological fluids for steroids and their metabolites, vitamins and nutrients. Coupled with extensive sample modification and/or cleanup, however, most clinical and environmental assays are performed using ESI or APCI - sacrificing time and throughput to satisfy

lower detection limit requirements, not afforded by modern commercial open-geometry APPI sources.

APPI is often targeted as suitable for only a niche range of compounds of low proton affinity, despite demonstrations to the contrary indicating the technique to be readily applicable to the analysis of both polar and non-polar compounds.[238] The ability to ionize polar compounds through proton transfer as well as non-polar compounds through charge exchange, positions APPI as the most universal atmospheric pressure ionization method. In a 2005 study, Cai et al. employed a generic LC-MS workflow to examine a panel of 201 pharmaceutical drug candidates, using APPI, APCI and ESI.[65] The APPI source was shown to effectively ionize 98% of the drug candidates surveyed, with APCI and ESI following behind at 91% respectively. Of the drugs subject to the study, APPI was also found to have the highest overall ionization efficiency of the three sources. Interestingly, the study was conducted using an AB/Sciex API 3000 mass analyzer equipped with a first-generation, closed-geometry Photospray source, including an extended field-free reaction zone. As such, we expect that comparable or even superior relative performance should be provided by the new field-free APPI source. Demonstrating relative APPI performance for the analysis of a broad range of compounds, using real analytical workflows will be the next step toward advancing technique acceptance.

### 3.1.1. Relevant Clinical and Environmental Sample Types

#### 3.1.1.1. Steroidal Analyses

Steroids comprise a class of bioactive compounds that consist of 4 conjoined cycloalkane rings, containing at least 17 carbons atoms in a fused gonane structure, shown in figure 3-1a. Additional functional groups attached to the steroidal backbone, as well as the oxidation state of the basic ring structures help

to define the compound's reactivity and functionality. Most steroids include alkane functional groups at carbon positions 10, 13 and 17. Cholesterol, shown in figure 3-1b, is an example of a basic precursor, waxy steroid alcohol, produced predominantly within the liver and utilized by the body in the production of hundreds of steroidal compounds within the adrenal glands or reproductive organs. Major clinical steroid classes include Progestogens, Estrogens, Androgens and Corticoids (figures 3-1c-f). Each is produced and regulated through metabolism and ultimately secreted from the body. Clinical scientists routinely use the determination of steroid levels within biological fluids like serum, plasma, urine and saliva, as a powerful diagnostic tool for the identification of deficiencies, irregularities and disease.

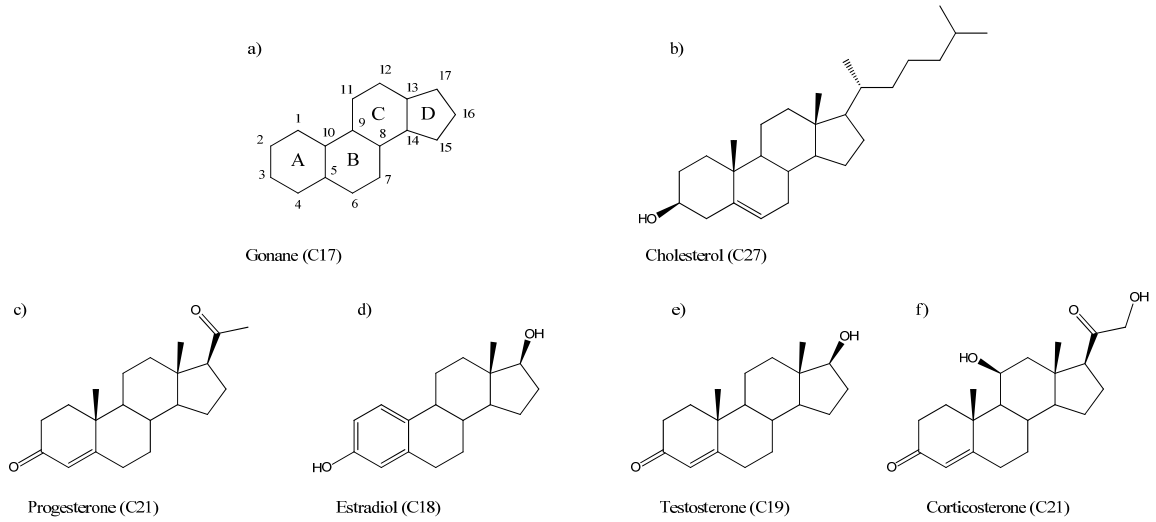


**Figure 3-1. Structures for a) gonane, b) cholesterol (containing 27 carbons), c) progesterone (a progestagen containing 21 carbons), d) estrogens (and estrogen containing 18 carbons), e) testosterone (an androgens containing 19 carbons) and f) coritcosterone (a corticoids containing 21 carbons).**

Historically, steroidal determinations have been performed using either tailored bioassays[239-241] or GC-MS,[242-244] however, both methods have considerable limitations. Immunoassays suffer from cross-reactivity, thus may lack selectivity, while GC-MS analysis is only amenable to highly volatile compounds, which are not thermally labile. Time-consuming derivatization methods are often required in order to enhance GC-MS performance, however, these too introduce a measure of uncertainty, while appreciably complicating sample preparation.[243,245,246] LC-

MS has been identified as possessing the greatest potential for improving the analysis of steroids, as well as their polar metabolites, taking advantage of the atmospheric pressure interface to provide high introduction efficiency for liquid samples with minimal preparation requirements.[247] Questions still remain, however, as to which ionization method is most suitable for routine clinical LC-MS workflows. Highly charged, polar steroid metabolites tend to be efficiently ionized by ESI, however, neutral steroids possessing limited acidic or basic functionalities continue to present a significant analytical challenge. As a result, it is inherently desirable to explore alternative ionization methods in order to identify and quantify neutral steroids, without the requirement for extensive sample cleanup or derivatization.

Although Electrospray is presently the most common source used for the general analysis of steroid neutrals and associated metabolites, APCI has garnered significant attention as an alternative candidate. Chemical ionization has been shown to demonstrate reduced ion suppression in the presence of complex biological matrices.[248-250] Co-eluting matrix elements are known to have a potentially drastic impact on ESI performance, disrupting the vapourization process, in-turn limiting ionization efficiency.[250] As a result, extensive sample preparation is required, often including: protein precipitation, liquid-liquid or solid phase extraction methods and time consuming chromatographic separations. Although the use of any one ionization source will never entirely obviate the need for sample preparation, minimizing the demand for extensive sample cleanup or modification will inevitable pay dividends toward sample throughput, as well as assay precision and accuracy.

Photoionization, analogous to APCI, has been shown to be less susceptible to ion suppression in comparison to ESI.[140,251] Both APCI and APPI methods employ a heated nebulizer to generate aerosol vapour from an LC eluent stream. In both instances, analyte ions are produced through a series of post-vapourization, gas-phase ion-molecule interactions. In contrast, the electrospray

ionization process is heavily dependent upon the electronic properties and volatility of the mobile phase composition and the ability to relinquish pre-ionized analyte species from charged solvent droplets into the source environment. Disruption of the vapourization process by involatile matrix components can be tied directly to a reduction in ESI efficiency. Matrix effects in APPI are thought to be attributed to gas-phase reactions, resulting in a depletion of the reagent ion population through interaction with interfering matrix components. These processes tend to have a less prominent impact on ionization efficiency than observed for ESI. Reduced susceptibility to matrix effects is a significant and often overlooked advantage afforded by APPI, particularly for the analysis of complex clinical samples, and high throughput workflows.

Photoionization has been cited frequently as a legitimate candidate for the analysis of neutral steroids throughout early development of the technique.[51,56,82] These reports focus upon use of the first generation, closed-geometry Photospray sources, providing an extended field-free reaction zone. This recognized advantage provided by the early field-free APPI sources would appear to have been lost, however, when transitioned to the modern, open-geometry orthogonal source designs.[60]

#### 3.1.1.2. Vitamin D Screening

Vitamin D is a non-polar, fat-soluble secosteroid required to stimulate the adsorption of calcium and phosphate within the intestines. It is also necessary to maintain calcium levels needed to facilitate bone growth. Of its two forms, shown in figure 3-2, Vitamin D2 (ergocalciferol) can be obtained through dietary consumption, while vitamin D3 (cholecalciferol) is produced in the skin through the absorption of UV light, typically from exposure to the sun. Clinically speaking, 25-OH-vitamin D2 and D3 metabolites are produced from their respective parent Vitamin D precursors within the liver.[252,253] 25-OH-vitamin D is

further metabolized in the kidneys to produce 1,25-$(OH)_2$-vitamin D2 and D3. The doubly hydroxylated forms of vitamin D are the most biologically active and are the most clinically significant. Unfortunately, the levels observed for these metabolites, even within healthy biological fluids, are typically quite low - often 500 to 1000 times lower in concentration than either of the mono-hydroxylated Vitamin D metabolites. Consequently, clinicians tend to rely upon the determination of 25-OH-Vitamin D2 and D3 to act as proxies for levels of both the parent vitamin D compounds and the doubly hydroxylated metabolites within biological fluids. Assays determining the parent vitamin D compounds are of limited relevance from a clinical standpoint, however, many processed food products are fortified with vitamin D, and thus rapid food-screening protocols are widely applicable.

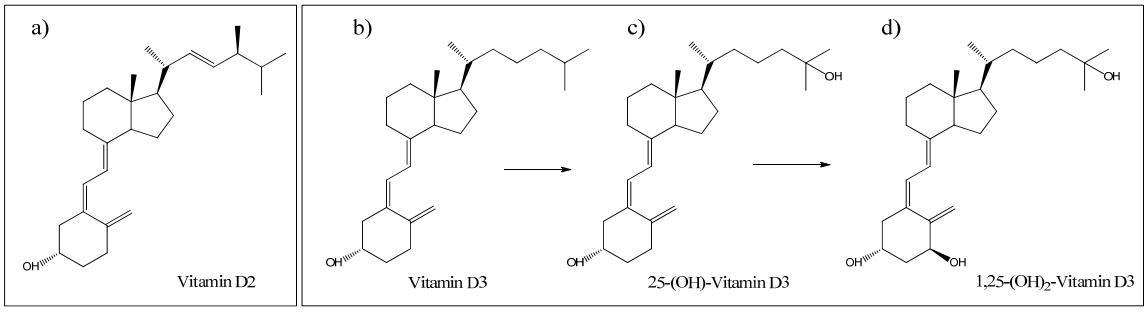


**Figure 3-2. Molecular structures for Vitamin D2 and D3, including both mono- and dihydroxy- metabolites.**

Routine vitamin D screening may be performed using competitive protein binding assays (CBPA),[254] radioimmunoassays (RIA)[255,256], enzyme immunoassays (EIA)[257] and chemiluminescent immunoassays (CLIA)[258], however, the current gold standard method simply utilizes HPLC with UV detection.[253,259,260] Recently, there has been interest in coupling common reverse-phase separation methods with MS detection, in an effort to improve assay sensitivity and accuracy. A few LC-MS methods for determination of vitamin D have been described utilizing Electrospray, however, most often APCI is found to provide better sensitivity with reduced sample preparation requirements.[261-264] Use of APPI for the

determination of vitamin D or its metabolites has only been reported in a couple of isolated instances, with little acceptance in the clinical field.[265,266]

#### 3.1.1.3. Polycyclic Aromatic Hydrocarbons

Polycyclic Aromatic Hydrocarbons are a class of fat-soluble atmospheric contaminants, produced through the incomplete combustion of organic materials such as petroleum fuels, coal and wood. They are ubiquitous environmental contaminants, often possessing carcinogenic or mutagenic properties and therefore must be monitored with some scrutiny.[267] PAHs consist of a series of 2 or more fused aromatic rings, including no additional functional groups. They tend to be relatively non-polar, possessing no acidic or basic functionalities. There are over 100 known PAHs compounds of which 16 have been identified as priority pollutants by the US and EU environmental protection agencies.

PAHs are routinely determined by either HPLC with fluorescence detection[268] or GC-MS,[269,270] however, the use of LC-MS methods is increasingly desired due to the potential for greater sensitivity and higher selectivity. APCI methods have been described providing adequate detection limits for some PAHs, while ESI methods are known to ineffectively ionize most highly non-polar analytes without derivatization.[153,271] The determination of PAHs is perhaps one of the key applications where modern open-geometry APPI sources currently hold some advantage, given the ability to ionize compounds with low proton affinity through charge exchange ionization.[51,132,153] Instrumental design modifications that lead to enhanced performance will inevitably increase the widespread acceptance of the APPI technique.

### 3.1.2. Sample Purification and Modification

Clinical LC-MS workflows inevitably require some measure of sample purification or modification prior to sample introduction. Over time, the repeated introduction

of protein macromolecules may clog LC columns, while smaller constituents can adversely affect the ionization process, increasing detection limits or contaminating the MS interface. For these reasons some measure of sample pre-treatment is generally necessary to preserve robustness and insure reproducible, accurate results.

Protein precipitation is perhaps the most widely applied sample cleanup procedure utilized in clinical LC-MS workflows.[272,273] Removal of proteins from a serum or plasma sample vastly improves column lifetime and often cannot be avoided. Techniques such as Liquid-Liquid Extraction (LLE),[264,274] and Solid Phase Extraction (SPE) [275-278] are often required to concentrate analytes or purify samples in an effort to limit endogenous interferences. Sample pre-treatment methods are routinely employed to reduce the impact of matrix suppression, however, each step places additional strain upon sample throughput and assay accuracy. Use of internal standards or isotope dilution methods are alternatives for improving accuracy in the face of matrix ion suppression, however, detection limits may still suffer as a result of reduced sensitivity. Additionally, suitable internal standards are often difficult to obtain for many clinical analytes, particularly steroidal metabolites.

Derivatization is another common sample pre-treatment method used to increase separation efficiency, volatility, selectivity or sensitivity for less polar analytes.[279-281] HPLC-ESI-MS methods commonly employ derivatization agents such as hydroxylamine or dansyl chloride to increase an analytes polarity through the attachment of basic nitrogen containing functional groups. Derivatized compounds may display higher or lower polarity, altering column retention and thus separation from early eluting matrix materials. Increased polarity and thus basicity also improves ionization efficiency for ESI methods often resulting in improved detection limits.

Sample purification and modification techniques may be performed on-line or with streamlined automated methodology, however, each will inevitably have a negative impact on assay throughput and accuracy. Extensive preparation workflows often result in sample dilution and also provide ample opportunity for analyte losses, carryover and contamination. Derivatization procedures in particular are costly and must be tailored specific to the functionalities presented by the analyte precursor, requiring a highly trained operator with thorough understanding of the chemistry involved. Reducing the requirement for extensive sample purification or modification procedures will inevitably improve the throughput and accuracy of LC-MS determinations.

### 3.1.3. Chromatography: High Throughput Analyses

Liquid chromatography can be thought of as a clinical scientist's most powerful sample pre-treatment tool. The physical separation *in time* of an analyte of interest from interfering matrix components provides a great advantage for the analysis of clinical samples including complex biological matrices. Chromatography inherently presents a significant barrier limiting sample throughput. The additional requirement for extensive sample purification, the use of trapping columns, solvent matrix matching and column re-equilibration should not be overlooked as limitations to an LC-MS workflow.

The pharmaceutical industry is perhaps the largest driving force for rapid, accurate LC-MS workflows as a means of reducing costs and increasing throughput and efficiency. Clinical researchers, however, also place a significant demand upon the need for rapid screening tools as it is more important to discern what a patient is suffering from, rather than what has killed them. Typical extended gradient LC methods, ranging in duration from minutes to hours, represent a significant bottleneck, throttling efficiency. The simplest workflow would see samples introduced immediately, without separation, to the MS via direct Flow Injection Analysis (FIA), as a narrow plug of sample inserted into a

continuous flow solvent stream. Since no physical separation is provided, direct FIA is only amenable to very clean samples with negligible interfering matrix components. Often times, water, urine, and saliva samples may be analyzed using simple “dilute and shoot” methodologies, however, some measure of chromatographic separation is still generally required. In these instances, high throughput, rapid screening methods may be utilized. Many of these methods employ high flow rates and isocratic solvent conditions in order to obviate the need for time-consuming column re-equilibration periods. Alternatively, recently introduced Ultra High Performance Liquid Chromatographs (UHPLCs) may be employed to reduce analysis times through use of separation columns containing small diameter column packing materials (typically < 2 μm), decreasing the mean free path and improving resolution and separation efficiencies.[282,283] In-turn, UHPLC systems must be operated under extremely high column backpressures. Rapid assays utilizing gradient methods are possible using UHPLC systems allowing the user to tailor separations, while maintaining analysis times below 5 minutes - a bench mark limit for high throughput LC workflows. Drawbacks to the use of UHPLC systems include requirement for dedicated instrumentation, and thus prohibitive cost, as well as the need for specialized LC columns that are capable of operation under the extreme pressures produced by UHPLC pumps.

An ideal high throughput LC workflow would of course present a minimal impact on analysis times, while still providing efficient analyte separation from interfering matrix elements. This is dependent on the degree to which ion source performance is altered by a particular matrix composition. Modern APPI and APCI are less susceptible to matrix ion suppression than ESI, and thus show additional promise for adaptation to high throughput clinical workflows. The next step in this line of research will be to determine if the new field-free APPI source provides a similar advantage for the analysis of real-biological samples under relevant high throughput reverse-phase LC-MS conditions.

## 3.2. Methods and Materials

### 3.2.1. Instrumentation

#### 3.2.1.1. Steroidal Analyses

The field-free, closed-geometry photoionization source described in Chapter 2 was employed for all analyses performed utilizing clinical and environmental LC-MS workflows. Lamp power was supplied using a custom HV power supply (electrical services, University of British Columbia, BC, Canada) with current restricted to 0.8 mA for all experiments. Offset transfer voltage was provided by an additional Stanford Research (Sunnyvale, CA) PS350 programmable DC HV supply. Transfer voltage, gas flow rates and source temperature were optimized to provide maximum sensitivity. Ion source and MS parameters were optimized for each analyte and adopted across all steroid determinations

The first mass analyzer used was an API 3200 triple quadrupole MS from Applied Biosystems/MDS Sciex (Concord, Ontario, Canada). An unmodified Turbo V source was used for all ESI and APCI analyses. A prototype open-geometry Photospray source, functionally identical to commercially available APPI sources, was also used without modification. MRM transitions selected for all steroidal analyses are summarized in table 3-1. In this study, estrone was found to display an $[M+H]^+$ base peak at m/z 271 in full spectrum scans, however, a peak of comparable intensity was also observed at m/z 253 corresponding to a water loss to product, $[M+H-H_20]^+$. The protonated estrone base peak was selected for all analyses, across all ion sources. The base peak for analysis of estradiol (m/z 255) was representative of a similar water loss product $[M+H-H_20]^+$. The estradiol dehydration product ion was selected for all applicable methods. MS parameters (EP, CXP, DP, CE, etc.) were optimized for each experiment, and were dependent on the mass analyzer utilized. All analyses were performed in positive mode with a scan time of 200 ms and a dwell time of 5 ms. The collision gas parameter tended to optimize toward a moderate value for each analyte, however, varying with each MS platform.

**Table 3-1. Steroid panel MRM transitions**

| Compound | Base Peak | Q1 mass | Q3 mass |
|---|---|---|---|
| Androstenedione | $[M+H]^+$ | 287.1 | 97.1 |
| Corticosterone | $[M+H]^+$ | 347.1 | 91.1 |
| Cortisone | $[M+H]^+$ | 361.3 | 163.3 |
| Estradiol | $[M+H-H_2O]^+$ | 255.1 | 159.1 |
| Estrone[a] | $[M+H]^+$ | 271.1 | 159.1 |
| Progesterone | $[M+H]^+$ | 315.4 | 109.1 |
| Testosterone | $[M+H]^+$ | 289.1 | 97.1 |

*a - Base peak for estrone was for $[M+H]^+$ however a comparibly large signal was also produceded for $[M+H-H2O]^+$.*

Early experiments utilizing chromatographic separation were performed using a Hewlett-Packard (Palo Alto, CA) 1100 series quaternary pump together with a Phenomenex (Torrance, CA) Luna, 100 x 2.0 mm C18 column with a 3 μm particle size unless otherwise specified. The pump was used to deliver all mobile phases at a total flow rate of 200 μL $min^{-1}$. Solvent A was deionized water, while solvent B was methanol, each containing 0.05% formic acid. A two-step gradient method, described in Table 3-2, was used to compare source performance while employing extensive matrix separation.

**Table 3-2. Gradient LC separation method**

| Time / min | Flow rate / μL/min | A (%)[a] | B (%)[a] |
|---|---|---|---|
| 0.0 | 200 | 80 | 20 |
| 1.0 | 200 | 80 | 20 |
| 3.0 | 200 | 30 | 70 |
| 7.0 | 200 | 5 | 95 |
| 12.0 | 200 | 5 | 95 |
| 12.1[b] | 200 | 80 | 20 |

*a - Mobile phase solvent A was DI water and solvent B was methanol. Both mobile phases included 0.05% forminc acid.*
*b - Two minute of column re-equilibration included between analyses*

Fast isocratic separations were performed with a 90:10 methanol/water solvent composition demonstrating the effects of matrix ion suppression during a suitable high throughput workflow. Flow injection experiments were performed using a 50:50 methanol/water mobile phase composition. APPI experiments required the infusion of toluene dopant at 20 μL/min using a syringe pump integrated with the mass spectrometer. The post-column infusion of analyte standards for the purpose of matrix effect characterization required a second Harvard Apparatus (Holliston, MA) syringe pump operated at a flow rate of 10 μL/min. Sample injections were performed manually using a switching valve integrated in the mass spectrometer with a 10 μL sample loop.

Mobile phase and dopant supplies were introduced separately through a novel, modified APCI nebulizer probe. Design of the modified heated nebulizer probe is detailed in Appendix 2. The modified probe utilizes two isolated flow paths to introduced mobile phase and dopant streams independently, eliminating concerns regarding solvent miscibility. Both solvent flows enter the nebulizer probe via stainless steel hypodermic capillaries and pass through a thermally controlled, high temperature region. Dopant flow is introduced through a short capillary, terminating within the heated probe where it is vapourized into the nebulizer gas (GS1). LC effluent was introduced through a longer capillary terminating 0.5 - 1.0 mm beyond the end of the probe assembly, analogous to the unmodified APCI design. The nebulizer gas (GS1), saturated in dopant vapour, was used to pneumatically assist the mobile phase vapourization process. Results obtained using the modified APCI probe are typically identical to those obtained using the standard probe design, however, without the potential signal instability attributable to solvent/dopant immiscibility.

Platform comparison experiments were conducted across three Applied Biosystems/MDS Sciex mass analyzers: A 3200 series triple quadrupole system, as well as a 4000 and a 5500 series QTrap. Platform experiments were

performed using a short isocratic method with mobile phase supplied using a PerkinElmer (Waltham, MA) 200 series LC pump with auto sampler. Solvent was supplied with a constant 80:20 methanol/water composition at 200 μL/min including 0.05% formic acid. Separation was performed using a Phenomenex (Torrance, CA) Luna, 100 x 2.0 mm C18 column with a 3 μm particle size and a 10-μL injection volume.

#### 3.2.1.2. Vitamin D Analyses

Vitamin D analyses were performed on an Applied Biosystems 5500 QTrap mass spectrometer. A Turbo V source operated in APCI mode was used to perform relevant source comparison experiments. The prototype field-free APPI source was operated using the method described previously for steroidal analyses. A conical flight tube with a 4:1 reduction in cross sectional area was employed. Fixed lamp current was provided using a stand-alone high voltage power supply designed to support first-generation, closed-geometry APPI sources. Offset transfer voltage was provided by an additional Stanford Research (Sunnyvale, CA) PS350 programmable DC HV supply. Lamp gas was supplied at 0.3 LPM from an independently regulated high purity nitrogen source. MRM transitions are summarized in Table 3-3. All MS parameters were optimized for each transition independently and maintained for all experiments.

**Table 3-3. Vitamin D final sample concentrations and MRM transitions**

| Compound | Concentration / μg/mL | Q1 mass[a] | Q3 mass |
|---|---|---|---|
| Vitamin D2 | 10 | 397.4 | 379.4 |
| | | 379.4 | 159.2 |
| Vitamin D3 | 10 | 385.3 | 367.4 |
| | | 367.4 | 159.2 |
| 25-(OH)-Vitamin D2 | 10 | 395.3 | 269.1 |
| | | 395.3 | 119.0 |
| 25-(OH)-Vitamin D3 | 10 | 383.3 | 229.2 |
| | | 383.3 | 211.1 |

*a - $[M+H-H20]^+$ ion selected in Q1 for both monohydroxy vitamin D metabolites. both $[M+H]^+$ and $[M+H-H20]^+$ ions evaluated for parent vitamin D analyses.*

Chromatography was performed using an Agilent Technologies (Santa Clara, CA) 1200 series quaternary LC pump including vacuum degasser and autosampler modules. A GC Sciences (Torrance, CA) Inertsil 5 cm - C18 column with a 2.1 mm diameter and 3.0 μm particle size was used to perform all vitamin D separations. Mobile phase was provided isocratically with a 95:5 methanol/water composition at a total flow rate of 400 μL/min without additives. A sample injection volume of 10 microlitres was used. For APPI analyses, toluene dopant was infused at 40 μL/min using a stand-alone Harvard Apparatus (Holliston, MA) syringe pump. LC and dopant flows were introduced to the field-free APPI source using the modified APCI probe described in appendix B.

#### 3.2.1.3. PAH Panel Analyses

Analysis of a standard PAH panel was performed using the LC and MS configurations described for the analysis of Vitamin D. Most PAHs were insufficiently ionized by APCI so a comparison study was instead performed against a prototype open-geometry Photospray source, functionally identical to commercially available sources. MS parameters independent of the ion source were optimized for the each analyte and maintained for all experiments. The MRM transitions summarized in Table 3-4 were specific to ionization through the charge exchange mechanism only, although in some instances ionization of suitably basic PAHs through proton transfer does occur, presenting a competing pathway.

A10-minute gradient method was employed for the analysis of the PAH panel using acetonitrile and deionized water without additives. Initial conditions utilized a 60:40 ACN/$H_20$ mobile phase composition, held for two minutes at a continuous flow rate of 250 μL/min. The organic component was then raised to 100% over then following 4 minutes and held for an additional 4 minutes. A 2-minute column re-equilibration period was included between trials. This method

used a 2-μL sample injection volume. A toluene dopant flow rate of 25 μL/min was adopted for both the Photospray and field-free APPI source.

**Table 3-4. PAH panel stock concentrations and MRM transitions**

| Compound | Concentrations[a] / μg/mL | Q1 mass | Q3 mass |
|---|---|---|---|
| Acenaphthene | 1000 | 154.1 | 126.1 |
| | | 154.1 | 153.1 |
| Acenaphthylene | 2000 | 152.1 | 126.1 |
| | | 152.1 | 151.1 |
| Anthracene | 100 | 178.1 | 152.1 |
| | | 178.1 | 176.1 |
| benzo(a)anthrecene | 100 | 228.1 | 150.1 |
| | | 228.1 | 226.1 |
| Benzo(a)pyrene | 100 | 252.1 | 224.1 |
| | | 252.1 | 250.1 |
| Benzo(b)fluoranthene | 200 | 252.1 | 224.1 |
| | | 252.1 | 250.1 |
| Benzo(k)fluoranthene | 100 | 276.1 | 246.1 |
| | | 276.1 | 274.1 |
| Benzo(ghi)perylene | 200 | 252.1 | 224.1 |
| | | 252.1 | 250.1 |
| Chrysene | 100 | 228.1 | 200.1 |
| | | 228.1 | 226.1 |
| Dibenzo(a,h)anthracene | 200 | 278.1 | 248.1 |
| | | 278.1 | 276.1 |
| Fluoranthene | 200 | 202.1 | 150.1 |
| | | 202.1 | 200.1 |
| Fluorene | 200 | 166.1 | 115.1 |
| | | 166.1 | 165.1 |
| Indo(1,2,3-cd)pyrene | 100 | 276.1 | 248.1 |
| | | 276.1 | 274.1 |
| Naphthalene | 1000 | 128.1 | 102.1 |
| | | 128.1 | 78.1 |
| Phenanthrene | 100 | 178.1 | 151.1 |
| | | 178.1 | 176.1 |
| Pyrene | 100 | 202.1 | 150.1 |
| | | 202.1 | 200.1 |

*a - Analyte concentrations were selected to provide similar relative signal intensities when analyzed using an LC-APCI-MS method . Stock solution diluted 1000x providing concentrations from 100-2000 μg/mL*

### 3.2.2. Chemicals

#### 3.2.2.1. Steroids Samples

Estrone, cortisone and progesterone were all obtained from Sigma Aldrich (St. Louis, MO) as dry solids at no less than 98% purity. Corticosterone, androstenedione, estradiol and testosterone samples were generously supplied as dry solids from MDS Sciex (manufacturer and purity unknown). HPLC grade methanol and toluene were obtained from Fisher Scientific (Fair Lawn, NJ), as was formic acid. Deionized water was produced using an in-house generator. Human serum matrix (2x charcoal stripped) was provided by MDS Sciex (Concord, ON, Canada). All analytes and solvents were used as purchased without further purification.

#### 3.2.2.2. Vitamin D and Metabolite Standards

Vitamin D2 and D3 standards were purchased as dry solid analytical standards at the highest available purity from Sigma Aldrich (St. Louis, MO). 25-(OH)-Vitamin D2 and D3 standards were obtained from AB/Sciex (Concord, ON, Canada), also as analytical standards at greater than 99% purity. HPLC grade methanol was obtained from Fisher Scientific (Fair Lawn, NJ). Deionized water was obtained from an in-house generator.

#### 3.2.2.3. PAH Standards

All PAHs summarized in table 3-4 were obtained as dry solid analytical standards from AB/Sciex (manufacturer and purity unknown). HPLC grade methanol, acetonitrile and methylene chloride were obtained from Fisher Scientific (Fair Lawn, NJ). Deionized water was obtained from an in-house generator.

### 3.2.3. Sample Preparation

#### 3.2.3.1. Steroid Analyses

*Stock analyte solutions:*

Analyte stock solutions were individually prepared for each of estrone, cortisone estradiol, androstenedione, corticosterone, testosterone and progesterone. Solid crystals were first dissolved to produce high concentration stock solutions each 1 mg/mL in HPLC methanol. Each solution was each further diluted to produce low concentration, 1 μg/mL standards in methanol.

*Protein precipitation (crashing) procedure:*

Serum matrix samples were received frozen with proteins precipitated by following method: Plasma samples were crash precipitated adding two parts acetonitrile to one part plasma. This solution was vortexed for 1 minute, and then centrifuged at 9000 rpm for 30 minutes. The supernatant was retained. Serum stock was purchased 2x charcoal stripped to reduce pre-existing steroidal interferences.

*Samples for flow injection, gradient and isocratic LC analysis:*

Samples for flow injection experiments were prepared by further dilution of the low concentration stock to produce single component standard solutions, each 100 ng/mL in 50:50 methanol/water. Two samples were prepared for gradient LC separation experiments, one containing pure steroid standards diluted to a final composition of 20:80 M/W. The other was adjusted and spiked with crashed serum to produce a matrix diluted by a factor of 10 in mobile phase. The matrix-containing sample was also prepared in 20:80 M/W to match gradient LC starting

conditions. Both samples were adjusted to provide analyte concentrations of 10 ng/mL cortisone, 20 ng/mL estrone and 10 ng/mL progesterone.

Three standard steroid mixtures were produced for isocratic analysis. Each was prepared using an identical procedure to those created for gradient analysis. The final composition for Steroid Panel A (both standard and matrix-spiked) was adjusted to 90:10 methanol/water to match the isocratic mobile phase composition. Final analyte concentrations of 10 ng/mL cortisone, 100 ng/mL estrone and 10 ng/mL progesterone were utilized. Steroid Panel B (both standard and matrix-spiked) was adjusted to 75:25 methanol/water. Final analyte concentrations of 5 ng/mL were selected for each of corticosterone, androstenedione, estradiol and testosterone. Steroid panel C was produced containing cortisone, progesterone and testosterone, each at 1 μg/mL, diluted in 80:20 methanol/water. Sample C was used to compare relative ion source performance across several MS platforms, each providing different sensitivity. Sample C required dilutions of 10, 100 and 1000 times in order to suit the performance of each mass analyzer surveyed. No additional biological matrix was included with sample C.

#### 3.2.3.2. Vitamin D and 25-(OH)-Vitamin D Metabolites

A multi-component Vitamin D standard was created containing Vitamin D2 and D3, as well as both 25-(OH)-Vitamin D2 and D3 metabolites. Each of the four analytes were dissolved in methanol to produce single component 10 mg/mL standard stock solutions. The stock solutions were then combined and diluted to create a 10 μg/mL multi-component standard with a 60:40 methanol/water solvent composition. No additional biological matrix was employed for the analysis of vitamin D or its metabolites.

#### 3.2.3.3. PAH Panel

A broad PAH panel was created through the serial dilution and combination of multiple single component standard solutions. Stock standards were prepared by individually dissolving pure dry solids in 1:1 methanol/methylene chloride. A standard PAH panel was prepared in methanol from the single component standards with final analyte concentrations ranging from 100 to 2000 μg/mL, as summarized in Table 3-4. The PAH panel was further diluted 1/1000 in 60:40 acetonitrile/water prior to analysis.

## 3.3. Results and Discussion

### 3.3.1. Steroidal Analyses

#### 3.3.1.1. Flow Injection Analysis

Figure 3-3 presents XIC signal intensities obtained for several single component steroid standards determined by flow injection using ESI, APCI, Photospray and the field-free APPI source. The closed-geometry, field-free APPI source provided the most advantage for the direct inject, “dilute and shoot” or rapid screening methods where matrix interferences are considered to be negligible. No additional biological matrix was introduced during this set of experiments. Although assumed to be reasonably pure, the presence and exact composition of possible interfering species within the standards is unknown. The prototype field-free source was demonstrated to provide order-of-magnitude scale improvement in sensitivity over the incumbent, open-geometry Photospray source across the range of steroids tested. This level of observed enhancement is consistent with values reported in chapter 2. The recognized improvement in sensitivity between the two APPI source designs is attributed to the presence of the extended field-free reaction zone provided by the field-free source.

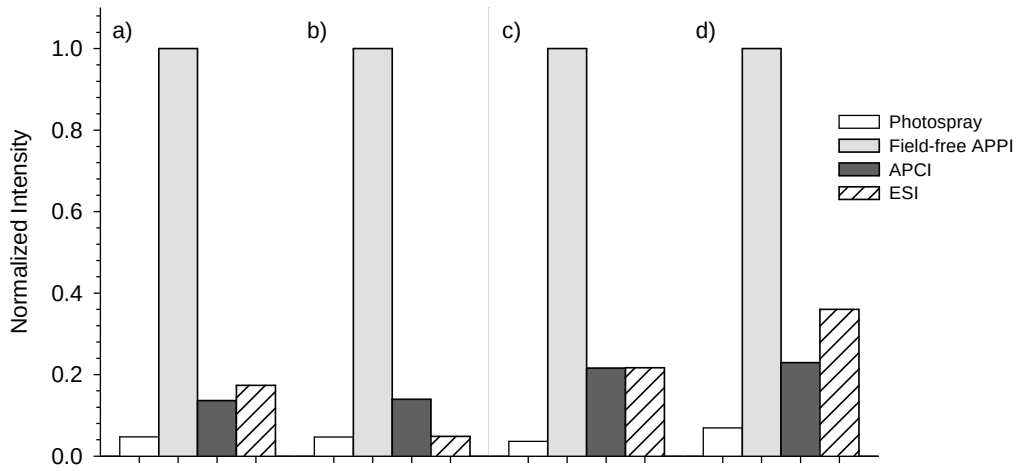


**Figure 3-3. Relative XIC signal intensities obtained for a) progesterone, b) estrone, c) cortisone, and d) testosterone standards introduced by flow injection using various ion sources.**

The addition of formic acid to all mobile phases was determined to be essential to ionization by ESI. An empirically ideal 0.05% v/v formic acid concentration was established for all analyses. Mobile phase additives provided insignificant or modest signal enhancement for APCI or the APPI sources (data not shown). Overall, signal improvement demonstrated by the field-free APPI source relative to APCI and ESI was noteworthy. APPI sensitivity was superior by an average of 6- and 10-fold for the range of steroids analyzed by direct flow injection. The most significant enhancement was obtained for estrone, demonstrating 20-fold greater signal intensity than ESI. This is particularly of interest, as estrogens are often identified as difficult to ionize by electrospray, due to a lack of highly acidic or basic functionalities and a localized steroidal ring structure.[278,284] The ability to provide improved sensitivity for the analysis of estrogen-like compounds could be regarded as a significant advantage associated with the field-free APPI source. In light of the complex nature of clinical sample matrices, direct flow injection methods are seldom ultimately useful. As a result, some form of chromatographic pre-treatment is generally required for the practical analysis of "real" clinical sample.

### 3.3.1.2. Gradient LC Separation

Figure 3-4 presents TIC chromatograms obtained for the gradient steroid panel including a crashed and diluted serum matrix. Optimized results for the closed-geometry, field-free prototype APPI, electrospray and open-geometry Photospray sources are provided. A simple two-stage, 12-minute gradient method was selected to demonstrate relative performance under conditions permitting extensive matrix separation. The three steroids were highly resolved under the selected conditions; however, in light of the relatively fast gradient utilized it is possible that co-eluting matrix elements may still persist. This would be more of a concern for samples prepared with reduced dilution or samples that have not been subject to charcoal stripping pre-treatment.

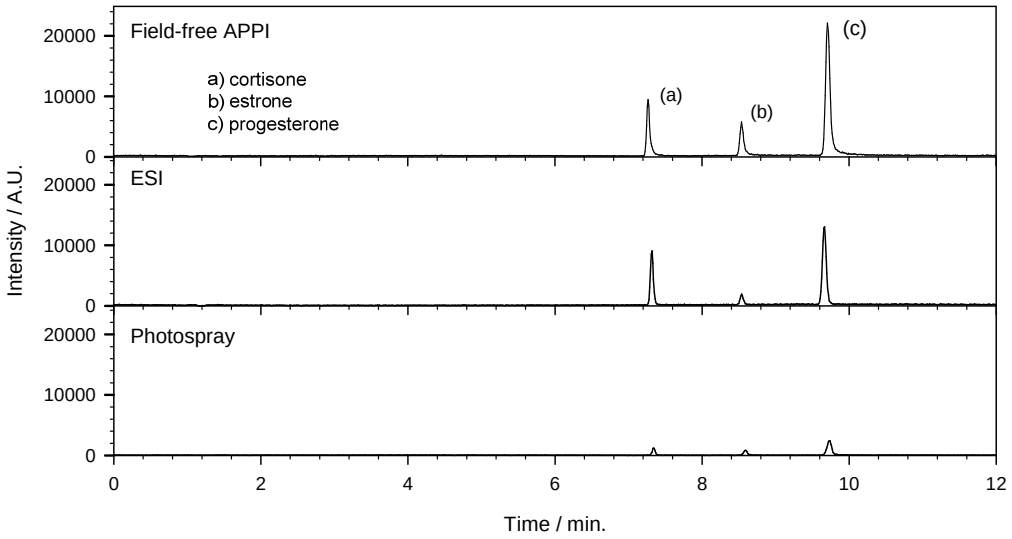


**Figure 3-4. TIC chromatograms presenting results for the analysis of steroid panel A using an extended gradient LC separation method.**

The field-free APPI source was shown to dramatically outperform the open-geometry Photospray source under gradient conditions. This result was anticipated, as both devices are expected to respond similarly in terms of matrix ionization suppression. The results suggest that exploitation of increased analyte ionization and/or transfer efficiency is again responsible for order-of-magnitude scale improvement in sensitivity. Interestingly, however, the performance

provided by ESI was found to be roughly comparable to the field-free APPI source for each of the steroids analyzed; this is in contrast to the order-of-magnitude improvement recognized through FIA. The field-free APPI still holds a clear advantage with respect to the determination of estrone, demonstrating 4 times better sensitivity that ESI. A comparison of peak areas obtained through both flow injection and gradient methods (data not shown) suggests that ESI signals were improved by a factor of 4 times on average when chromatographic separation was employed. The exact cause of the observed signal enhancement is unknown, however, it may be attributable to the separation of the various analytes from interfering matrix components that are co-introduced during FIA, even when relatively clean, single component standards are utilized; this may be particularly true for the analysis of highly concentrated standards. Peak areas obtained using both the open-geometry and field-free sources were virtually identical when comparing gradient and flow injection methods. This observation is consistent with advantages previously recognized for APPI sources with respect to susceptibility to ionization suppression. These early results suggest that ESI sources benefit the most from some measure of chromatography in order to provide reliable, accurate results. Conversely, the APPI sources responded more favourably to factors affecting ionization suppression, which could lend these sources toward dilute and shoot, rapids screening assays. Further experimentation would of course be required to confirm these hypotheses.

#### 3.3.1.3. Isocratic High Throughput LC Separation

We now take a closer look at the effects of matrix ion suppression on the relative performance provided by each ion source under high throughput isocratic conditions. Analyses were spread across a number of sample and MS platforms in order to gain a broad appreciation for relative performance and build confidence in the results obtained. LC parameters were selected to produce fast isocratic methods, suitable for high throughput or rapid screening analyses. Figure 3-5a presents chromatograms comparing the field-free APPI, ESI and

Photospray sources utilizing a short 5-minute isocratic method (methanol/water, 90:10 v/v +0.05% formic acid). The first panel demonstrates signal response for a standard mixture of cortisone, estrone and progesterone, in the absence of crashed serum matrix. All three analyte peaks are fully resolved, eluting within 4-minutes. The results indicate that the field-free APPI source again provided the best sensitivity for the analysis of all three steroids - a similar relative outcome to that obtained under gradient conditions.

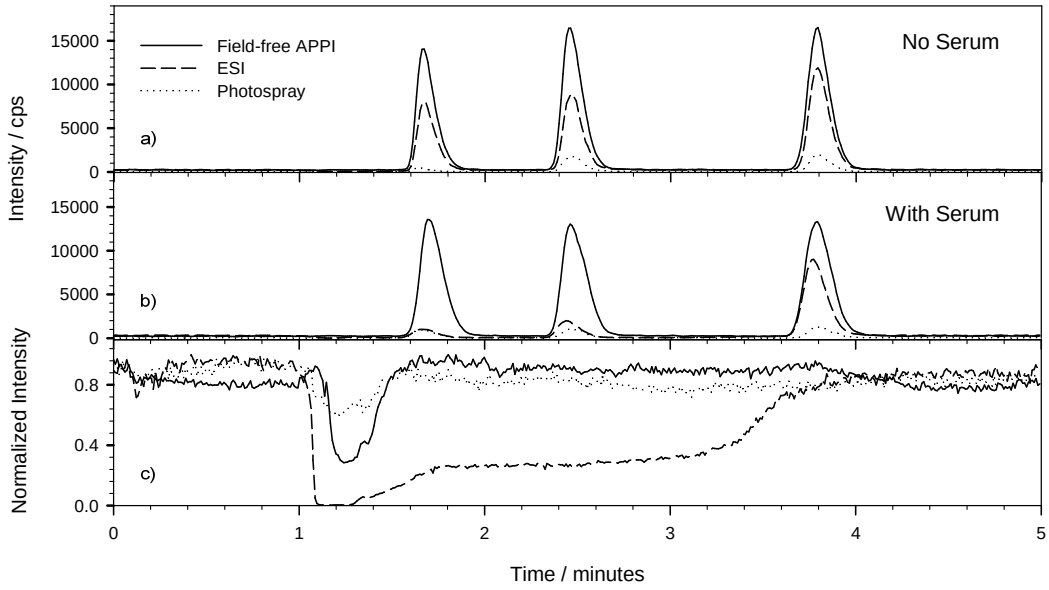


**Figure 3-5. TIC chromatograms comparing the field-free APPI source to ESI and the open-geometry Photospray source for the analysis of Steroid Panel A. a) standards only, b) including crashed serum matrix and c) visualization of matrix ionization suppression using post column infusion of Steroid Panel A with the on-column injection of blank serum.**

Figure 3-5b provides chromatograms also obtained for the steroid panel under the same high throughput conditions, however, now with the addition of crashed serum matrix. The results saw a dramatic suppression of the first two analyte signals obtained using the ESI source, corresponding to cortisone and estrone. Little to no signal suppression was observed for either of the APPI sources. The overall effect of serum matrix ion suppression is further visualized in Figure 3-5c, through Post-Column Infusion, PCI. Injection of blank serum on-column, along with the steady-state introduction of all three steroids post-column visually demonstrates the extent and duration of signal suppression for each ion source.

Suppression was shown to be considerably more severe for ESI than either the prototype field-free APPI or Photospray sources. The electrospray process was completely hindered for approximately 20 seconds upon the initial elution of the serum matrix plug. The background signal level did not fully recover for an additional 2-3 minutes. We expect the extent of ion suppression to be further pronounced for the analysis of plasma samples, or simply for serum samples prepared with reduced dilution.

Expanding the range of steroids determined under relevant high throughput, rapid-screening workflows, Figure 3-6 provides XIC chromatograms obtained for the analysis of steroid panel B using a modern 5500 series QTrap instrument. Moving to a high-performance instrument platform provides the sensitivity and detection limits required to enable “real,” trace level clinical determinations.

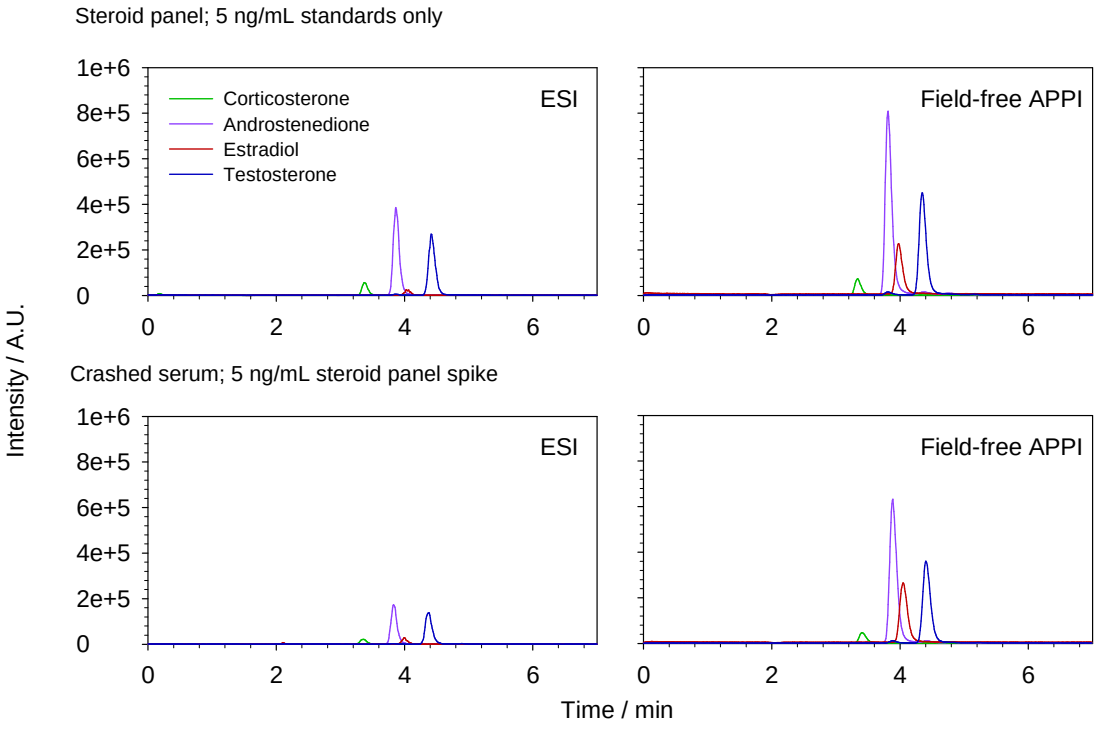


**Figure 3-6. XIC chromatograms comparing the field-free APPI source to ESI for the analysis of steroid panel B on a modern 5500 series QTrap instrument. Top panels – analysis of standards only, bottom panels – crashed serum matrix spiked with steroid panel.**

The top two panels in figure 3-6 demonstrates the optimized relative performance for ESI and the field-free APPI source for the determination of Steroid Panel B in the absence of additional biological matrix. In order to constrain all eluted analytes to within a 5-minute window, it was not possible to completely resolve all four steroid peaks. The method does provide an initial 3-minute window for the chromatographic isolation of matrix interferences prior to the first analyte elution.

For the analysis of standards only, best results were once again obtained for the field-free APPI source, providing 2-4 times better sensitivity than ESI for all steroids except for estradiol, which was superior by about 7 fold. Similar to estrone, estradiol is an estrogen and a clinically significant biomarker, routinely determined to evaluate reproductive health. The bottom series of panels shown in figure 3-6 demonstrate the effect of serum ion suppression upon the signals obtained using each ion source. Signals obtained by ESI were each reduced by 50% or more under this set of high throughput LC conditions. Signals obtained using the field-free APPI source were suppressed by only 10-20%. Although not free from matrix suppression, the field-free source provides a clear advantage for the rapid analysis of steroids within complex biological matrices. Coupled with enhanced sensitivity, the field-free APPI source provided the best results for high throughput steroidal determinations. Sensitivity is, however, only one factor in the determination of detection limits. The standard deviation associated with the background signal must also be considered as increased noise levels will also impact both limits of detection and quantification. For completeness, associated detection limits determined based upon $3\sigma_{Blank}$ are summarized in table 3-5.

**Table 3-5. Detection limits for steroids in panel B**

| Compound | MRM (Q1/Q3) | ESI/ pg | FF-APPI / pg |
|---|---|---|---|
| Androstenedione | 2871/97.1 | 0.2 | 0.07 |
| Estradiol | 255.1/159.1 | 2.1 | 0.3 |
| Testosterone | 289.1/97.0 | 0.3 | 0.08 |
| Corticosterone | 347.1/91.0 | 1.6 | 0.5 |

### 3.3.1.4. MS Platform Comparison

We have to this point assumed that relative source performance is transferable from one MS platform to the next, independent of the ion sampling efficiency of the interface involved. The following experiment was intended to confirm that the relative performance improvement recognized for the field-free APPI source is preserved across various MS platforms. Figure 3-7 summarizes XIC signal intensities obtained for the analysis of Steroid Panel C, using the field-free APPI source, ESI and Photospray, across three MS platforms.

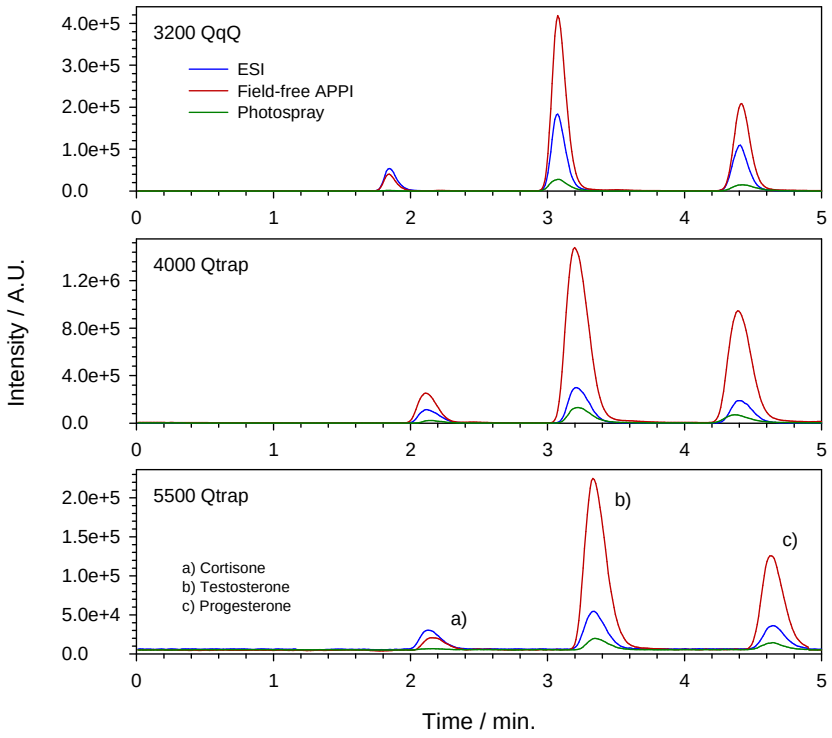


**Figure 3-7. TIC chromatograms obtained for Steroid Panel C (standards only, no additional biological matrix added) utilizing a simple high-throughput isocratic method. Results compare relative sensitivity provided by ESI, Photospray and the field-free APPI source, across a variety of MS platforms.**

Each MS utilizes a different geometric interface configuration, including varying sampling orifice diameters, ion focusing elements and vacuum pumping capacities. The API 3200 and 4000 QTrap instruments utilize 250 and 340 μm diameter orifice nozzles respectively. Both instruments also employ a grounded skimmer cone after the orifice plate, prior to entering Q0. The 5500 QTrap

incorporates a high transmission QJet ion guide in place of a skimmer cone, as well as an even larger 620 μm orifice diameter. The increased orifice sampling efficiency provided by the 5500 interface is coupled with increased pumping capacity in order to maintain vacuum requirements. Independent of these instrumental differences, the relative signal intensities summarized in figure 3-7 demonstrate only minor variation from instrument-to-instrument, for any of the three steroids determined.

#### 3.3.1.5. Reproducibility

Instrument and method reproducibility was assessed for the field-free APPI source using the repeated injection of crashed serum matrix, spiked with steroid panel C. Overnight stability assessment was performed using the high throughput isocratic method described for the platform comparison experiments above. Figure 3-8 shows XIC traces obtained for testosterone, during a reproducibility test consisting of 40 consecutive injections of steroid panel C including a crashed serum matrix. Reproducibility was determined to be better than 3% RSD by peak area, with no evidence of matrix carryover observed from run-to-run.

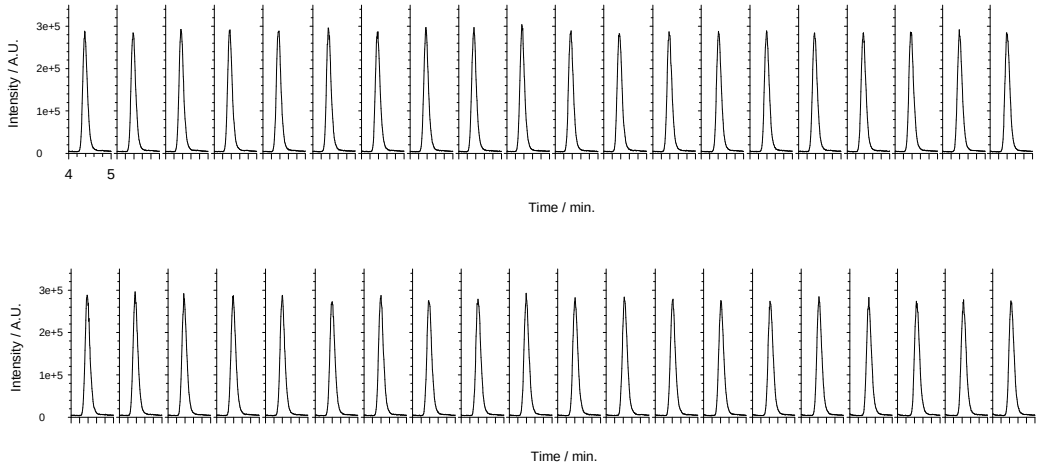


**Figure 3-8. XIC traces for testosterone (289/109) extracted from MRM data obtained for the analysis of Steroid Panel C using a short 5 minute isocratic method. Reproducibility was assessed for the field-free APPI source using 40 consecutive injections of crashed serum matrix spiked with the steroid panel. Standard deviation was less than 3% by peak area.**

### 3.3.2. Determination of Vitamin D

High throughput Vitamin D screening by LC-MS is complicated for a number of reasons. Without derivatization, all forms of vitamin D are poorly ionized by ESI and APCI - particularly at levels suitable for determination within biological fluids. Additionally, due to their limited polarity, neutral forms of Vitamin D tend to be well retained under typical reverse-phase conditions, leading to extended LC run-times, particularly at modest mobile phase flow rates. This section will quickly demonstrate the relative performance of the field-free APPI source for the determination of Vitamin D and its monohydroxy- metabolites using a simple, short isocratic separation method, suitable for routine screening.

Figure 3-9 presents overlaid XIC traces obtained for both APCI and the field-free APPI source. No additional biological matrix was utilized for these trials so the effect of matrix suppression on resultant signals is still uncharacterized. The clinically significant 25-(OH)-Vitamin D metabolites were first to elute followed by the parent Vitamin D compounds after a 4-minute delay. Best results for the determination of all four compounds were obtained using the field-free APPI source, providing a 5-9 fold improvement in sensitivity over APCI. In this method, mobile phase composition was maintained at 95:5 methanol/water and a flow rate of 400 μL/min for the purposes of reducing analysis times, however, it is unlikely that an assay would require both compounds to be determined simultaneously within a single assay. The LC-MS parameters and MRM transitions were selected in order to optimize results for the APCI source. The method was then quickly adapted to the APPI source; as a result, we expect relative performance to improve with additional source optimization. These results indicate the potential for order-of-magnitude scale performance enhancement utilizing a field-free APPI source design. Implications of higher sensitivity obviously include improved detection limits (provided background noise levels remain constant); however, there may also be the potential to

transition future rapid screening Vitamin D assays to less costly MS platforms – increasing the practicality of routine clinical screening by LC-MS.

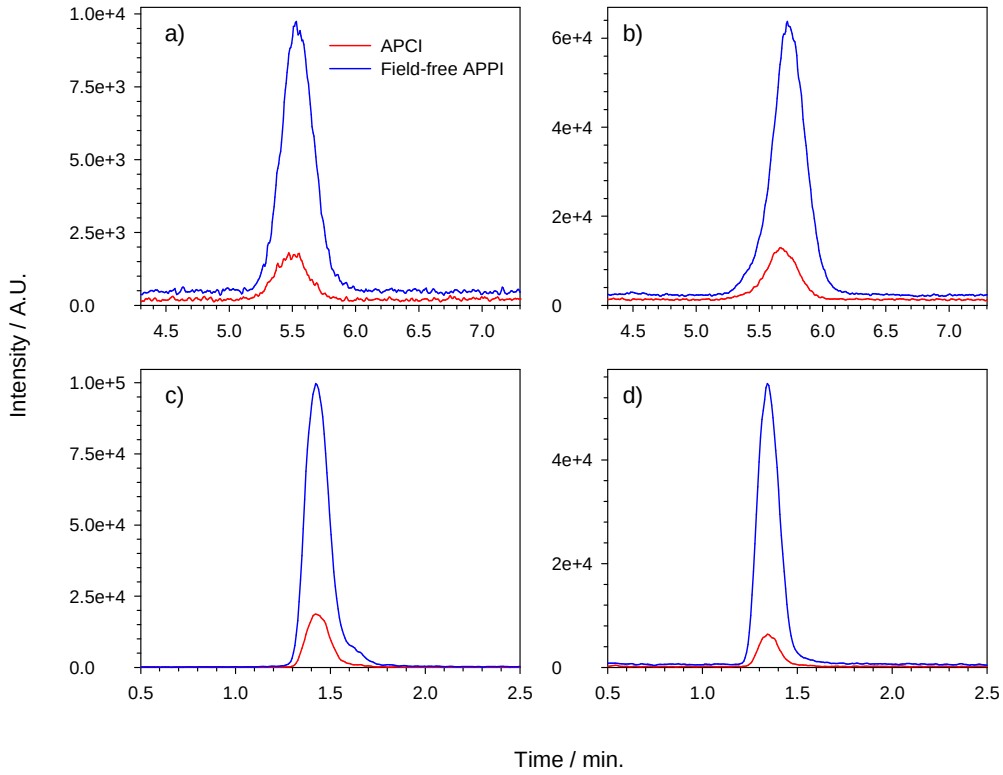


**Figure 3-9. Overlaid XIC traces obtained for the analysis of a) Vitamin D2, b) Vitamin D3, c) 25-(OH)-Vitamin D2 and d) 25-(OH)-Vitamin D3, using a short isocratic LC method. Results demonstrate the relative performance of APCI and the field-free APPI source.**

### 3.3.3. Analysis of a PAH Panel

For completeness, the performance of the field-free source was evaluated against an open-geometry Photospray source for the determination of a PAH panel containing 16 PAHs of relevant environmental concern. APPI is already widely recognized as the principle ionization method for the analysis of PAHs by LC-MS, however, improved performance is always desirable. Figure 3-10 presents total ion chromatograms obtained using both ion sources for the analysis of the PAH panel. Chlorobenzene was utilized as the dopant, providing better overall results than toluene. Although many peaks were only partially resolved, the results demonstrate the relative sensitivity enhancement provided

by the field-free source, attainable using a relatively short 10-minute gradient method. Improvements on an order-of-magnitude scale have been demonstrated.

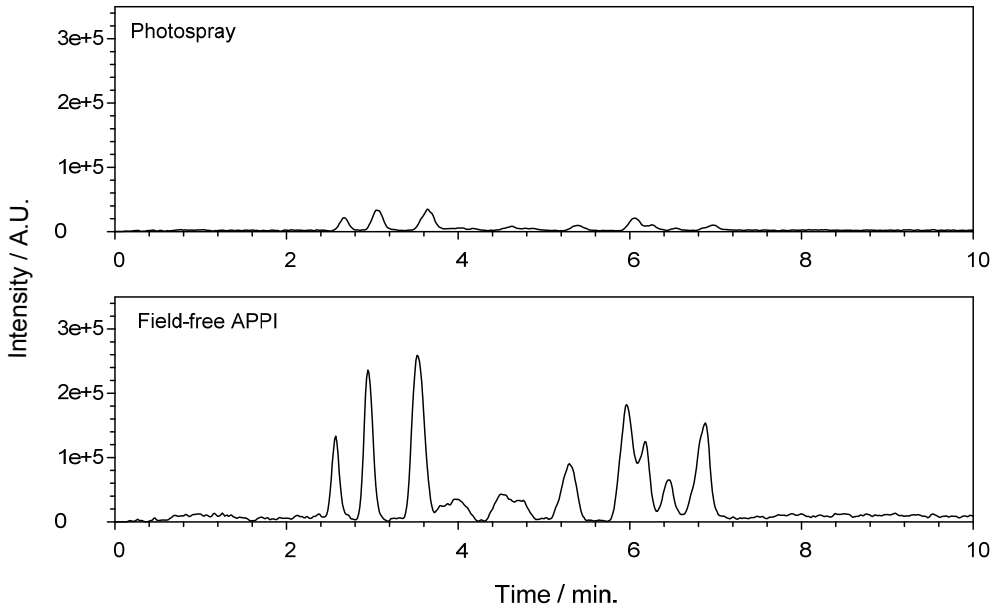


**Figure 3-10. TIC chromatograms obtained for the analysis of a 16 component PAH panel. Relative sensitivity for the Photospray and field-free APPI sources is demonstrated.**

Figure 3-11 provides selected XIC signals obtained for several of the PAH transitions, overlaid to explicitly demonstrate relative enhancement. Signals for the earliest eluting PAHs are enhanced by 6-10 times, while later eluting, more basic compounds are enhanced by a factor of 20 or more. Although the analysis of PAHs has become the de facto standard application used to demonstrate APPI sources performance, LC-MS is still infrequently adopted for routine environmental screening. The start-up cost for performing LC-MS assays tends to be quite prohibitive relative to HPLC-fluorescence or GC-MS based analyses. Improved detection limits, however, may allow for highly sensitive and selective determinations to be made using lower end MS platforms, reducing instrumental costs, ultimately impacting widespread acceptance.

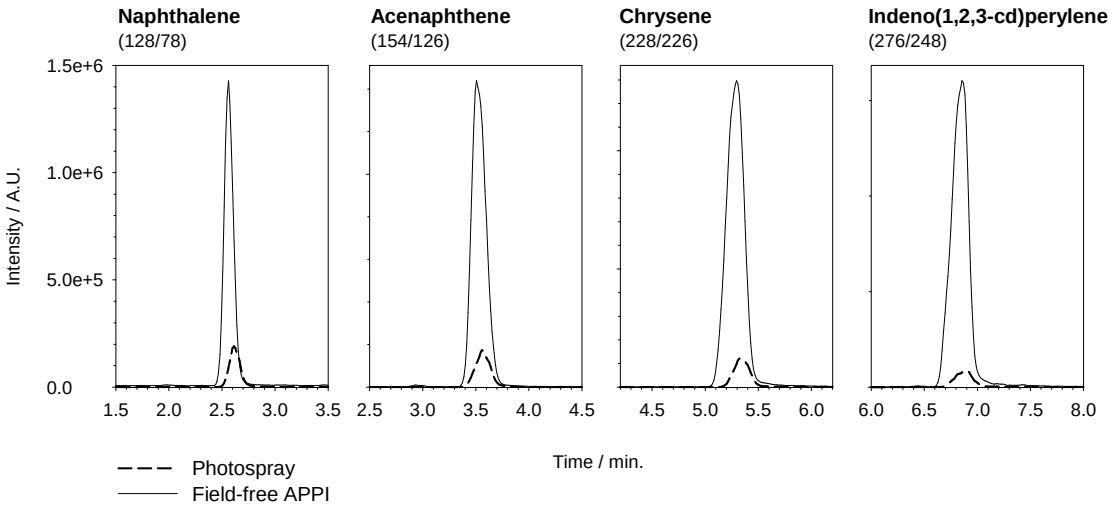


**Figure 3-11. Selected XIC traces obtained for a range of compounds extracted from the MRM analysis of a 16 component standard PAH panel. Signals overlaid to demonstrate the relative performance of the Photospray and field-free APPI sources.**

## 3.4. Conclusions

This chapter has presented the results for several experiments intended to evaluate the performance of the field-free APPI source, relative to other commonly adopted API sources. The focus of these analyses has been the determination of clinically relevant analytes using rapid screening workflows. Performance evaluations focused primarily upon the growing clinical market, as the needs of the health sciences shifts toward routine, accurate, high throughput assays, where ESI and APCI often fail to provide adequate performance.

The field-free APPI source was shown to routinely provide the most sensitivity for all compounds surveyed, including both polar and non-polar analytes. The ability to ionize the widest range of compounds positions the field-free APPI as the most universal ionization method. The potential for order-of-magnitude improvement in sensitivity for many key analyte classes such as estrogens, vitamin D metabolites and environmental significant PAHs has also been highlighted.

Historically, an additional benefit to APPI is a reduced susceptibility to matrix ionization suppression, particularly relative to ESI.[27] This effect has been demonstrated for the field-free APPI source through the analysis of a variety of steroids spiked within crashed serum matrices. APPI signals were often largely unaffected by the co-introduction of serum matrix elements, where electrospray ionization was entirely hindered under the same conditions. The variable extent of ion suppression is thought to be dependent upon the sample matrix involved, as well as the amount of sample pre-treatment utilized and chromatographic performance. In the following chapter we will thoroughly explore instrumental factors contributing to matrix ion suppression, focusing on the analysis of an expanded range of clinically relevant samples.

# Chapter 4. Matrix Ion Suppression and Enhancement: Characterization and Control

We continue to develop a general understanding for the performance of the new field-free APPI source relative to alternative ionization methods such as ESI and APCI. Matrix interferences derived from the analysis of biological samples are a real and significant concern. Samples requiring considerable sample clean-up or extensive chromatography to mitigate matrix effects will have an obvious impact on overall throughput, creating limitations for rapid screening LC-MS workflows. Quantifying the role of ion suppression or enhancement, however, is often an ill-defined, arbitrary practice, due to the inherent variability of matrix effects. APPI may provide an advantage with respect to matrix effects; however, is it a quantifiable benefit?

## 4.1. Introduction

Liquid Chromatography – Mass Spectrometry has emerged as perhaps the most sensitive and accurate technique available for routine bioanalysis. The accuracy and detection limits provided by an LC-MS assay, however, may be significantly affected by co-introduced matrix elements. The matrix of a sample is considered to be all components other than the analyte. Matrix effects with respect to chemical analysis may be defined as the effect a matrix presents upon the analyte signal response. This could include either the enhancement or suppression of an analytical signal, as a result of the interaction between the analyte and any matrix components.

In LC-MS, matrix effects generally concern the suppression of analyte ionization, resulting from the presence of co-eluting matrix components. This definition may be expanded, however, to include changes to ion transmission efficiency, as well as changes leading to an increase in MS background levels. The matrix of a

sample is not limited to the biological elements presented by the sample, but also the components introduced through sample preparation, chromatography and any modifiers introduced to aid the ionization process. In LC-MS, a matrix will include all solvents (including dopants), additives, and contaminant interferences, as well as the co-retained biological components carried through the sample preparation process.

Matrix ion suppression is particularly common for ESI based LC-MS methods.[250] Ionization within electrospray sources is thought to proceed through either an ion evaporation or charged residue mechanism.[11] Figure 4-1 provides details describing these mechanisms, both resulting in the eventual formation of gas-phase analyte ions.

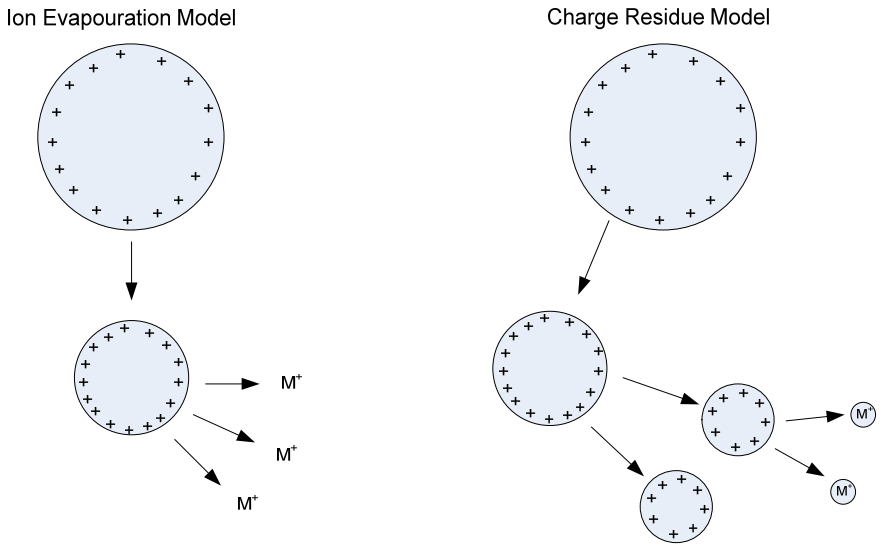


**Figure 4-1. Schematics describing the ion evaporation and charged residue mechanisms.**

Both mechanisms commence with the analyte contained within highly charged solvent droplets in a pre-ionized state. The ion evaporation model is thought to be the dominant process responsible for the ionization of small polar compounds.[285] As highly charged droplets traverse the source environment they begin to shrink through the evaporation of solvent. When the droplets reach a critical radius the field strength at the droplets surface becomes large enough to

eject individual solvated analyte ions into the gas-phase. The charge residue mechanism is more applicable to macromolecules.[7] In this model, highly charged droplets will continuously divide through fission until they contain on average a single analyte molecule. A protein for example will remain trapped within the charged droplet until all solvent molecules have evapourated, leaving a charged gas-phase analyte ion. In both mechanisms the analyte must be pre-ionized prior to reaching the gas-phase. Both methods are also heavily reliant on the physical and electronic properties of the mobile phase composition in order to efficiently generate free gas-phase analyte ions.

A reduction or enhancement in analyte ionization efficiency with ESI is commonly associated with the co-elution of endogenous phospholipids retained through sample preparation, however, the presence of salts or analyte metabolites may also play a role in ion suppression.[286] Co-introduced interferences may compete with the analyte for surface space upon the charged droplets, reducing the efficiency of analyte desolvation. Alternatively, non-volatile matrix components such as lipids or mobile phase modifiers may alter the volatility, viscosity or surface tension of the charged solvent droplets, reducing ionization efficiency as well. Competition for surface space and charge resulting from co-eluting analytes or metabolites may also be the cause of linear dynamic range restrictions associated with ESI determinations at concentrations above $10^{-5}$ M.[287] As a result of these concerns, matrix effects play a significant role in routine bioanalysis by ESI and must be thoroughly investigated to insure precise, accurate results.

APCI has been shown to suffer less severely from matrix ion suppression than ESI.[249,250,288] The sample eluent flow in an APCI-LC-MS method is efficiently vapourized using a heated gas stream. APCI mechanisms proceed within the gas-phase through a series of ion-molecule reactions utilizing an abundant supply of reagent ions. Since ionization occurs entirely post vapourization, ion suppression within APCI workflows is thought to result from a competition for

charge between the analyte and co-eluting sample components. This effect is typically much less impactful than observed for the suppression mechanisms at play in ESI sources, lending APCI suitably toward the analysis of samples containing complex matrices that would otherwise require extensive cleanup or chromatography. APCI, however, often presents reduced sensitivity relative to ESI, which may in turn limit applicability.

Similar to APCI, a number of sources have described APPI-LC-MS workflows to be less susceptible to matrix ion suppression than ESI.[289-292] As previously discussed, ionization in APPI is also the result of critical gas-phase ion-molecule reactions. Ion suppression in APPI is thought to be linked to a disruption of these processes. Co-eluting matrix components may abduct charge from the reagent ion population, consisting primarily of photoionized dopant radical cations or acidic protonated solvent clusters. A reduction in the concentration of the reagent ions through these competitive pathways will inevitably reduce analyte ionization efficiency within APPI sources that are reliant upon maintaining an excess population of reagent ions. Alternatively, charge may be removed directly from the ionized analyte through direct interaction with sufficiently basic co-eluted matrix components. The relative contributions of these processes are unknown, however, it is certain that APPI sources are not free from matrix effects. As such, matrix effects must also be considered for any APPI-LC-MS method, in order to ensure accurate and precise results.

### 4.1.1. Evaluating Matrix Effects in LC-MS

A clinical LC-MS assay must provide accurate, reliable results. Ionization suppression presents the opportunity for false negative determinations, while less commonly, ion enhancement may lead to false positive reporting - particularly a concern for pharmaceutical or forensic analyses. Before any LC-MS/MS method may be validated, it must be first thoroughly evaluated for the

effects various matrices may place upon the results obtained.[286,293] There are two common methods for evaluating the impact of matrix effects upon LC-MS workflows: Post-Column Infusion, and Post-Extraction Addition. Both methods were briefly deployed in the previous chapter to evaluate the effect a human serum matrix placed upon the determination of a panel of steroids. These techniques will be utilized extensively in this section to further characterize matrix effects and determine how they may be controlled or mitigated within the field-free APPI source based upon the selection of ion source parameters.

#### 4.1.1.1. Post-Column Infusion (PCI)

Post-Column Infusion has become a standard method for visualizing the effect that a particular matrix will have upon an LC-MS assay.[294,295] Figure 4-2 presents a simple plumbing diagram, typically adopted for PCI experiments. Chromatographic separation is performed for a sample containing only blank biological matrix. A pure standard solution containing only the analyte of interest is infused through a T-union, combining with the column eluent flow just prior to entering the ion source. A steady-state signal is produced at an MRM transition corresponding to the analyte. The blank matrix sample passes through the column, separating the various biological elements and interferences as a function of time. As the matrix components elute, they suppress the steady-state analyte signal (generally as an extended plug), allowing the expected degree and duration of matrix ion suppression or enhancement to be visualized.

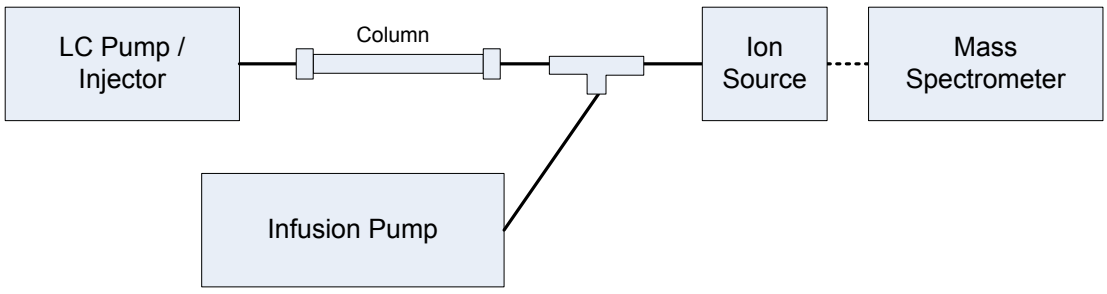


**Figure 4-2. Solvent flow plumbing diagram typically adopted for post-column infusion (PCI) experiments.**

Although primarily a qualitative approach, PCI can provide quantitative data characterizing the degree of suppression relative to the baseline analyte signal, as well as the time required for the signal to return to some percentage (typically 95%) of the initial, uninhibited level. Results obtained through post-column infusion require previous knowledge of the expected analyte retention time. To be useful, PCI experiments also require that a suitable reference matrix be available including all components of the sample matrix, ideally excluding the analyte of interest. PCI experiments may also be time consuming, as best results are obtained when infusing only pure single component analyte standards, meaning each analyte should be characterized separately. This is particularly important for ESI where co-eluting analytes and their metabolites may compete for space upon the surface of charged solvent droplets at elevated gross concentrations.

#### 4.1.1.2. Post Extraction Addition

Post extraction addition is a technique suitable for providing relevant quantitative information regarding the effect matrix ion suppression has upon each analyte in a particular sample.[295,296] In these analyses, two samples are evaluated: one containing only pure mobile phase solvent, spiked with each of the analytes of interest, the other containing blank biological matrix that has been subject to the full sample preparation workflow and then finally spiked to an identical concentration with analyte standards. Both samples are then analyzed using an appropriate LC-MS method. Matrix effects (ME) can be evaluated for each analyte independently using equation 19,

$$ME\,(\%) = B\ /\ A \times 100$$

where A represents the analyte signal response obtained for the sample containing standards only and B is the response for the sample containing a

biological matrix. An ME(%) of 100 indicates that the matrix had no effect on the analyte response. The degree of ion suppression will be indicated by an ME(%) < 100, while ion enhancement is evident from an ME(%) > 100.

#### 4.1.1.3. Robust Linear Regression (RLR)

Robust Linear Regression (RLR),[297,298] may be applied as an extension of Post Extraction Addition, providing a measure for comparing two sets of data or analytical methods, where results are known to have a high degree of variability - the evaluation of matrix effects represents an ideal example. In order to build confidence within results comparing multiple methods, RLR may be employed to reduce the error associated with random fluctuations in a dataset. A standard calibration curve relates two sets of data: one well known (x-axis), and the other measured, containing a high degree of uncertainty (y-axis). In RLR, both sets of data are uncertain. In our example, matrix effects are investigated by plotting analyte peak areas obtained for a sample containing standards only (x-axis), against peak areas obtained for a sample containing the analyte as wells as additional biological matrix components (y-axis). This process is repeated across a range of analyte concentrations in order to build a dataset to which linear regression may be applied. An ideal slope, $m_{RLR}$, of unity denotes that no significant matrix effects are observed. A slope less than one is indicative of matrix ion suppression, while a slope greater than one points to ion enhancement. Nguyen et al. used RLR to investigate the effect an assortment of biological matrices play upon the determination of estrogens, using an ESI-LC-MS method coupled with a variety of sample preparation techniques.[299] RLR was employed to establish confidence within their results. Using this method, they were able to establish which sample matrices required additional preparation measures to reduce ion suppression, furthering assay accuracy. They also used RLR as a diagnostic tool to discern which matrices required only minimal sample preparation and could potentially be analyzed using only pure analyte standards

for the production of calibration curves. Evaluation criterion was established stipulating that $m_{RLR}$ must fall within the range $0.9 < m_{RLR} < 1.1$, in order to yield a positive result. RLR experiments are non-trivial and are somewhat uncommon within the realm of chemical analysis. Such methods require both a significant investment in time and additional rigorous sample preparation. There is a general lack of consensus regarding how LC-MS workflows should be evaluated for matrix effects for purpose of method validation.[300] The implementation of robust regression methods could in the future become a standard component in the validated assessment of matrix effects, offering an improved degree of statistical confidence and reproducibility.

## 4.2. Methods and Materials

### 4.2.1. Instrumentation

Matrix effect characterization experiments were performed upon an Applied Biosystems / MDS Sciex (Concord, ON, Canada) API 3200 series triple quadrupole mass spectrometer. An unmodified Turbo V source was utilized in both ESI and APCI modes. ESI determinations were made using the following optimized ion source conditions: Probe voltage = 5500 V, GS1 = 45, GS2 = 50 and source temperature = 500 $^{o}$C. APCI determinations utilized the following ion source conditions: GS1 = 30 psi, nebulizer temperature = 400 $^{o}$C and discharge current = 4 nA.

The prototype field-free APPI source described in chapter 2 was used for all experiments, including a 4:1 reducing flight tube. Lamp power was supplied using a high voltage power supply, originally designed for use with first generation MDS Sciex field-free Photospray sources. Offset transfer voltage was provided using a stand-alone Stanford Research (Sunnyvale, CA) PS350 programmable DC high voltage supply. Lamp gas was provided from an independently regulated, high purity nitrogen supply at 0.3 LPM. APPI source conditions

optimized at a heated nebulizer temperature of 275 $^{o}$C, with GS1 set to 30 psi. A supply of toluene dopant was infused at 20 μL/min using a syringe pump integrated within the mass spectrometer. All analyses were performed in positive mode with a scan time of 100 ms and a dwell time of 5 ms.

Optimized MS parameters are summarized in Table 4-1. A single MRM transition was monitored for each analyte. The $[M+H]^+$ ion was not observed for androsterone at significant sensitivity. A base peak corresponding to $[M-H_2O+H]^+$ was observed using APCI and ESI, however, the most intense transition found for APPI, (255.2 $\rightarrow$ 159.1), corresponds to a second water loss $[M-2{\cdot}H_2O+H]^+$. This MRM transition is identical to that typically adopted for estradiol (also the product of water loss), leading to order-of-magnitude superior sensitivity by APPI. Estradiol itself was also evaluated using a transition corresponding to the same water loss product, however, retention times varied significantly, allowing for the discrete determination of both analytes. Estrone also yielded a substantial water loss product (m/z 253.2), however, the strongest signal was observed for the $[M+H]^+$ ion. An optimized MRM transition 271.1 $\rightarrow$ 133.0 was monitored for all experiments. All other compounds utilized MRM transitions corresponding to the selection of the $[M+H]^+$ pseudo molecular ion.

**Table 4-1. MS parameters optimized for steroid panel D**

| Compound | Concentration / ppm | Q1 | Q3 | CE | CXP | DP | EP | RT / min |
|---|---|---|---|---|---|---|---|---|
| Cortisone | 1 | 361.1 | 163.1 | 33 | 4 | 50 | 6 | 1.51 |
| Estradiol | 1 | 255.2 | 159.1 | 25 | 3 | 35 | 3 | 1.81 |
| Estrone | 1 | 271.1 | 133.0 | 35 | 3 | 37 | 4 | 1.84 |
| Testosterone | 0.1 | 289.1 | 109.1 | 40 | 3 | 46 | 6 | 1.95 |
| Progesterone | 0.1 | 315.2 | 97.0 | 45 | 3 | 47 | 5 | 2.33 |
| Pregnanediol | 1 | 285.1 | 81.0 | 51 | 3 | 43 | 5 | 3.05 |
| Androsterone | 1 | 255.2 | 159.1 | 25 | 3 | 35 | 3 | 3.22 |

Chromatographic separation was performed isocratically using a Gilson (Middleton, WI) LC pump to provide pre-mixed mobile phase solvents at constant flow rate of 200 µL/min. A 90:10 methanol/water, 0.05% formic acid solvent composition was selected to provide retention times suitable for a high throughput clinical screening LC-MS workflow. All analytes were eluted in less than 5 minutes with an additional 2 minutes provided for column cleanup between injections. 10 µL injections of a steroid panel (table 4-1) were made on-column (Phenomenex, Luna C18, 3µ, 100 x 2 mm) using a manually activated switching valve integrated within the mass spectrometer. For APPI analyses, LC effluent and dopant flows were introduced independently through the modified APCI probe described in Appendix B. For PCI experiments, a second stand-alone Harvard syringe pump (Holliston, MA) was used to provide the continuous infusion of analyte standards at 10 µL/min. The PCI flow was combined with the LC effluent using a T-union prior to entering the ion source.

### 4.2.2. Chemicals

All analytes were initially purchased as dry solids at no less than 97% purity. Cortisone, estradiol, testosterone, and progesterone were purchased from Sigma (St. Louis, MO). Estrone, pregnanediol and androsterone were kindly donated by AB/Sciex (original manufacturer unknown), previously dissolved in methanol to produce standard solutions, each 1 mg/mL. HPLC grade methanol, toluene and formic acid were purchased from Fisher Scientific (Fair Lawn, NJ). Deionized water was obtained from an in-house generator. Human serum and plasma (k2 EDTA) were obtained from Bioreclamations Inc. (Westbury, NY). Surine, simulated urine, was obtained from Dyna-tek (Lenexa, KS).

### 4.2.3. Sample Preparation

Cortisone, estradiol, testosterone, and progesterone solids were individually dissolved in methanol to produce 1 mg/mL stock solutions from which serial dilutions would be made. Single component standards for each of the analytes

were diluted in mobile phase to 1 μg/mL for the purpose of evaluating matrix effects through PCI. These standards were also used to optimize MS and ion source conditions. Finally, a new steroid panel was created incorporating each of the high concentration analyte standards. Final relative concentrations for each analyte are provided in table 4-1. Further dilutions were made as required to perform robust regression analyses.

Human serum (2x charcoal stripped), human plasma (2x charcoal stripped), and Surine, simulated urine, were utilized as representative clinical matrices. Serum and plasma matrices were protein precipitated using the following procedure: 600 μL of matrix was placed in a conical vial to which an additional 1200 μL of methanol was added. The vial was capped and vortexed for 30 seconds. The solution was then chilled for 30 minutes at $4^{o}$C. The vials were then centrifuged for 30 minutes at 9000 rpm. The supernatant was retained and filtered at 0.22 μm. The crashed matrices were then spiked with the steroid panel to produce solutions with a range of analyte concentrations (including matrix containing blanks). Each sample was finally diluted to match isocratic mobile phase conditions. Samples containing the standard steroid panel only (no additional biological matrix added) were produced to match the concentration range and solvent composition of the matrix containing samples.

The simulated urine samples were filtered at 0.22 μm and then diluted in pure solvents to match mobile phase conditions. A 1/10 dilution factor was achieved with respect to the concentration of the stock Surine matrix. Surine samples were spiked with the steroid panel to produce a series of samples, ranging in analyte concentration. A second series of samples was produced, analogous to the serum and plasma samples described above, containing analyte concentrations identical to the Surine containing samples, however, utilizing pure solvents in place of the biological matrix.

## 4.3. Results and Discussion

### 4.3.1. Matrix Suppression Under Optimized Ion Source Conditions

Figure 4-3 presents chromatographic results obtained for the determination of the steroid panel under isocratic, high throughput conditions. Overlaid TIC traces obtained with and without the introduction of crashed human plasma provide a demonstration of the effect a particularly complex matrix may have upon ion source performance.

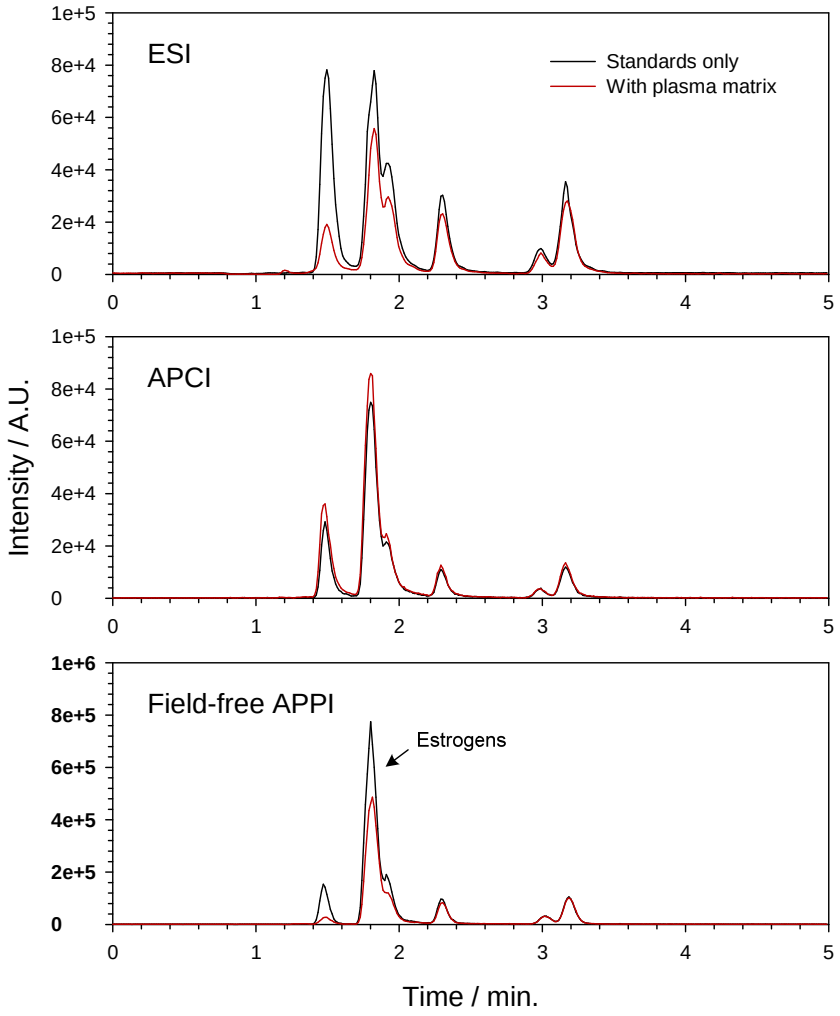


**Figure 4-3. Overlaid TIC chromatograms demonstrating the effect of a crashed plasma matrix upon results obtained for the analysis of a steroid panel using, ESI, APCI and the field-free APPI source. Signal suppression or enhancement is demonstrated relative to signals obtained for the analysis of pure standards.**

Under the selected LC conditions, it was not possible to fully resolve the peaks coinciding with estradiol, estrone and testosterone, however, each of the four remaining analytes was sufficiently isolated. It should be noted that the scales for the chromatograms obtained by ESI and APCI are equivalent, however, the scale for the field-free APPI source is extended by an order-of-magnitude, again demonstrating relative sensitivity enhancement, particularly for estrogens. The results presented in figure 4-3 were obtained under ion source conditions optimized to provide maximum analyte sensitivity. APCI was the source least affected by the introduction of the plasma matrix, with the field-free APPI and ESI sources following respectively. Although APPI signals experienced significant ion suppression, particularly for the earliest eluted analytes, the duration of sensitivity loss appears to be short lived relative to ESI. APCI signals were largely enhanced on the whole by the co-eluted plasma matrix. Signal enhancement with APCI is not uncommon and can in-turn lead to false positive reporting.[301,302] Internal standards may be used to mitigate the effects of signal enhancement or suppression provided suitable isotopically labeled standards are available.

A direct comparison of overlaid chromatograms may appear telling, however, this method will inevitably contain a high degree of run-to-run variability, limiting an accurate assessment of matrix effects. In order to build confidence within the results, robust linear regression was employed and the evaluation of matrix suppression between sources was repeated. Figure 4-4 presents data summarizing an RLR analysis based upon XIC peak areas isolated for cortisone, as a component of the steroid panel. Cortisone was the earliest eluting analyte (RT = 1.51 min.) under the selected LC conditions and was also the most polar of the steroids scrutinized.

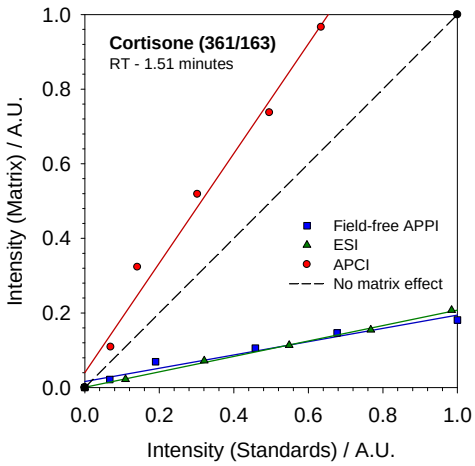


**Figure 4-4. Results summarizing the robust regression analysis based upon XIC peak areas isolated for cortisone. Results compare the signals obtained for the analysis of the steroid panel spiked within a crashed plasma matrix (y-axis) with those obtained using only pure standards (x-axis). ESI, APCI and the field-free APPI source are compared.**

In this experiment, peak areas are plotted for standards only against peak areas obtained for solutions containing crashed plasma matrix - this process was repeated over a range in analyte concentrations. Each data point represents the average of three trials, alternating between pure analyte standards and spiked plasma. The trendline obtained for each ion source provides a measure for quantifying matrix effects. The dashed line represents a theoretical case indicating the absence of matrix effects. Strassnig et al. offered that if signal intensities obtained for two different matrices agree within a confidence limit of 95%, the result of RLR should be a slope of 1.[303] For the analysis of cortisone, ESI and APPI performance were clearly affected the most by the addition of the plasma matrix, presenting RLR slopes of 0.21 and 0.18 respectively. This implies that under the selected set of conditions, cortisone signals are expected to be suppressed approximately 80%. The signals obtained for cortisone using APCI were enhanced by 40% ($m_{RLR}$ = 1.41). Clearly none of the ion sources were free from matrix effects, however, the results suggest that the APCI source would be the least susceptible method for the analysis of cortisone in crashed human plasma under the selected high throughput isocratic conditions. Expanding the RLR method to the entire steroid panel, Figure 4-5 provides regression slopes obtained for each analyte, spiked within a variety of biological

matrices. The results are presented as a function of retention time and may be correlated to each of the analytes using table 4-1. The matrices analyzed included a) diluted Surine (simulated urine), b) crashed serum and c) crashed plasma. The dashed line once again represents a theoretical absence of matrix effects. The field-free APPI source provided the most resistance to ion suppression or enhancement for the analysis of the simulated urine sample. Only the estrogens eluting at 1.9 minutes were subject to sufficient ionization suppression to warrant additional sample treatment (based upon the condition $0.9 < m_{RLR} < 1.1$). The APCI source again experienced significant ionization enhancement in response to the presence of the co-eluting Surine matrix. The effect was consistent for each of the analytes determined from the steroid panel, under the selected LC conditions. ESI responded the least favourably to the Surine matrix, fluctuating between analyte signal enhancement and suppression for the range of steroids tested.

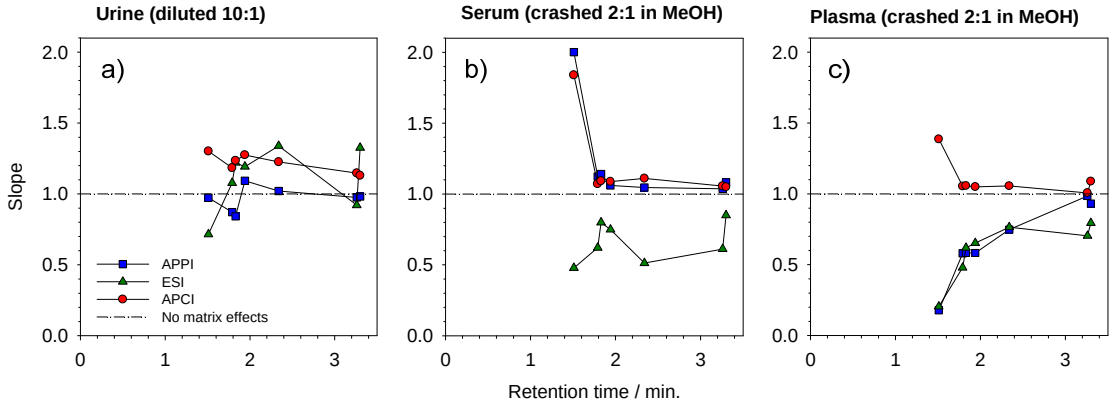


**Figure 4-5. Results obtained for the analysis of the entire steroid panel comparing signals obtained with and without the addition of biological matrices through RLR. Slopes ($m_{RLR}$) for each analyte are plotted against retention time. Analytes may be identified based upon the retention times described in Table 4-1.**

For the analysis of the crashed serum sample (figure 4-5, panel b), ESI signals were each suppressed by more than 20% with the exception of Androsterone, the latest eluting compound. APCI and the field-free APPI source responded both similarly and favourably. In each case, only cortisone experienced significant ionization enhancement, with all other analytes being largely resistant to matrix effects. Blank plasma injections presented no significant signals for

cortisone (data not shown), so we may assume that signal enhancement in this case is a purely matrix induced effect. The root cause of ionization enhancement in APCI and APPI is poorly understood, however, we assume this to be the result of a gas-phase process. Ionization enhancement in APCI has been shown to be more prominent with high organic solvent concentration, similar to the conditions utilized here.[304] As a result, some degree of ionization enhancement is not unusual or unexpected. Similarly, ion suppression within these sources could result from the formation of solid neutral analyte precipitates with co-eluted matrix elements, post-vapourization.[304] An alterative suppression mechanism with the APPI source could result from a competition for available charge between the analyte neutrals and basic matrix components. This could lead to depletion in the reagent ion population, and could thus impact analyte ionization efficiency. In either case, matrix effects are likely the result of an overall combination of mechanisms and are expected to be both compound and assay dependent.

Crashed plasma (figure 4-5, panel c) represents the most complex of the matrices scrutinized. Similar to the analysis of serum, APCI responded quite well to the presence of the plasma matrix. Signals for the field-free APPI and ESI sources were significantly suppressed indicating that additional sample preparation methods should be employed. To summarize, across each of the matrices and analytes surveyed, ESI was by far the least resistant to matrix effects with only 2 of the 21 analytes responding favourably to presence of complex biological matrices under the selected high throughput LC conditions. APPI and APCI responded the best to matrix effects, with 10 and 11 of the analytes being insignificantly suppressed or enhanced respectively.

### 4.3.2. Characterizing Matrix Effects Within the Field-free APPI Source

Matrix effects are assumed to be compound dependent. A number of reports have suggested that the degree of suppression or enhancement can vary significantly between analytes of varying polarity.[286,294,295] This principle effect

was quickly evaluated for the field-free APPI source using post-column infusion to visualize the suppression of each analyte component included within the steroid panel for the analysis of crashed plasma. Figure 4-6 presents normalized XIC chromatograms obtained for the PCI of the full steroid panel. With the exception of the XIC for cortisone, each of the steroids responded nearly identically to the presence of co-eluted matrix materials. In each case, suppression began with the elution of the matrix plug at 1.2 minutes and did not return to 95% of the baseline level for approximately 1.5 minutes (although a small, unidentified suppression event also occurs at ~ 7 minutes).

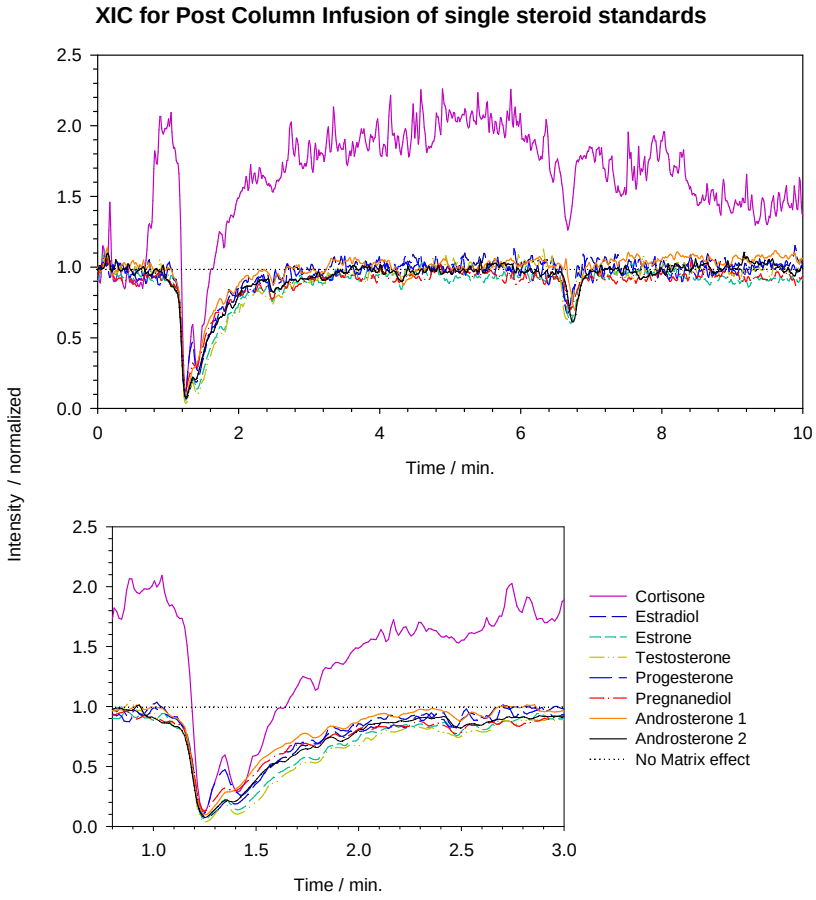


**Figure 4-6. Overlaid and normalized XIC chromatograms obtained through post-column infusion, for the analysis of blank, crashed human serum. Results demonstrate the degree and duration of ion enhancement and suppression experienced by each of the analytes included within the steroid panel. Each analyte was infused as a pure single component standard solution. Experimental ion source conditions optimized to provide maximum analyte sensitivity.**

Aside from cortisone, the data suggests that the effects of matrix suppression may be assumed similar for compounds possessing the same basic structure or containing common functionalities. The anticipated degree of matrix suppression can then be estimated for additional compounds (of similar polarity) based upon retention times determined for analytical standards under the same separation conditions. Given the results for cortisone, however, a method must still be verified in order to avoid false positive or negative reporting, particularly for highly polar, early eluting compounds.

### 4.3.3. A Parametric Evaluation of Matrix Effects

Post-column infusion was also used to evaluate the impact of variable ion source parameters upon resulting matrix effects. Others have demonstrated that ion source conditions and geometry may influence the degree of matrix ion suppression or enhancement.[305] We have previously observed that for the general analysis of steroids through proton transfer, the field-free APPI source tends to optimize empirically toward lower nebulizer temperatures. Figure 4-7 presents PCI results for testosterone, monitoring XIC response for the analysis of crashed plasma over a range of vapourizer temperatures. At low temperatures (i.e. 275$^{o}$C), the degree of ion suppression was minimized. Signal suppression began at around the 1-minute mark and was sustained for approximately 2-minutes. At higher temperatures (i.e. 475$^{o}$C), however, the degree and duration of suppression was amplified, extending for nearly 10 minutes post-injection, before returning to the baseline level. This observation further lends optimization of field-free APPI for steroidal assays, toward low temperature source conditions.

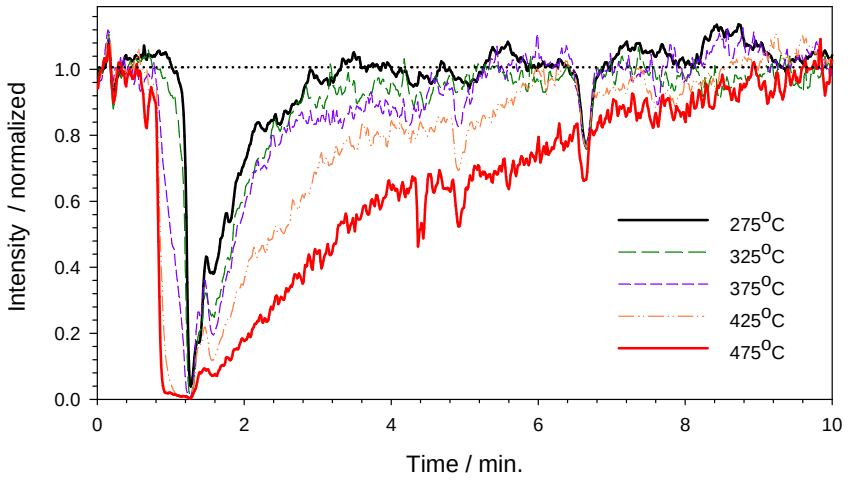


**Figure 4-7. PCI results obtained for testosterone, monitoring XIC response for the introduction of crashed, blank human plasma at a variety of heated nebulizer temperatures.**

Any attempt to assign a mechanism to this observation would be speculation at this point, however, we feel the result is noteworthy and should be considered during method development. It would be interesting to explore the temperature effect for alternative analyte classes such as highly polar pharmaceutical metabolites or non-polar environmental compounds, ionized through the charge exchange mechanism.

The parametric investigation of ion source conditions was extended to include nebulizer gas flow rate. Figure 4-8 provides results for PCI experiments monitoring the effect of GS1 pressure upon the degree of plasma induced matrix suppression. The XIC for testosterone was again monitored while varying the GS1 parameter from 20 to 80 psi. The offset transfer voltage was correspondingly adjusted to provide maximum analyte sensitivity, in response to the change in axial ion velocity associated with the nebulizer gas flow rate. The degree of ion suppression associated with the elution of the plasma matrix was observed to decrease steadily with increased nebulizer gas pressure. This is of course opposite to the trend used to optimize sensitivity for the analysis of most steroids.

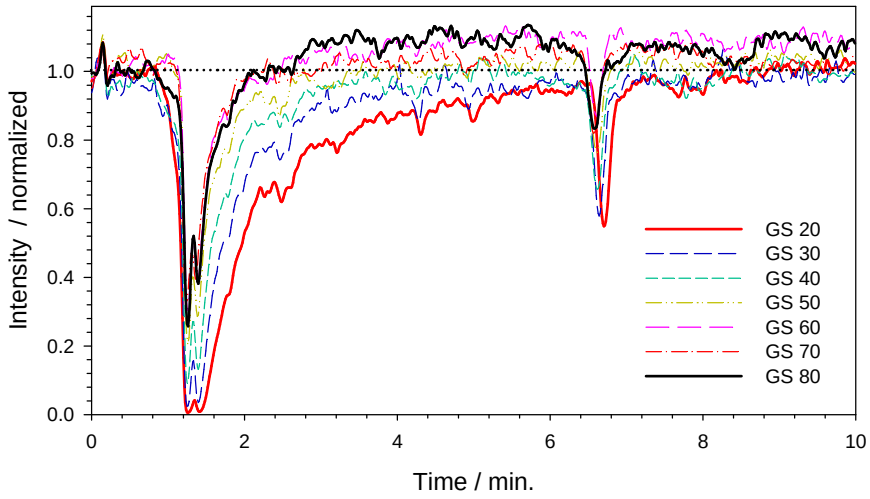


**Figure 4-8. PCI experiments monitoring the effect of nebulizer gas flow (GS1) upon the degree of matrix suppression induced by the introduction of crashed human plasma. XIC results for the infusion of testosterone are provided.**

In order to build confidence within these observations, the effect of nebulizer gas flow rate upon resultant ion suppression was characterized using the robust regression method. The first panel in figure 4-9 demonstrates the effect of GS1 on $m_{RLR}$ obtained for cortisone. The slope is shown to increase with decreased nebulizer gas pressure, approaching unity at GS1 = 80, indicating that a very high resistance to matrix effects is achieved. The second panel extends the RLR analysis to the rest of the steroid panel, monitoring $m_{RLR}$ as a function of GS1 for each component of the steroid panel. The general trend for each analyte appears to be improved resistance to ion suppression with increasing nebulizer gas flow. Under the selected high throughput isocratic conditions, while adopting a nebulizer gas pressure of 80 psi, it was determined that each of the 7 analytes exhibited no significant ion suppression or enhancement (satisfied by the condition: $0.9 < m_{RLR} < 1.1$).

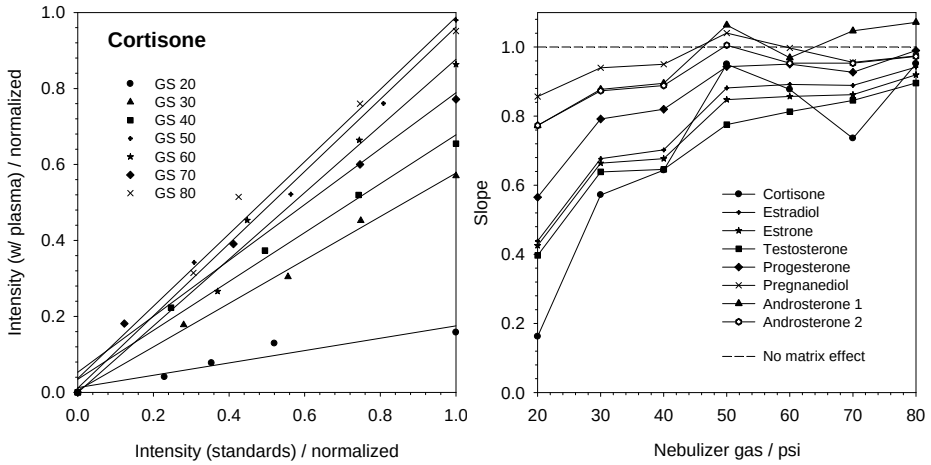


**Figure 4-9. (left) Effect of nebulizer gas pressure (GS1) upon XIC results obtained for cortisone, introduced as a component of the steroid panel. Results are examined through robust linear regression. (right) RLR results expanded to the entire steroid panel showing $m_{RLR}$ as a function of nebulizer gas pressure for each analyte.**

The evaluation was extended to a practical demonstration through the analysis of spiked plasma containing the steroid panel. Figure 4-10 presents overlaid TIC chromatograms obtained for the determination of the steroid panel spiked within a plasma matrix and within pure solvents only. The results compare both the maximum and the minimum GS1 settings. At low gas flow (GS1 = 20 psi), the TIC was suppressed dramatically, particularly for the first four eluted analytes. Moving to 80 psi, absolute signal intensities were diminished by about 50% on average. This trade-off in sensitivity, however, was balanced by the apparent elimination of ion suppression at the higher nebulized gas flow rate. Although at this point we may only speculate as to the underlying mechanisms responsible for this effect, our results present an important new finding that should not be overlooked. The ability to manage the degree of matrix suppression through parametric optimization could represent another valuable advantage for the field-free APPI source for routine high throughput workflows. Provided suitable sensitivity is within reach, an APPI-LC-MS method may be adjusted parametrically to provide fast, accurate determinations that are minimally susceptible to matrix effects.

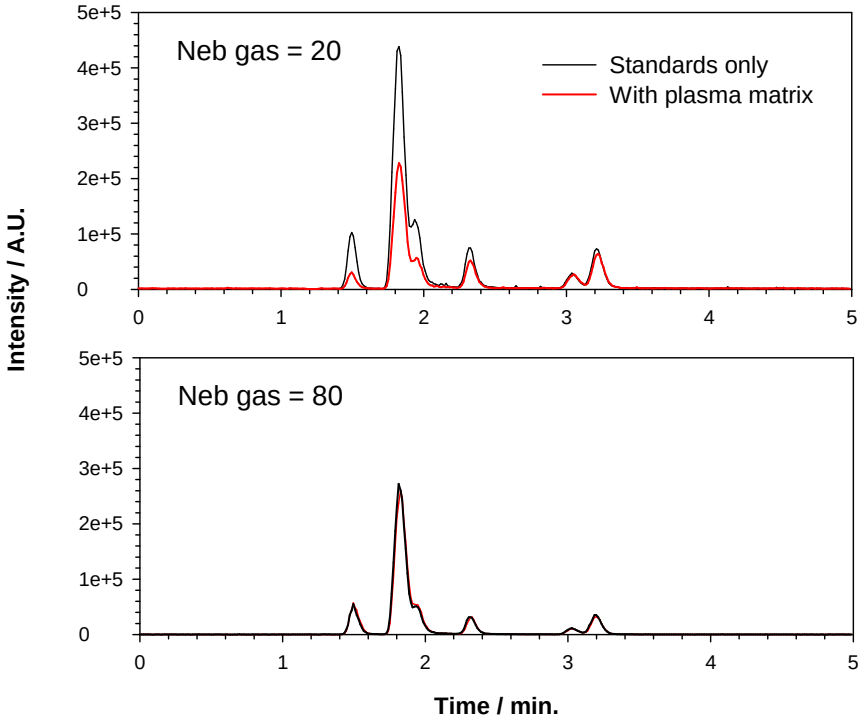


**Figure 4-10. Overlaid TIC chromatograms obtained for the determination of the steroid panel spiked within a crashed plasma matrix and within pure solvents only. Chromatograms compare results obtained at low (20 psi) and high (80 psi) GS1 pressure settings.**

In chapter 2 we identified that analyte ion production will increase with a decrease in nebulizer gas flow (see section 2.3.1.1). Lower flow rates are assumed to result in an effective increase in the gas-phase neutral analyte concentration and in-turn improved analyte ion yield. We speculate the same could be said for the matrix concentration; at high nebulizer gas pressures (i.e. 80 psi) the concentration of matrix components would be effectively diluted. A potential consequence of this would be a decrease in the consumption of solvent cluster reagent ions through interaction with interfering matrix neutrals. This represents a potential mechanism which could be used to explain the reduced matrix effects observed at high nebulizer gas settings; however, further investigation is needed to confirm this hypothesis. This newly identified effect linking nebulizer gas flow rate to matrix effects could impact assay optimization. A trade-off is presented where sensitivity may be sacrificed to provide reduced susceptibility to matrix effects. Under conditions where matrix effects are

presumed to be minimal, GS1 may be tailored toward lower values providing improved analyte sensitivity.

Post-column infusion was again utilized to determine if geometric source parameters have an impact on the degree of matrix ion suppression. Increasing the length of the field-free reaction zone (flight tube length) has also been shown to correlate with increased analyte sensitivity (see section 2.3.3.1). Figure 4-11 shows the normalized results of a PCI experiment characterizing the analysis of the steroid panel, while surveying a range of flight tube lengths. The XIC traces shown for testosterone appear to be largely insensitive to the change in flight tube length with respect to the severity of ion suppression. Similarly, figure 4-12 demonstrates that the degree of ion suppression is unaffected by the restriction of the field-free reaction zone profile, produced through the adaptation of various conical shaped flight tubes. Decreasing the flight tube diameter has been shown to have a significant affect on analyte ionization efficiency (see section 2.3.3.2), however, no correlation was observed to the effects of matrix suppression. These experiments suggest that matrix effects within the field–free APPI source are not likely connected to changes in ion transmission. That said, changes to nebulizer gas flow rate will likely affect ion transfer efficiency to some extent, however, the true impact of this parameter has yet to be determined.

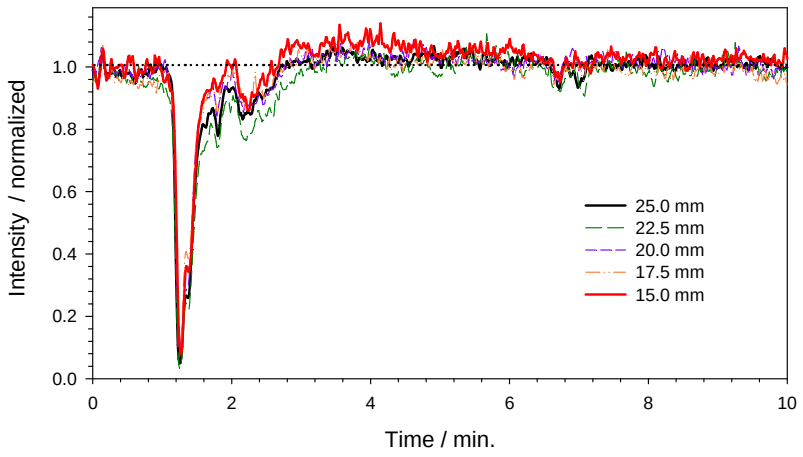


**Figure 4-11. Normalized XIC results for the post-column infusion of a testosterone standard, demonstrating the effect of flight tube length on ion suppression or enhancement. Results shown for the introduction of blank crashed human plasma.**

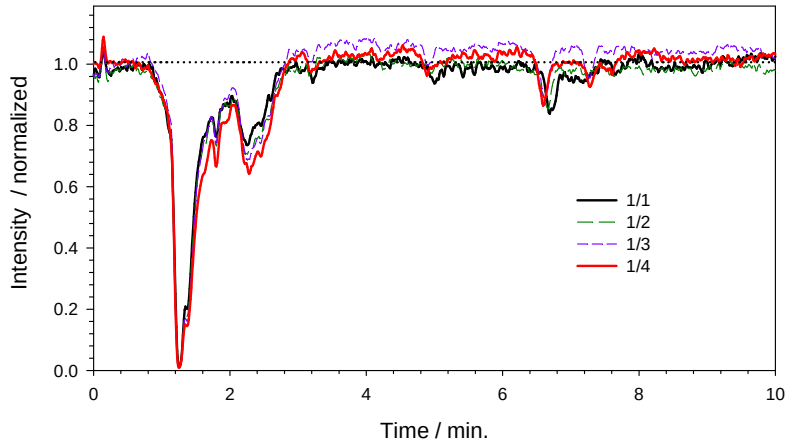


**Figure 4-12. Normalized XIC results for the post-column infusion of a testosterone standard, demonstrating the effect of flight tube diameter upon the matrix effects observed for the analysis of crashed human plasma.**

## 4.4. Conclusions

Limited susceptibility to matrix effects is an advantage commonly associated with APPI sources, particularly when compared to ESI. These reports, however, are often largely empirical and seldom provide a thorough evaluation with statistical confidence. In this chapter we used a robust linear regression method to characterize the relative merits of APCI, ESI and the new field-free APPI source with respect to their resistance to matrix ion suppression or enhancement. The post-column infusion technique was also utilized as a quick diagnostic tool for qualitatively visualizing matrix effects. Under ion source conditions selected to optimize analyte sensitivity, APCI was shown to suffer least from matrix effects. Further, signals obtained for the analysis of Surine, serum and plasma were often enhanced with APCI. Over-estimated results present the potential for false positive reporting, and are every bit as significant as results influenced by ion suppression. APPI responded similarly to APCI, however, suffered more under the influence of the highly complex crashed plasma matrix. As expected, matrix effects influenced ESI the most drastically, positioning it as the least attractive ion source for high throughput, rapid screening workflows.

A short parametric analysis of the factors influencing matrix effects within the field-free APPI source was also completed. This study yielded two interesting results: First, matrix effects may be minimized through use of lower heated nebulizer temperatures, at least for the analysis of steroids within some biological matrices. Second, nebulizer gas flow rate, GS1, was shown to have a direct impact on the degree and duration of matrix suppression within the APPI source. As an example, for the analysis of crashed human plasma, use of a high GS1 setting was shown to effectively eliminate the impact of matrix ion suppression for the determination of a steroid panel. The mechanisms surrounding these condition dependent matrix effects are still uncertain, and will require further study. These observations do suggest that there is potential to control or minimize the role matrix effects, allowing one to tailor an assay toward either highly sensitive or highly accurate steroidal determinations.

# Chapter 5. Discussion and Conclusions

In this concluding chapter we will revisit the objectives and motivations presented at the beginning of this research project. Like any body of work extending over many years, research goals were forced to continually evolve with the development of new ideas and discoveries, leading to fresh avenues of research. Several preliminary objectives were successfully accomplished, while others must now be transferred to the realm of future research. Still, other findings and results will be summarized that were not anticipated by the author at the project's onset. The final section of this dissertation will include a number of suggested research topics that the author believes could present interesting directions for future device development, characterization and application.

## 5.1. Summary of Research Objectives

### 5.1.1. Development of a Next Generation APPI Source

There are currently two distinct APPI ion source design configurations: first-generation closed-geometry devices incorporating an elongated, field-free reaction zone, and open-geometry devices that do not include any provision for extended ion-molecule reactivity. The latter of these device designs are today the only commercially manufactured APPI sources available for LC-MS applications. To this end, however, there is evidence to suggest that the early field-free design may provide the best overall performance of the two configuration alternatives. To our knowledge, until now, there has never been a comprehensive head-to-head comparison of the two APPI methods, with the expressed intention of evaluating relative performance.

Our preliminary goal was satisfied with the production of a prototype, orthogonal geometry field-free APPI source, modeled upon the dimensions and functionality of the first-generation APPI sources. This device incorporated a stainless steel

source block, including an extended field-free reaction region, mounted to the outlet of a heated nebulizer. The prototype device was built around a modified housing of a TurboV ion source facilitating a performance comparison against a commercially available, open-geometry Photospray source.

Our field-free device was found to provide significantly enhanced performance over the incumbent Photospray design, routinely delivering order-of-magnitude scale improvements in sensitivity for the analysis of a variety of clinically and environmentally important analytes. In a second performance comparison, the field-free source was evaluated against a prototype, Syagen technologies, open-geometry APPI source. This device incorporated a proprietary high radiant output RF photoionization lamp. Similar relative performance was observed between the field-free source and the alternative open-geometry source design. Most importantly, this study has finally demonstrated through head-to-head comparison, that increased lamp energy does not tend to lead to improved analyte ionization efficiency – a long-standing claim of the manufacturer.

The performance of the prototype device was thoroughly characterized, evaluating the role of various user optimizable source parameters, including nebulizer positioning and temperature, lamp and nebulizer gas flow rates, transfer field voltage and lamp current. Analyses were repeated numerous times for a range of sample types and under a variety of LC conditions, in order to build confidence within our results. The device was shown to be robust and easily optimizable allowing for maximum sensitivity and reproducibility. Operation of the prototype device presented no limitations that are not experienced by current alternative MS ion source designs.

A cursory examination of various geometric source block dimensions was also performed, leading to an improved understanding of the factors that may ultimately limit source performance. Most significantly, it was identified that increases to the length of the field-free reaction zone provided proportional

improvements to overall performance, taking advantage of the kinetics associated with the analyte ion formation and loss processes. Based upon our preliminary evaluations, we determined that increasing field-free length will lead to an increase in analyte sensitivity, at least until the population of reagent ions has been exhausted or alternative ion loss mechanisms become a significant factor.

The impact of charge recombination was also considered as theory suggests that it should represent the dominant ion loss process within the field-free source design. The in-source recombination of positive and negative charge carriers within the field-free region will lead to a continual decrease in total ion current delivered, with increased flight tube length. Our hypothesis suggests that ion transmission is ultimately space-charge limited, therefore provided a larger percentage of analyte ion current is maintained, improved overall analyte ion transmission through the MS interface can be recognized by reducing the TIC. Open-geometry sources that exclude an extended field-free region limit ion recombination as a result of near-immediate charge separation. These devices have been shown to produce significantly higher total ion currents than are attainable with the field-free source design. Despite increased total ion currents, however, the open-geometry sources fail to provide superior analyte sensitivity. The mechanisms proposed supporting these empirical observations are at best speculative, however, opening the door for future consideration.

Early results were presented at industry conferences and a significant amount of excitement was generated. APPI technologies are under-employed, exclusively utilized for the niche analysis of highly non-polar analytes. Order-of-magnitude scale enhancement to sensitivity for the analysis of PAHs, flame-retardants, and petrochemical products positions field-free APPI as an attractive potential successor to current open-geometry APPI sources. Questions still remained, however, as to how the performance of the field-free source compares with

alternative ionization methods such as ESI and APCI for the analysis of more polar analytes.

### 5.1.2. Characterization Relative to ESI and APCI

First-generation field-free APPI sources were shown to be competitively amenable to the analysis of a variety of polar analytes. The shift to manufacture of exclusively open-geometry APPI devices has led to performance delivery below that attainable with ESI and often times APCI sources. As a result, the modern widespread adaptation of APPI within these fields has been restricted. Here, however, we have demonstrated that the field-free APPI source, may once again establish the potential for APPI to provide significantly enhanced ionization efficiency over the traditional sources, at least for the analysis of clinically important polar steroids.

The relative performance of our field-free device was evaluated through the analysis of a broad panel of steroids using flow injection, extended gradient and high throughput isocratic LC methods. The field-free source was shown to routinely out-perform ESI and APCI for all analytes tested. These relative results were consistent with early reports, which cited enhanced performance using first-generation APPI sources. Best results were obtained for the determination of estrogens, again providing order-of-magnitude sensitivity enhancement over ESI. The response for most other steroids indicated advanced sensitivity ranging from 2-5 fold, while demonstrating superior resistance to ion suppression, resulting from the analysis of human serum. The sensitivity attained for the analysis of both neutral forms of vitamin D and their metabolites was also considered. The field-free APPI source was found to provide 5-9 fold greater sensitivity than APCI using a fast isocratic LC method. Clearly, the potential has been demonstrated for APPI to provide the best overall performance for the analysis of both polar and non-polar clinical analytes.

### 5.1.3. Evaluation of Matrix Effects

In his 2005 review paper, Taylor described matrix effects as the Achilles' heel of LC-ESI-MS spectrometry, a testament to the potentially destructive impact of ion suppression or enhancement upon the accuracy of real chemical determinations.[295] APPI has been described through numerous outlets as being less susceptible than ESI to matrix effects, however, this is seldom demonstrated quantitatively with a high degree of confidence. We feel this is an important and often overlooked attribute associated with APPI that justifies further recognition and exploration.

In Chapter 4 we compared the performance of the field-free APPI source with both ESI and APCI for the analysis of a broad panel of clinically relevant analytes spiked within several complex biological matrices including: human plasma, serum, and a simulated urine matrix. A novel Robust Linear Regression method was applied to quantify, with confidence, ion suppression among sources using a high throughput LC-MS screening method. As expected, ESI was by far the most susceptible to ion suppression, furthering the need for rigorous sample preparation. APPI and APCI were not immune to matrix effects, however, the results indicate that for routine analysis they certainly represent superior options to ESI. These results were generally reproducible and consistent, however, they were also shown to be variably dependent on the source parameter selection, separation and mobile phase conditions, and analyte polarity.

Our most interesting results were obtained for the field-free source for the analysis of the clinical steroid panel within a complex crashed plasma matrix. Two parametric correlations were discovered. First, the extent and duration of ion suppression was profoundly dependent upon vapourizer temperature. This effect was characterized through post-column infusion, leading to the conclusion that, for best results, APPI methods should be optimized toward reduced temperatures. The second correlation considers that ion suppression varied inversely with nebulizer gas flow rate (GS1). While operating at elevated flows, it

was observed that susceptibility to matrix effects could be dramatically reduced or even eliminated. This effect coincides, however, with reduced analyte sensitivity, presenting a trade off in which sensitivity could be sacrificed in order to improve assay accuracy. The mechanisms behind our parametric observations have yet to be established, however, they do represent exciting new benefits associated with APPI methods.

## 5.2. Future Research Directions

### 5.2.1. Performance Evaluation for Alternative Sample Types

This report considered a relatively narrow range of compounds and sample types. Non-polar analytes such as PAHs for example, were already known to ionize most effectively using APPI. Conversely, the determination of an assortment of steroids was selected repeatedly to compare source performance using a relevant class of compounds of particular interest to the rapidly expanding clinical research field. It is now necessary to expand the performance evaluation to additional analyte classes. This could include pharmaceutical compounds and even various clinically important metabolites such as basic steroid glucuronides. Many of these compounds may already be efficiently ionized by ESI and even APCI, however, this should not preclude the use of APPI. Additionally, the analysis of oil and petroleum samples represents the fastest growing application for APPI technologies. Application of the field-free APPI source to this field would require the development of a new prototype suitable for interfacing with high-resolution MS technologies; however, the potential for improved sensitivity could be very attractive to petrochemical researchers.

### 5.2.2. Continued Source Optimization

The primary goal of this research project was to establish through head-to-head comparison, the relative merits of the open- and closed-geometry APPI source

designs. From this work, a prototype orthogonal field-free APPI source was created. The device geometry, however, was only briefly refined and remains far from optimized. Further efforts are needed to develop the current field-free device based upon the principles of primary reagent ion production, secondary ion-molecule reaction chemistry and ultimately analyte ion transmission.

A key geometric parameter requiring additional attention should be the optimization of the extended field-free reaction length. We have yet to establish true limits to analyte ion formation and transmission based upon the modification of the flight tube dimensions. At what point does increased flight tube length no longer result in improved analyte sensitivity? We expect that ion transmission through the MS sampling orifice will be ultimately space charge limited. Total ion current was shown to decrease continuously with increased field-free length – the result of unimpeded charge recombination. An evaluation of ion current transmission could be used to optimize ion transfer through the orifice plate based upon the modification of the field-free transit length. Ion currents leaving the field-free region could be tailored to match the acceptance limits of the MS interface. This future empirical work was described in more detail within the theory and discussion sections of chapter 2 and should be considered among the logical next steps toward device optimization.

### 5.2.3. Dopant Considerations, Delivery, and Source Introduction

There has been a general movement to increase the fundamental understanding of the dopant chemistry, deemed critical to APPI source performance. Many novel dopant candidates (including numerous mixtures) have been explored, with the intention to enhance APPI sensitivity. Today there is still much to learn, however, concerning the link between geometric source design and the mechanisms surrounding reagent ion chemistry. Appendix A briefly touched upon some observations that evolved along this path. Here we discussed the effect of flight tube length upon the ionization yield for some non-polar PAHs

through the charge transfer pathway using alternative dopants such as anisole and chlorobenzene. There is still much work to be done in order to generate a complete understanding of the fundamental APPI mechanisms and how they might be affected by device design.

Dopant flow is an additional concern. Dopant is generally delivered using a dedicated mechanical solvent pump or stand-alone syringe infusion pump. Both of these methods, however, introduce prohibitive costs as well as technical limitations, opening the door for alternative methods. Appendix B presents previous work related to the development of a novel pneumatic solvent delivery system. Although this design was shown to be functionally suitable for APPI dopant delivery, a refined, sophisticated design including automated control could lead to improved robustness, ease-of-use and reproducibility. We envision that a dopant delivery device based upon the design presented in appendix B could one day be included with all APPI sources.

The introduction of dopant to the ion source presents another significant technical concern. There are again a variety of options available to APPI users. Modern AB/Sciex Photospray sources utilize a crude auxiliary nebulizer to vapourize dopant into the heated nebulizer gas stream. This method is ostensibly effective, however, we postulate that this design will suffer from carryover issues, should modification of the dopant composition be necessary. Otherwise, all Syagen style open-geometry APPI sources provide no dedicated means for introducing dopant. Instead, dopant must be added directly to the LC effluent either as part of the pre-mixed solvent composition, or through post-column addition through a T-union. This latter method tends to lead to solvent miscibility issues, often impairing signal stability as a consequence of effluent sputtering. Appendix C introduced a Y-tube dopant introduction probe that was intended to address these concerns. This device performed adequately for our purposes, however, it was not found to be particularly robust or easily serviceable. A refined design or an all-together alternative means of discretely

introducing dopant would definitely benefit APPI usability, improve flow stability and aid to minimize carryover concerns.

### 5.2.4. Further Characterization of Matrix Effects

In chapter 4 we presented results describing the parametric control of matrix ion suppression with the field-free APPI source through the analysis of a steroid panel spiked within a human plasma matrix. To our knowledge, no similar parametric effects have been previously reported for APPI or any other ionization method. A lot of work is now necessary to properly characterize these observations, as the underlying mechanisms are still undetermined. It was discerned that the degree and duration of matrix ion suppression could be influenced by both vapourizer temperature and nebulizer gas flow rate. It was determined that field-free transit length and diameter had no discernable effect on the impact of ion suppression. Aside from this handful of variables little is certain regarding these effects. It is unknown if similar effects will be applicable to the other ionization methods like APCI or ESI. We also lack evidence to support these effects being universal phenomena. Do they apply only to the analysis of neutral steroid compounds? Do the effects translate to non-polar molecules, ionized through the charge transfer mechanism? Does dopant reagent ion chemistry play a role? Matrix effects are a real and significant concern that is widely known to impact the accuracy and the validity of analytical determinations. We believe that moderating the effects of ion suppression and enhancement could play a critical role in routine LC-MS method development.

### 5.2.5. Dual Mode Source Development

APPI is already regarded as the most universal LC-MS ionization method, amenable to the analysis of both polar and non-polar compounds. Of these compounds, however, photoionization may of course not provide the highest sensitivity or lowest detection limits, simply the broadest overall compound

coverage. In some instances it may be desirable to have the ability to analyze highly polar compounds through ESI or ESI-like functionality without having to switch between ion sources. A dual-mode source could be developed to satisfy this requirement, incorporating the functionality of both APPI and ESI into a single robust device. The concern, however, would of course be that compromise might be necessary to adapt both ionization methods. Dual-mode sources often provide performance that could be described as offering the “worst of both worlds”, rather than the “best of both worlds”.

## 5.3. Concluding Remarks

The most important test for the field-free APPI source will occur within the coming years, if industry or other researchers adopt the technology. APPI is no longer young and it is far from a novel technique. Our device mimics the design of its first-generation predecessors in both function and geometry. Both devices, in their time, have now been demonstrated to provide the best relative overall performance for the analysis of the broadest range of compounds. Slowly but surely the fundamental mechanisms governing APPI performance are also becoming increasingly well understood, however, it has been established that there is still room to grow. Continued geometric optimization can still lead to additional performance dividends, inevitably furthering technique acceptance.

As exciting as the potential for APPI technologies may be, momentum is the key to sustaining its development. In 2004, similar momentum was lost following the shift to exclusively open-geometry APPI platforms, presenting only devices that stifled performance expectations. Now there is an opportunity to correct this mistake. Science may search for alternatives, however, ultimately the best alternatives must still be embraced. The largest hurdle will be swaying the minds of industry. ESI and APCI are thoroughly entrenched as industry standard technologies. These sources are often operated as “black boxes” for generating

ions – sample goes in, ions come out. APPI is mistakenly viewed as more convoluted – a niche technique requiring high user input and offering limited extensive benefit. This isn't to say that APPI hasn't attracted its followers and applications, however, it remains viewed as a novel technique, applicable only to a restricted range of non-polar compounds. This perception is simply not true. We have confidence that given the opportunity, supported by its universality and improved performance, field-free APPI could ultimately supplant other ionization methods as the backbone of the clinical and pharmaceutical LC-MS workflow.

# Bibliography


[1] Gillespie, T. A., & Winger, B. E. (2011). Mass spectrometry for small molecule pharmaceutical product development: a review. *Mass Spectrometry Reviews*, *30*, 479- 490.

[2] Dooley, K. C. (2003). Tandem mass spectrometry in the clinical chemistry laboratory. *Clinical Biochemistry*, *36*, 471- 481.

[3] Covey, T. R., Thomson, B. A., & Schneider, B. B. (2009). Atmospheric pressure ion sources. *Mass Spectrometry Reviews*, *28*, 870- 897.

[4] Grebe, S. K. G., & Singh, R. J. (2011). LC-MS / MS in the clinical laboratory – Where to from here? *Clinical Biochemistry Rev*, *32*, 5-31.

[5] Dooley, K. C. (2003). Tandem mass spectrometry in the clinical chemistry laboratory. *Clinical Biochemistry*, *36*, 471- 481.

[6] Ouweland, J. M. W. van den, & Kema, I. P. (2012). The role of liquid chromatography – tandem mass spectrometry in the clinical laboratory. *Journal of Chromatography B*, *883-884*, 18-32. Elsevier B.V.

[7] Dole, M., Mack, L. L., Hines, R. L., Mobley, R. C., Ferguson, L. D., & Alice, M. B. (1968). Molecular beams of macroions. *Journal of Chemical Physics*, *49*, 2240-2249.

[8] Fenn, J. B. (1993). Ion formation from charged droplets: Roles of geometry, energy and time. *American society for mass spectrometry*, *4*, 524-535.

[9] Gaskell, S. J. (1997). Electrospray: principles and practice. *Journal of mass spectrometry*, *32*, 677-688.

[10] Bruins, A. P. (1998). Mechanistic aspects of electrospray ionization. *Journal of Chromatography A*, *794*, 345-357.

[11] Kebarle, P., & Verkerk, U. H. (2009). Electrospray: from ions in solution to ions in the gas phase, what we know now. *Mass Spectrometry Reviews*, *28*, 898- 917.

[12] Wilm, M. (2011). Principles of electrospray ionization. *Molecular & Cellular Proteomics*, *10*(7).

[13] Crotti, S., Seraglia, R., & Traldi, P. (2011). Some thoughts on electrospray ionization mechanisms. *European journal of mass spectrometry*, *17*, 85-99.

[14] Cole., R. B. (1997). Electrospray ionization mass spectrometry: fundamentals, instrementation, and applications. Wiley, New York.

[15] Schneider, B. B. (2002). New methods and instrumentation for electrospray ionization - mass spectrometry. University of British Columbia, Vancouver, BC.

[16] Iribarne, J. V., & Thomson, B. A. (1976). On the evaporation of small ions from charged droplets. *Journal of Chemical Physics*, *64*(6), 2287-2294.

[17] Kind, T. *UC Davis: Fiehn Metabolics Lab.* Mass Spectrometry Adduct Calculator. http://fiehnlab.ucdavis.edu/staff/kind/Metabolomics/MS-Adduct-Calculator/

[18] Byrdwell, W. C. (2001). Atmospheric pressure chemical ionization mass spectrometry for analysis of lipids. *Lipids*, *36*(4), 327-346.

[19] Balogh, M. P. (2006). Ionization revisited. *LCGC North America*, *24*(12), 1-6.

[20] Carroll, D. I., Dzidic, I., Stillwell, R. N., Haegele, K. D., & Horning, E. C. (1975). Atmospheric pressure ionization mass spectrometry: Corona discharge ion source for use in liquid chromatograph-mass spectrometer-computer analytical system. *Analytical chemistry*, *47*(14), 2369-2373.

[21] Good, A., Durden, D. A., & Kebarle, P. (1970). Ion – molecule reactions in pure nitrogen and nitrogen containing traces of water at total pressures 0.5 – 4 torr . Kinetics of clustering reactions forming H+(H2O)n. *Journal of Chemical Physics*, *52*, 212-221.

[22] Zenobi, R., & Knochenmuss, R. (1998). Ion formation in MALDI mass spectrometry. *Mass Spectrometry Reviews*, *17*, 337-366.

[23] Dreisewerd, K. (2003). The desorption process in MALDI. *Chemical Reviews*, *103*(2), 395-425.

[24] Knochenmuss, R. (2006). Ion formation mechanisms in UV-MALDI. *Analyst*, *131*, 966-986.

[25] Gibson, G. T. T., Mugo, S. M., & Oleschuk, R. D. (2009). Nanoelectrospray emitters: Trends and perspectives. *Mass Spectrometry Reviews*, *28*, 918- 936.

[26] Raffaelli, A., & Saba, A. (2003). Atmospheric pressure photoionization mass spectrometry. *Mass spectrometry reviews*, *22*, 318- 331.

[27] Robb, D. B., & Blades, M. W. (2008). State-of-the-art in atmospheric pressure photoionization for LC/MS. *Analytica chimica acta*, *627*(1), 34-49.

[28] Syage, J. A., Short, L. C., & Cai, S.-S. (2008). Atmospheric pressure photoionization - The second source for LC-MS. *LCGC North America*, *26*(3), 287-296.

[29] Marchi, I., Rudaz, S., & Veuthey, J.-L. (2009). Atmospheric pressure photoionization for coupling liquid-chromatography to mass spectrometry: A review. *Talanta*, *78*, 1-18.

[30] U.S. Secretary of Commerce, NIST Chemical Webbook, 2011, http://webbook.nist.gov/chemistry/name-ser.html

[31] Hunter, K. C., & East, A. L. L. (2002). Properties of C-C bonds in n-alkanes: Relevance to cracking mechanisms. Journal of Physical Chemistry A, 106, 1346-1356

[32] SCIEX Photospray ion source operator's manual; December 2002.

[33] Kauppila, T. J., Kotiaho, T., Kostiainen, R., & Bruins, A. P. (2004). Negative ion-atmospheric pressure photoionization-mass spectrometry. Journal of the American Society for Mass Spectrometry, 15, 203-11.

[34] Song, L., Wellman, A. D., Yao, H., & Bartmess, J. E. (2007). Negative ion-atmospheric pressure photoionization: Electron capture, dissociative electron capture, proton transfer, and anion attachment. *Journal of the American Society for Mass Spectrometry*, *18*, 1789-1798.

[35] McEwen, C. N., & Larsen, B. S. (2009). Ionization mechanisms related to negative ion APPI, APCI, and DART. *Journal of the American Society for Mass Spectrometry*, *20*, 1518-1521. American Society for Mass Spectrometry.

[36] Song, L., Dykstra, A. B., Yao, H., & Bartmess, J. E. (2009). Ionization mechanism of negative ion-direct analysis in real time : A comparative study with negative ion-atmospheric pressure photoionization. *Journal of the American Society for Mass Spectrometry*, *20*, 42-50.

[37] Creasy, W. R., & Connor, R. O. (2005). Detection of chemical-weapons related arsenic compounds using atmospheric pressure photoionization (APPI) LC / MS. *Proceedings of the 53rd ASMS Conference, San Antonio, TX. June 5–9*.

[38] Delobel, A., Roy, S., Touboul, D., Gaudin, K., Germain, D. P., Baillet, A., et al. (2006). Atmospheric pressure photoionization coupled to porous graphitic carbon liquid chromatography for the analysis of globotriaosylceramides . Application to Fabry disease. *Journal of mass spectrometry*, *41*, 50-58.

[39] Kéki, S., Török, J., Nagy, L., & Zsuga, M. (2008). Atmospheric pressure photoionization mass spectrometry of polyisobutylene derivatives. *Journal of the American Society for Mass Spectrometry*, *19*, 656-665.

[40] Ross, M. S., & Wong, C. S. (2010). Comparison of electrospray ionization, atmospheric pressure photoionization , and anion attachment atmospheric pressure photoionization for the analysis of hexabromocyclododecane enantiomers in environmental samples. *Journal of Chromatography A*, *1217*, 7855-7863.

[41] Driscoll, J. N. (1977). Evaluation of a new photoionization detector for organic compounds. *Journal of chromatography*, *134*, 49-55.

[42] Jaramillo, L. F., & Driscoll, J. N. (1979). Analysis of therapeutic and commonly abused drugs in serum and urine by gas-liquid chromatography using a photoionization detector. *Drugs*, *186*, 637-644.

[43] Caslda, M. E., & Caslda, K. C. (1980). Application of a unified theory of gas chromatographic photoionization detector response to a 10.2 eV detector. *Journal of chromatography*, *200*, 35-45.

[44] Freedman, A. N. (1980). The photoionization detector. Theory, performance and applications a low-level monitor of oil vapour. *Journal of chromatography*, *190*, 263-273.

[45] Senum, G. I. (1981). Quenching or enhancement of the response of the photoionization detector. *Journal of chromatography*, *205*, 413 - 418.

[46] Bairn, M. A., Eatherton, R. L., & Hill, H. H. (1983). Ion mobility detector for gas chromatography with a direct photoionization source. *Analytical chemistry*, *55*, 1761-1766.

[47] Schmermund, J. T., & Locke, D. C. (1975). A universal photoionization detector for liquid chromatography. *Analytical letters*, *8*(9), 611-625.

[48] Locke, D. C., Dhingra, B. S., & Baker, A. D. (1982). Liquid-phase photoionization detector for liquid chromatography. *Analytical chemistry*, *54*, 447-450.

[49] Driscoll, J. N., Conron, D. W., Ferioli, P., Krull, I. S., & Kie, K. H. (1984). Trace analysis of organic compounds by high-performance liquid chromatography with photoionization detection. *Journal of chromatography*, *302*, 43-50.

[50] Jorgenson, J. W., with Jos S. M. De Wit. (1987). Photoionization detector for open-tubular liquid chromatography. *Journal of chromatography*, 201-212.

[51] Robb, D. B., Covey, T., & Bruins, A. (2000). Atmospheric pressure photoionization: an ionization method for liquid chromatography-mass spectrometry. *Analytical chemistry*, *72*(15), 3653-3659.

[52] Syage, J. A., Evans, M. D., & Hanold, K. A. (2000). Photoionization mass spectrometry. *American Laboratory*, *32*(24), 24-29.

[53] Robb, D. B., & Blades, M. W. (2005). Effects of solvent flow, dopant flow, and lamp current on dopant-assisted atmospheric pressure photoionization (DA-APPI) for LC-MS. Ionization via proton transfer. *Journal of the American Society for Mass Spectrometry*, *16*, 1275-1290.

[54] Impey, G., Kieser, B., & Alary, J.-françois. (2001). The analysis of polycyclic aromatic hydrocarbons (PAHs) by LC/MS/MS using a new atmospheric pressure photoionization source. *Proceedings of the 49th ASMS Conference on Mass Spectrometry and Allied Topics, Chicago, Illinois, May 27-31*.

[55] Cormia, P. H., Fischer, S. M., & Miller, C. A. (2001). Analysis of polyaromatic hydrocarbons by atmospheric pressure photoionization LC/MS. *Proceedings of the 49th ASMS Conference on Mass Spectrometry and Allied Topics, Chicago, Illinois, May 27-31*.

[56] Bruins, A. P., Robb, D. B., Peters, H. A. M., & Jacobs, P. L. (2000). Atmospheric pressure photoionization (APPI) for high sensitivity LC/MS in bioanalysis. *Proceedings of the 48th ASMS Conference on Mass Spectrometry and Allied Topics, Long Beach, California, June 11-15*.

[57] Jacobs, P. L., Peters, H. A. M., & Swaanen, C. H. (2000). Atmospheric pressure photoionization (APPI) and APCI compared for metabolic profiling using testosterone and related steroids. *Proceedings of the 48th ASMS Conference on Mass Spectrometry and Allied Topics, Long Beach, California, June 11-15*.

[58] Robb, D. B., & Blades, M. W. (2006). Factors affecting primary ionization in dopant-assisted atmospheric pressure photoionization (DA-APPI) for LC/MS. *Journal of the American Society for Mass Spectrometry*, *17*, 130-138.

[59] Covey, T., Jong, R., Javahari, H., Liu, C., Thomson, C., & LeBlanc, Y. (2001). Design optimization of atmospheric pressure chemical ionization instrumentation. *Proceedings of the 49th ASMS Conference on Mass Spectrometry and Allied Topics, Chicago, Illinois, May 27-31*.

[60] Jacobs, P. L., Ingelse, B. A., Peters, H. A. M., & Swaanen, C. H. (2004). APPI revisited for earlyADME applications using a Photospray source on the Sciex API 4000. *Proceedings of the 52nd ASMS Conference on Mass Spectrometry and Allied Topics, Nashville, Tennessee, May 23 - 27*.

[61] Yang, C., & Henion, J. (2002). Atmospheric pressure photoionization liquid chromatographic–mass spectrometric determination of idoxifene and its metabolites in human plasma. *Journal of Chromatography A*, *970*, 155-165.

[62] Hsieh, Y., Merkle, K., & Wang, G. (2003). Zirconia-based column high-performance liquid chromatography/atmospheric pressure photoionization tandem mass spectrometric analyses of drug molecules in rat plasma. *Rapid Communications in Mass Spectrometry*, *17*, 1775-1780.

[63] Greig, M. J., Ventura, M., Bolaños, B., Quenzer, T., Pham, C., Shi, S. D., et al. (2004). Applications of APPI-MS for drug discovery. *Proceedings of the 52nd ASMS Conference on Mass Spectrometry and Allied Topics, Nashville, Tennessee, May 23 - 27*.

[64] Theron, H. B., Coetzee, C., Sutherland, F. C. W., Wiesner, J. L., & Swart, K. J. (2004). Selective and sensitive liquid chromatography – tandem mass spectrometry method for the determination of levonorgestrel in human plasma. *Journal of Chromatography B*, *813*, 331-336.

[65] Cai, Y., Kingery, D., McConnell, O., & Bach II, A. C. (2005). Advantages of atmospheric pressure photoionization mass spectrometry in support of drug discovery. *Rapid Communications in Mass Spectrometry*, *19*, 1717-1724.

[66] Wang, G., Hsieh, Y., & Korfmacher, W. A. (2005). Comparison of atmospheric pressure chemical ionization, electrospray ionization, and atmospheric pressure photoionization for the determination of cyclosporin A in rat plasma. *Analytical chemistry*, *77*, 541-548.

[67] Sun, R., Jayaratna, H., Pugh, M., Overdorf, G., & Gehrke, M. (2006). A fast LC/APPI-MS method for quantification of D9-THC and 11-OH-D9-THC in human plasma. *Proceedings of the 54th ASMS Conference, Seattle, WA. May 28-June 1*.

[68] Cai, S.-suan, Hanold, K. A., & Syage, J. A. (2007). Comparison of atmospheric pressure photoionization and atmospheric pressure chemical ionization for normal-phase LC / MS chiral analysis of pharmaceuticals. *Analytical chemistry*, *79*, 2491-2498.

[69] Hsieh, Y., Duncan, C. J. G., Lee, S., & Liu, M. (2007). Comparison of fast liquid chromatography/tandem mass spectrometric methods for simultaneous determination of cladribine and clofarabine in mouse plasma. *Journal of Pharmaceutical and Biomedical Analysis*, *44*, 492-497.

[70] Martens-lobenhoffer, J., Reiche, I., Uwe, T., Monkemuller, K., & Malfertheiner, P. (2007). Enantioselective quantification of omeprazole and its main metabolites in human serum by chiral HPLC–atmospheric pressure photoionization tandem mass spectrometry. *Journal of Chromatography B*, *857*, 301-307.

[71] Theron, H. B., Merwe, M. J. V. D., Swart, K. J., & Westhuizen, J. H. V. D. (2007). Employing atmospheric pressure photoionization in liquid chromatography/tandem mass spectrometry

to minimize ion suppression and matrix effects for the quantification of venlafaxine and O-desmethylvenlafaxine. *Rapid Communications in Mass Spectrometry*, *21*, 1680-1686.

[72] Pereira, A. S., Bicalho, B., Ilha, J. O., & Nucci, G. D. (2008). Analysis of dihydropyridine calcium channel blockers using negative ion photoionization mass spectrometry. *Journal of chromatographic science*, *46*, 35-41.

[73] Short, L. C., & Syage, J. A. (2008). Electrospray photoionization ( ESPI ) liquid chromatography / mass spectrometry for the simultaneous analysis of cyclodextrin and pharmaceuticals and their binding interactions. *Rapid Communications in Mass Spectrometry*, *22*, 541-548.

[74] Borges, N. C., Mazuqueli, A., Moreno, R. A., Astigarraga, R. B., Sverdloff, C. E., Alexandre, P. G. R., et al. (2009). Cyproterone acetate quantification in human plasma by high-performance liquid chromatography coupled to atmospheric pressure photoionization tandem mass spectrometry. *Arzneimittelforschung*, *59*(7), 335-344.

[75] Hommerson, P., Khan, A. M., Bristow, T., Harrison, M. W., Jong, G. J. de, & Somsen, G. W. (2009). Drug impurity profiling by capillary electrophoresis/mass spectrometry using various ionization techniques. *Rapid Communications in Mass Spectrometry*, *23*, 2878-2884.

[76] Marchi, I., Schappler, J., Veuthey, J.-luc, & Rudaz, S. (2009). Development and validation of a liquid chromatography–atmospheric pressure photoionization–mass spectrometry method for the quantification of alprazolam, flunitrazepam, and their main metabolites in haemolysed blood. *Journal of Chromatography B*, *877*, 2275-2283.

[77] Ramesh, M., Ramesh, V., Raju, B., S, R., Kumaraswamy, G., Markondaiah, B., et al. (2009). Diastereomeric differentiation of Oppolzer sultam derivatives using electrospray ionization and atmospheric pressure photo ionization tandem mass spectrometry. *Journal of mass spectrometry: Letters*, *44*, 1114-1118.

[78] Rhourri-Frih, B., Chaimbault, P., Claude, B., Lamy, C., Andre, P., & Lafosse, M. (2009). Analysis of pentacyclic triterpenes by LC–MS . A comparative study between APCI and APPI. *Journal of mass spectrometry*, *44*, 71-80.

[79] Wang, I.-T., Feng, Y.-T., & Chen, C.-Y. (2010). Determination of 17 illicit drugs in oral fluid using isotope dilution ultra-high performance liquid chromatography/tandem mass spectrometry with three atmospheric pressure ionizations. *Journal of Chromatography B*, *878*, 3095-3105.

[80] Garcia-Ac, A., Segura, P. A., Viglino, L., Gagnon, C., & Sauve, S. (2011). Comparison of APPI, APCI and ESI for the LC-MS/MS analysis of bezafibrate, cyclophosphamide, enalapril, methotrexate and orlistat in municipal wastewater. *Journal of mass spectrometry*, *46*, 383-390.

[81] He, J., & Shamsi, S. A. (2011). Chiral micellar electrokinetic chromatography-atmospheric pressure photoionization of benzoin derivatives using mixed molecular micelles. *Electrophoresis*, *32*, 1164-1175.

[82] Alary, J.-françois, Berthemy, A., Tuong, A., & Uzabiaga, M.-F. (2000). Comparative LC-MS/MS analysis of four neurosteroids compounds and their acetyl-pentafluorobenzyl derivatives using a photoionization ion source and a conventional atmospheric-pressure chemical

ionization source. *Proceedings of the 48th ASMS Conference on Mass Spectrometry and Allied Topics, Long Beach, California, June 11-15* (Vol. 3000).

[83] Bruins, A. P., Robb, D. B., Peters, H. A. M., & Jacobs, P. L. (2000). Atmospheric pressure photoionization (APPI) for high sensitivity LC/MS in bioanalysis. *Proceedings of the 48th ASMS Conference on Mass Spectrometry and Allied Topics, Long Beach, California, June 11-15*.

[84] Leinonen, A., Kuuranne, T., & Kostiainen, R. (2002). Liquid chromatography/mass spectrometry in anabolic steroid analysis - optimization and comparison of three ionization techniques: electrospray ionization, atmospheric pressure chemical ionization and atmospheric pressure photoionization. *Journal of mass spectrometry*, *37*, 693-698.

[85] Trosken, E. R., Straube, E., Lutz, W. K., Volkel, W., & Patten, C. (2004). Quantitation of lanosterol and its major metabolite FF-MAS in an inhibition assay of CYP51 by azoles with atmospheric pressure photoionization based LC-MS/MS. *American society for mass spectrometry*, *15*, 1216-1222.

[86] Kushnir, M. M., Neilson, R., Roberts, W. L., & Rockwood, A. L. (2004). Cortisol and cortisone analysis in serum and plasma by atmospheric pressure photoionization tandem mass spectrometry. *Clinical Biochemistry*, *37*, 357 - 362.

[87] Guo, T., Chan, M., & Soldin, S. J. (2004). Steroid profiles using liquid chromatography–tandem mass spectrometry with atmospheric pressure photoionization source. *Archives of Pathology & Laboratory Medicine*, *128*, 469-475.

[88] Kushnir, M. M., Neilson, R., Roberts, W. L., & Rockwood, A. L. (2004). Cortisol and cortisone analysis in serum and plasma by atmospheric pressure photoionization tandem mass spectrometry. *Clinical Biochemistry*, *37*, 357 - 362.

[89] Grant, R. (2005). Development of LC-APPI-MS/MS for clinical analysis of steroids. *Proceedings of the 53rd ASMS Conference, San Antonio, TX. June 5–9*.

[90] Pereira, A. dos S., Oliveira, L. S. O. B., Mendes, G. D., Gabbai, J. J., & Nucci, G. D. (2005). Quantification of betamethasone in human plasma by liquid chromatography–tandem mass spectrometry using atmospheric pressure photoionization in negative mode. *Journal of Chromatography*, *828*, 27-32.

[91] Lembcke, J., Ceglarek, U., Fiedler, G. M., Baumann, S., Leichtle, A., & Thiery, J. (2005). Rapid quantification of free and esterified phytosterols in human serum using APPI-LC-MS/MS. *Journal Of Lipid Research*, *46*, 21-26.

[92] Tang, J. X., Tsao, R., & Longfellow, C. (2005). LC-APPI-MS of steroids and small organic molecules using photospray ion source. *Proceedings of the 53rd ASMS Conference on Mass Spectrometry and Allied Topics, San Antonio, TX, June 5- 9*.

[93] Soldin, O. P., Guo, T., Weiderpass, E., Tractenberg, R. E., Hilakivi-Clarke, L., & Soldin, S. J. (2005). Steroid hormone levels in pregnancy and 1 year postpartum using isotope dilution tandem mass spectrometry. *Fertility and Sterility*, *84*(3), 701-710.

[94] Trosken, E. R., Fischer, K., Volkel, W., & Lutz, W. K. (2006). Inhibition of human CYP19 by azoles used as antifungal agents and aromatase inhibitors, using a new LC–MS/MS method for the analysis of estradiol product formation. *Toxicology*, *219*, 33-40.

[95] Yamamoto, A., Kakutani, N., Yamamoto, K., Kamiura, T., & Miyakoda, H. (2006). Steroid hormone profiles of urban and tidal rivers using LC/MS/MS equipped with electrospray ionization and atmospheric pressure photoionization sources. *Environmental Science & Technology*, *40*, 4132-4137.

[96] Guo, T., Taylor, R. L., Singh, R. J., & Soldin, S. J. (2006). Simultaneous determination of 12 steroids by isotope dilution liquid chromatography-photospray ionization tandem mass spectrometry. *Clinica chimica acta*, *372*, 76-82.

[97] Hilhorst, M., Merbel, N. van de, Hendriks, G., & Horst, E. van der. (2007). Experiences with the quantitative determination of steroids by LC-MS/MS. *Proceedings of the 55th ASMS Conference, Indianapolis, IN. June 3-7*.

[98] Mendes, G. D., Hamamoto, D., Ilha, J., Pereira, S., & De Nucci, G. (2007). Anastrozole quantification in human plasma by high-performance liquid chromatography coupled to photospray tandem mass spectrometry applied to pharmacokinetic studies. *Journal of Chromatography B*, *850*, 553-559.

[99] Hommerson, P., Khan, A. M., Jong, G. J. D., & Somsen, G. W. (2008). Comparison of electrospray ionization and atmospheric pressure photoionization for coupling of micellar electrokinetic chromatography with ion trap mass spectrometry. *Journal of Chromatography A*, *1204*, 197-203.

[100] Lerma-Garcia, M. J., Ramis-Ramos, G., Herrero-Martinez, J. M., & Simo-Alfonso, E. F. (2008). Classification of vegetable oils according to their botanical origin using sterol profiles established by direct infusion mass spectrometry. *Rapid Communications in Mass Spectrometry*, *22*, 973-978.

[101] Okano, M., Sato, M., Ikekita, A., & Kageyama, S. (2009). Analysis of non-ketoic steroids 17α-methylepithiostanol and desoxymethyl-testosterone in dietary supplements. *Drug Testing and Analysis*, *1*, 518-525.

[102] Lien, G.-W., Chen, C.-Y., & Wang, G.-S. (2009). Comparison of electrospray ionization, atmospheric pressure chemical ionization and atmospheric pressure photoionization for determining estrogenic chemicals in water by liquid chromatography tandem mass spectrometry with chemical derivatizations. *Journal of chromatography. A*, *1216*, 956-966.

[103] Harwood, D. T., & Handelsman, D. J. (2009). Development and validation of a sensitive liquid chromatography–tandem mass spectrometry assay to simultaneously measure androgens and estrogens in serum without derivatization. *Clinica Chimica Acta*, *409*, 78-84.

[104] Zhang, F., Bartels, M. J., Geter, D. R., Carr, M. S., McClymount, L. E., Marino, T. A., et al. (2009). Simultaneous quantitation of testosterone, estradiol, ethinyl estradiol, and 11-ketotestosterone in fathead minnow fish plasma by liquid chromatography/positive atmospheric pressure photoionization tandem mass spectrometry. *Rapid Communications in Mass Spectrometry*, *23*, 3637-3646.

[105] Zhang, C., Zhai, S., Liang, W., Jiang, J., & Lou, H. (2009). Highly sensitive analysis of norethisterone in human serum by LC coupled with atmospheric pressure photoionization tandem mass spectrometry. *Chromatographia*, *69*, 665-670.

[106] Borges, N. C., Astigarraga, R. B., Sverdloff, C. E., Galvinas, P. R., Silva, W. M. da, Rezende, V. M., et al. (2009). A novel and sensitive method for ethinylestradiol quantification in human plasma by high-performance liquid chromatography coupled to atmospheric pressure photoionization (APPI) tandem mass spectrometry: Application to a comparative pharmacokinetics study. *Journal of Chromatography B*, *877*, 3601-3609.

[107] Chen, H.-C., Kuo, H.-W., & Ding, W.-H. (2009). Determination of estrogenic compounds in wastewater using liquid chromatography–tandem mass spectrometry with electrospray and atmospheric pressure photoionization following desalting extraction. *Chemosphere*, *74*, 508-514.

[108] Lih, F. B., Titus, M. A., Mohler, J. L., & Tomer, K. B. (2010). Atmospheric pressure photoionization tandem mass spectrometry of androgens in prostate cancer. *Analytical chemistry*, *82*, 6000-6007.

[109] Borgesa, N. C. do C., Astigarraga, R. B., Sverdloffa, C. E., Borgese, B. C., Paivaa, T. R., Galvinas, P. R., et al. (2011). Budesonide quantification by HPLC coupled to atmospheric pressure photoionization (APPI) tandem mass spectrometry. Application to a comparative systemic bioavailability of two budesonide formulations in healthy volunteers. *Journal of Chromatography B*, *879*, 236-242.

[110] Matejicek, D. (2011). On-line two-dimensional liquid chromatography–tandem mass spectrometric determination of estrogens in sediments. *Journal of Chromatography A*, *1218*, 2292-2300.

[111] Zhang, F., Rick, D. L., Kan, L. H., Perala, A. W., Geter, D. R., Lebaron, M. J., et al. (2011). Simultaneous quantitation of testosterone and estradiol in human cell line (H295R) by liquid chromatography/positive atmospheric pressure photoionization tandem mass spectrometry. *Rapid Communications in Mass Spectrometry*, *25*, 3123-3130.

[112] Adamec, J., Jannasch, A., Huang, J., Hohman, E., Fleet, J. C., Peacock, M., et al. (2011). Development and optimization of an LC-MS/MS-based method for simultaneous quantification of vitamin D2, vitamin D3, 25-hydroxyvitamin D2 and 25- hydroxyvitamin D3. *Journal of separation science*, *34*, 11-20.

[113] Parker, D. L., Rybak, M. E., & Pfeiffer, C. M. (2012). Phytoestrogen biomonitoring: an extractionless LC-MS/MS method for measuring urinary isoflavones and lignans by use of atmospheric pressure photoionization (APPI). *Analytical and Bioanalytical Chemistry*, *402*, 1123-1136.

[114] Matejicek, D. (2012). Multi heart-cutting two-dimensional liquid chromatography–atmospheric pressure photoionization-tandem mass spectrometry method for the determination of endocrine disrupting compounds in water. *Journal of Chromatography A*, *1231*, 52- 58.

[115] Chen, W.-L., Wang, G.-S., Gwo, J.-C., & Chen, C.-Y. (2012). Ultra-high performance liquid chromatography/tandem mass spectrometry determination of feminizing chemicals in river

water, sediment and tissue pretreated using disk-type solid-phase extraction and matrix solid-phase dispersion. *Talanta*, *89*, 237-245.

[116] Delobel, A., Touboul, D., & Laprévote, O. (2005). Structural characterization of phosphatidylcholines by atmospheric pressure photoionization mass spectrometry. *European journal of mass spectrometry*, *11*, 409-417.

[117] Roy, S., Delobel, A., Gaudin, K., Touboul, D., Germain, D. P., Baillet, A., et al. (2006). Liquid chromatography on porous graphitic carbon with atmospheric pressure photoionization mass spectrometry and tandem mass spectrometry for the analysis of glycosphingolipids. *Journal of Chromatography A*, *1117*, 154-162.

[118] Cai, S.-S., & Syage, J. A. (2006). Comparison of atmospheric pressure photoionization, atmospheric pressure chemical ionization, and electrospray ionization mass spectrometry for analysis of lipids. *Analytical chemistry*, *78*, 1191-1199.

[119] Muller, A., Mickel, M., Geyer, R., Ringseis, R., Eder, K., & Steinhart, H. (2006). Identification of conjugated linoleic acid elongation and Beta-oxidation products by coupled silver-ion HPLC APPI-MS. *Journal of Chromatography B*, *837*, 147-152.

[120] Cai, S.-S., & Syage, J. A. (2006). Atmospheric pressure photoionization mass spectrometry for analysis of fatty acid and acylglycerol lipids. *Journal of Chromatography A*, *1110*, 15-26.

[121] Delobel, A., Roy, S., Touboul, D., Gaudin, K., Germain, D. P., Baillet, A., et al. (2006). Atmospheric pressure photoionization coupled to porous graphitic carbon liquid chromatography for the analysis of globotriaosylceramides. Application to Fabry disease. *Journal of mass spectrometry*, *41*, 50-58.

[122] Cai, S.-S., Short, L. C., Syage, J. A., Potvin, M., & Curtis, J. M. (2007). Liquid chromatography–atmospheric pressure photoionization-mass spectrometry analysis of triacylglycerol lipids - Effects of mobile phases on sensitivity. *Journal of Chromatography A*, *1173*, 88-97.

[123] Muñoz-garcia, A., Ro, J., Brown, J. C., & Williams, J. B. (2008). Cutaneous water loss and sphingolipids in the stratum corneum of house sparrows, Passer domesticus L., from desert and mesic environments as determined by reversed phase high-performance liquid chromatography coupled with atmospheric pressure photospray i. *Journal of Experimental Biology*, *211*, 447-458.

[124] Karuna, R., Eckardstein, A. von, & Rentsch, K. M. (2009). Dopant assisted-atmospheric pressure photoionization (DA-APPI) liquid chromatography–mass spectrometry for the quantification of 27-hydroxycholesterol in plasma. *Journal of Chromatography B*, *877*, 261-268.

[125] Ronsein, G. E., Prado, F. M., Mansano, F. V., Oliveira, M. C. B., Medeiros, M. H. G., Miyamoto, S., et al. (2010). detection and characterization of cholesterol-oxidized products using HPLC coupled to dopant assisted atmospheric pressure photoionization tandem mass spectrometry. *Analytical chemistry*, *82*(17), 7293-7301.

[126] Merbel, N. C. van de, Bronsema, K. J., Hout, M. W. J. van, Nilsson, R., & Sillén, H. (2011). A validated liquid chromatography–tandem mass spectrometry method for the quantitative

determination of 4Beta-hydroxycholesterol in human plasma. *Journal of Pharmaceutical and Biomedical Analysis*, *55*, 1089-1095.

[127] Castro-perez, J., Previs, S. F., Mclaren, D. G., Shah, V., Herath, K., Bhat, G., et al. (2011). In vivo D2O labeling to quantify static and dynamic changes in cholesterol and cholesterol esters by high resolution LC/MS. *Journal Of Lipid Research*, *52*, 159-169.

[128] Herchi, W., Trabelsi, H., Salah, H. B., Zhao, Y. Y., Boukhchina, S., Kallel, H., et al. (2012). Changes in the triacylglycerol content of flaxseeds during development using liquid chromatography- atmospheric pressure photoionization-mass spectrometry (LC-APPI-MS). *African Journal of Biotechnology*, *11*(4), 904-911.

[129] Gaudin, M., Imbert, L., Libong, D., Chaminade, P., Brunelle, A., Touboul, D., et al. (2012). Atmospheric pressure photoionization as a powerful tool for large-scale lipidomic studies. *Journal of the American Society for Mass Spectrometry*, *23*, 869-879.

[130] Imbert, L., Gaudin, M., Libong, D., Touboul, D., Abreu, S., Loiseau, P. M., et al. (2012). Comparison of electrospray ionization , atmospheric pressure chemical ionization and atmospheric pressure photoionization for a lipidomic analysis of Leishmania donovani. *Journal of Chromatography A*, *1242*, 75-83.

[131] Kania, M., Skorupinska-Tudek, K., Swiezewska, E., & Danikiewicz, W. (2012). Atmospheric pressure photoionization mass spectrometry as a valuable method for the identification of polyisoprenoid alcohols. *Rapid Communications in Mass Spectrometry*, *26*, 1705-1710.

[132] Moriwaki, H., Ishitake, M., Yoshikawa, S., Miyakoda, H., & Alary, J.-F. (2004). Determination of polycyclic aromatic hydrocarbons in sediment by liquid chromatography–atmospheric pressure photoionization–mass spectrometry. *Analytical Sciences*, *20*, 375-377.

[133] Itoh, N., Aoyagi, Y., & Yarita, T. (2006). Optimization of the dopant for the trace determination of polycyclic aromatic hydrocarbons by liquid chromatography/dopant-assisted atmospheric-pressure photoionization/mass spectrometry. *Journal of Chromatography A*, *1131*, 285-288.

[134] Ding, Y. S., Ashley, D. L., & Watson, C. H. (2007). Determination of 10 carcinogenic polycyclic aromatic hydrocarbons in mainstream cigarette smoke. *Journal of agricultural and food chemistry*, *55*, 5966-5973.

[135] McCulloch, R. D., Robb, D. B., & Blades, M. W. (2008). A dopant introduction device for atmospheric pressure photoionization with liquid chromatography/mass spectrometry. *Rapid Communications in Mass Spectrometry*, *22*, 3549-3554.

[136] Chu, S., & Letcher, R. J. (2008). Analysis of fluorotelomer alcohols and perfluorinated sulfonamides in biotic samples by liquid chromatography-atmospheric pressure photoionization mass spectrometry. *Journal of Chromatography A*, *1215*, 92-99.

[137] Itoh, N., Narukawa, T., Numata, M., Aoyagi, Y., Yarita, T., & Takatsu, A. (2009). Mechanism of ionization of polycyclic aromatic hydrocarbons by a toluene/anisole mixture as a dopant in liquid chromatography/dopant-assisted atmospheric-pressure photoionization/mass spectrometry. *Polycyclic Aromatic Compounds*, *29*, 41-55.

[138] Cai, S.-S., Syage, J. A., Hanold, K. A., & Balogh, M. P. (2009). Ultra performance liquid chromatography-atmospheric pressure photoionization-tandem mass spectrometry for high-sensitivity and high-throughput analysis of U.S. Environmental Protection Agency 16 priority pollutants polynuclear aromatic hydrocarbons. *Analytical chemistry*, *81*, 2123-2128.

[139] Rodil, R., Schrader, S., & Moeder, M. (2009). Non-porous membrane-assisted liquid–liquid extraction of UV filter compounds from water samples. *Journal of Chromatography A*, *1216*, 4887-4894.

[140] Rodil, R., Schrader, S., & Moeder, M. (2009). Comparison of atmospheric pressure photoionization and electrospray ionization mass spectrometry for the analysis of UV filters. *Rapid Communications in Mass Spectrometry*, *23*, 580-588.

[141] Itoh, N., Aoyagi, Y., & Takatsu, A. (2009). Certified reference material for quantification of polycyclic aromatic hydrocarbons in sediment from the National Metrology Institute of Japan. *Analytical and Bioanalytical Chemistry*, *393*, 2039-2049.

[142] Smith, D. R., Robb, D. B., & Blades, M. W. (2009). Comparison of dopants for charge exchange ionization of nonpolar polycyclic aromatic hydrocarbons with reversed-phase LC-APPI-MS. *Journal of the American Society for Mass Spectrometry*, *20*, 73-79.

[143] Ehrenhauser, F. S., Wornat, M. J., Valsaraj, K. T., & Rodriguez, P. (2010). Design and evaluation of a dopant-delivery system for an orthogonal atmospheric-pressure photoionization source and its performance in the analysis of polycyclic aromatic hydrocarbons. *Rapid Communications in Mass Spectrometry*, *24*, 1351-1357.

[144] Smoker, M., Tran, K., & Smith, R. E. (2010). Determination of polycyclic aromatic hydrocarbons (PAHs) in shrimp. *Journal of agricultural and food chemistry*, *58*, 12101-12104.

[145] Lintelmann, J., Franca, M. H., Hübner, E., & Matuschek, G. (2010). A liquid chromatography–atmospheric pressure photoionization tandem mass spectrometric method for the determination of azaarenes in atmospheric particulate matter. *Journal of Chromatography A*, *1217*, 1636-1646.

[146] Hollosi, L., & Wenzl, T. (2011). Development and optimisation of a dopant assisted liquid chromatographic-atmospheric pressure photo ionisation-tandem mass spectrometric method for the determination of 15+1 EU priority PAHs in edible oils. *Journal of Chromatography A*, *1218*, 23-31.

[147] Lung, S.-C. C., & Liu, C.-H. (2011). High-sensitivity analysis of six synthetic musks by ultra-performance liquid chromatography-atmospheric pressure photoionization-tandem mass spectrometry. *Analytical chemistry*, *83*, 4955-4961.

[148] Hutzler, C., Luch, A., & Filser, J. G. (2011). Analysis of carcinogenic polycyclic aromatic hydrocarbons in complex environmental mixtures by LC-APPI-MS/MS. *Analytica Chimica Acta*, *702*, 218-224.

[149] Ahmed, A., Choi, C. H., Choi, M. C., & Kim, S. (2012). Mechanisms behind the generation of protonated ions for polyaromatic hydrocarbons by atmospheric pressure photoionization. *Analytical chemistry*, *84*, 1146-1151.

[150] Thuong, M. B. T., Catala, C., Colas, C., Schaeffer, C., Dorsselaer, A. van, Mann, A., et al. (2012). Trimethoxyarene as a highly ionizable tag for reaction analysis by atmospheric pressure photoionization mass spectrometry (APPI/MS): Exploration of heterocyclic synthesis. *European journal of organic chemistry*, 85-92.

[151] Li, L., Huhtala, S., Sillanpää, M., & Sainio, P. (2012). Liquid chromatography–mass spectrometry for C60 fullerene analysis: optimisation and comparison of three ionisation techniques. *Analytical and Bioanalytical Chemistry*, *403*, 1931-1938.

[152] Sioud, S., Amad, M., & Al-Talla, Z. A. (2012). Multicomponent mixed dopant optimization for rapid screening of polycyclic aromatic hydrocarbons using ultra high performance liquid chromatography coupled to atmospheric pressure photoionization high-resolution mass spectrometry. *Rapid Communications in Mass Spectrometry*, *26*, 1488-1496.

[153] Ghislain, T., Faure, P., & Michels, R. (2012). Detection and monitoring of PAH and oxy-PAHs by high resolution mass spectrometry:Comparison of ESI, APCI and APPI source detection. *Journal of the American Society for Mass Spectrometry*, *23*, 530-536.

[154] Cai, S.-S., Stevens, J., & Syage, J. A. (2012). Ultra high performance liquid chromatography–atmospheric pressure photoionization-mass spectrometry for high-sensitivity analysis of US Environmental Protection Agency sixteen priority pollutant polynuclear aromatic hydrocarbons in oysters. *Journal of Chromatography A*, *1227*, 138-144.

[155] Debrauwer, L., Riu, A., Jouahri, M., Rathahao, E., Jouanin, I., Antignac, J.-P., et al. (2005). Probing new approaches using atmospheric pressure photo ionization for the analysis of brominated flame retardants and their related degradation products by liquid chromatography–mass spectrometry. *Journal of Chromatography A*, *1082*, 98-109.

[156] Riu, A., Zalko, D., & Debrauwer, L. (2006). Study of polybrominated diphenyl ethers using both positive and negative atmospheric pressure photoionization and tandem mass spectrometry. *Rapid Communications in Mass Spectrometry*, *20*, 2133-2142.

[157] Cariou, R., Antignac, J.-P., Debrauwer, L., Maume, D., Monteau, F., Zalko, D., et al. (2006). Comparison of analytical strategies for the chromatographic and mass spectrometric measurement of brominated flame retardants: 1. Polybrominated diphenylethers. *Journal of chromatographic science*, *44*, 489-497.

[158] Jhong, Y.-J., & Ding, W.-H. (2007). Method optimization for quantitation of decabromodiphenyl ether in sedi- ments and earthworms using liquid chromatography/atmospheric pres- sure photoionization tandem mass spectrometry. *Rapid Communications in Mass Spectrometry*, *21*, 4158-4161.

[159] Lagalante, A. F., & Oswald, T. D. (2008). Analysis of polybrominated diphenyl ethers (PBDEs) by liquid chromatography with negative-ion atmospheric pressure photoionization tandem mass spectrometry (LC/NI-APPI/MS/MS): application to house dust. *Analytical and Bioanalytical Chemistry*, *391*, 2249-2256.

[160] Bacaloni, A., Callipo, L., Corradini, E., Giansanti, P., Gubbiotti, R., Samperi, R., et al. (2009). Liquid chromatography–negative ion atmospheric pressure photoionization tandem mass spectrometry for the determination of brominated flame retardants in environmental water and industrial effluents. *Journal of Chromatography A*, *1216*, 6400-6409.

[161] Abdallah, M. A.-elwafa, Harrad, S., & Covaci, A. (2009). Isotope dilution method for determination of polybrominated diphenyl ethers using liquid chromatography coupled to negative ionization atmospheric pressure photoionization tandem mass spectrometry: Validation and application to house dust. *Analytical chemistry*, *81*, 7460-7467.

[162] Zhou, S. N., Reiner, E. J., Marvin, C., Kolic, T., Riddell, N., Helm, P., et al. (2010). Liquid chromatography–atmospheric pressure photoionization tandem mass spectrometry for analysis of 36 halogenated flame retardants in fish. *Journal of Chromatography A*, *1217*, 633-641.

[163] Mascolo, G., Locaputo, V., & Mininni, G. (2010). New perspective on the determination of flame retardants in sewage sludge by using ultrahigh pressure liquid chromatography–tandem mass spectrometry with different ion sources. *Journal of Chromatography A*, *1217*(27), 4601-4611.

[164] Ross, M. S., & Wong, C. S. (2010). Comparison of electrospray ionization, atmospheric pressure photoionization, and anion attachment atmospheric pressure photoionization for the analysis of hexabromocyclododecane enantiomers in environmental samples. *Journal of Chromatography A*, *1217*, 7855-7863.

[165] Letcher, R. J., & Chu, S. (2010). High-sensitivity method for determination of tetrabromobisphenol-S and tetrabromobisphenol-A derivative flame retardants in great lakes herring gull eggs by liquid pressure photoionization-tandem mass spectrometry. *Environmental Science & Technology*, *44*, 8615-8621.

[166] Debrauwer, L., Marteau, C., Zalko, D., & Chevolleau, S. (2010). Is LC-MS APPI coupling an alternative to LC-MS coupling for highly brominated PBDEs analysis? *Spectra Analyse*, *39*(276), 38-44.

[167] Calvosa, F. C., & Lagalante, A. F. (2010). Supercritical fluid extraction of polybrominated diphenyl ethers (PBDEs) from house dust with supercritical 1, 1, 1, 2-tetrafluoroethane (R134a). *Talanta*, *80*, 1116-1120.

[168] Zhou, S. N., Reiner, E. J., Marvin, C. H., Helm, P. A., Shen, L., & Brindle, I. D. (2011). Liquid chromatography/atmospheric pressure photoionization tandem mass spectrometry for analysis of Dechloranes. *Rapid Communications in Mass Spectrometry*, *25*, 436-442.

[169] Itoh, N., Otake, T., Aoyagi, Y., Matsuo, M., & Yarita, T. (2009). Application of pesticide quantification in unpolished rice by LC-dopant-assisted atmospheric pressure photoionization-MS. *Chromatographia*, *70*, 1073-1078.

[170] Osaka, I., Yoshimoto, A., Nozaki, K., Moriwaki, H., Awasaki, H. K., & Rakawa, R. A. (2009). Simultaneous LC/MS analysis of hexachlorobenzene and pentachlorophenol by atmospheric pressure chemical ionization (APCI) and photoionization (APPI) methods. *Analytical Sciences*, *25*, 1373-1376.

[171] Yamamoto, A., Miyamoto, I., Kitagawa, M., Moriwaki, H., Miyakoda, H., Awasaki, H., et al. (2009). Analysis of chlorothalonil by liquid chromatography/mass spectrometry using negative-ion atmospheric pressure photoionization. *Analytical Sciences*, *25*, 693-697.

[172] Yoshioka, N., Akiyama, Y., Matsuoka, T., & Mitsuhashi, T. (2010). Rapid determination of five post-harvest fungicides and metabolite in citrus fruits by liquid chromatography/time-of-flight mass spectrometry with atmospheric pressure photoionization. *Food Control*, *21*, 212-216.

[173] Gu, C., & Shamsi, S. A. (2010). CEC-atmospheric pressure ionization MS of pesticides using a surfactant-bound monolithic column. *Electrophoresis*, *31*, 1162-1174.

[174] Roetering, S., Nazarov, E. G., Borsdorf, H., & Weickhardt, C. (2010). Effect of dopants on the analysis of pesticides by means of differential mobility spectrometry with atmospheric pressure photoionization. *International Journal of Ion Mobility Spectrometry*, *13*, 47-54.

[175] Capriotti, A. L., Foglia, P., Gubbiotti, R., Roccia, C., Samperi, R., & Laganà, A. (2010). Development and validation of a liquid chromatography/atmospheric pressure photoionization-tandem mass spectrometric method for the analysis of mycotoxins subjected to commission regulation (EC) No. 1881/2006 In cereals. *Journal of Chromatography A*, *1217*, 6044-6051.

[176] Kruve, A., Haapala, M., Saarela, V., Franssila, S., Kostiainen, R., Kotiaho, T., et al. (2011). Feasibility of capillary liquid chromatography–microchip-atmospheric pressure photoionization–mass spectrometry for pesticide analysis in tomato. *Analytica Chimica Acta*, *696*, 77-83.

[177] Yoshioka, N., Asano, M., Kuse, A., Matsuoka, T., Akiyama, Y., Mitsuhashi, T., et al. (2012). Rapid and sensitive quantification of paraquat and diquat in human serum by liquid chromatography/time-of-flight mass spectrometry using atmospheric pressure photoionization. *Forensic Toxicol*, *30*, 135-141.

[178] Yamamoto, A., Terao, T., Hisatomi, H., Kawasaki, H., & Arakawa, R. (2012). Evaluation of river pollution of neonicotinoids in Osaka City (Japan) by LC/MS with dopant-assisted photionisation. *Journal of Environmental Monitoring*, *14*, 2189-2194.

[179] Kawano, S.-ichi, Murata, H., Mikami, H., Mukaibatake, K., & Waki, H. (2006). Method optimization for analysis of fullerenes by liquid chromatography/ atmospheric pressure photoionization mass spectrometry. *Rapid Communications in Mass Spectrometry*, *20*, 2783-2785.

[180] Talyzin, A. V., Tsybin, Y. O., Purcell, J. M., Schaub, T. M., Shulga, Y. M., Noreus, D., et al. (2006). Reaction of hydrogen gas with C60 at elevated pressure and temperature: Hydrogenation and cage fragmentation. *Journal of Physical Chemistry A*, *110*, 8528-8534.

[181] Song, L., Wellman, A. D., Yao, H., & Adcock, J. (2007). Electron capture atmospheric pressure photoionization mass spectrometry: analysis of fullerenes, perfluorinated compounds, and pentafluorobenzyl derivatives. *Rapid Communications in Mass Spectrometry*, *21*, 1343-1351.

[182] Isaacson, C. W., & Bouchard, D. (2010). Asymmetric flow field flow fractionation of aqueous C60 nanoparticles with size determination by dynamic light scattering and quantification by liquid chromatography atmospheric pressure photo-ionization mass spectrometry. *Journal of Chromatography A*, *1217*, 1506-1512.

[183] Hockaday, W. C., Hwang, Y. S., Masiello, C. A., & Li, Q. (2010). Mass spectrometry of non-colloidal fullerenes in waters containing natural organic matter. *Proceedings of the 239th ACS National Meeting, San Francisco, CA, March 21-25*.

[184] Chen, H.-chang, & Ding, W.-hsien. (2012). Determination of aqueous fullerene aggregates in water by ultrasound-assisted dispersive liquid–liquid microextraction with liquid chromatography–atmospheric pressure photoionization-tandem mass spectrometry. *Journal of Chromatography A*, *1223*, 15-23.

[185] Nunez, O., Gallart-Ayala, H., Martins, C. P. B., Moyano, E., & Galceran, M. T. (2012). Atmospheric pressure photoionization mass spectrometry of fullerenes. *Analytical Chemistry*, *84*, 5316-5326.

[186] Purcell, J. M., Hendrickson, C. L., Rodgers, R. P., & Marshall, A. G. (2006). Atmospheric pressure photoionization Fourier transform ion cyclotron resonance mass spectrometry for complex mixture analysis. *Analytical Chemistry*, *78*(16), 5906-5912.

[187] Purcell, J. M., Rodgers, R. P., Hendrickson, C. L., & Marshall, A. G. (2007). speciation of nitrogen containing aromatics by atmospheric pressure photoionization or electrospray ionization Fourier transform ion cyclotron resonance mass spectrometry. *Journal of the American Society for Mass Spectrometry*, *18*, 1265-1273.

[188] Witt, M. (2007). Crude oil analysis by Fourier transform ion cyclotron resonance mass spectrometry using different ionization techniques. *Proceedings of the 55th ASMS Conference, Indianapolis, IN. June 3-7*.

[189] Purcell, J. M., Hendrickson, C. L., Rodgers, R. P., & Marshall, A. G. (2007). Atmospheric pressure photoionization proton transfer for complex organic mixtures cyclotron resonance mass spectrometry. *Journal of the American Society for Mass Spectrometry*, *18*, 1682-1689.

[190] Purcell, J. M., Juyal, P., Kim, D.-G., Rodgers, R. P., Hendrickson, C. L., & Marshall, A. G. (2007). Sulfur speciation in petroleum: Atmospheric pressure photoionization or chemical derivatization and electrospray ionization Fourier transform ion cyclotron resonance mass spectrometry. *Energy & Fuels*, *21*, 2869-2874.

[191] Li, F., Hsieh, Y., & Korfmacher, W. A. (2008). High-performance liquid chromatography-atmospheric pressure photoionization/tandem mass spectrometry for the detection of 17alpha-ethinylestradiol in hepatocytes. *Journal of Chromatography B*, *870*, 186-191.

[192] Qian, K., Mennito, A. S., Edwards, K. E., & Ferrughelli, D. T. (2008). Observation of vanadyl porphyrins and sulfur-containing vanadyl porphyrins in a petroleum asphaltene by atmospheric pressure photonionization Fourier transform ion cyclotron resonance mass spectrometry. *Rapid Communications in Mass Spectrometry*, *22*, 2153-2160.

[193] Rodgers, R. P., McKenna, A. M., Purcell, J. M., Smith, D. F., & Marshall, A. G. (2008). Speciation of nitrogen, oxygen and sulfur species in unconventional crudes by electrospray ionization and atmospheric pressure photoionization Fourier transform ion cyclotron resonance mass spectrometry. *Proceedings of the 236th ACS National Meeting, Philadelphia, PA, August 17-21*.

[194] Haapala, M., Purcell, J. M., Saarela, V., Franssila, S., Rodgers, R. P., Hendrickson, C. L., et al. (2009). Microchip atmospheric pressure photoionization for analysis of petroleum by Fourier transform ion cyclotron resonance mass spectrometry. *Analytical Chemistry*, *81*(7), 2799-2803.

[195] McKenna, A. M., Purcell, J. M., Rodgers, R. P., & Marshall, A. G. (2009). Identification of Vanadyl porphyrins in a heavy crude oil and raw asphaltene by atmospheric pressure photoionization Fourier transform ion cyclotron resonance (FT-ICR) mass spectrometry. *Energy & Fuels*, *23*(9), 2122-2128.

[196] Atolia, E., McKenna, A. M., Rodgers, R. P., Reddy, C. M., Nelson, R. K., & Marshall, A. G. (2010). 3D graphical analysis of ultrahigh-resolution FT-ICR mass spectrometry data: compositional comparison of a crude oil and associated production deposit. *American Chemical Society, Division of Petroleum Chemistry*, *55*(1), 171-172.

[197] Purcell, J. M., Merdrignac, I., Rodgers, R. P., Marshall, A. G., Gauthier, T., & Guibard, I. (2010). Stepwise structural characterization of asphaltenes during deep hydroconversion processes determined by atmospheric pressure photoionization (APPI) Fourier transform ion cyclotron resonance (FT-ICR) mass spectrometry. *Energy & Fuels*, *24*, 2257-2265.

[198] Na, J., Chung, S., Bae, E., Kim, H., & Kim, S. (2010). Identification of chemical components in shale oils and comparison to conventional crude. *Proceedings of the Pacifichem, International Chemical Congress of Pacific Basin Societies, Honolulu, HI, Dec 15-20*.

[199] Barrow, M. P., Witt, M., Headley, J. V., & Peru, K. M. (2010). Athabasca oil sands process water: characterization by atmospheric pressure photoionization and electrospray ionization Fourier transform ion cyclotron resonance mass spectrometry. *Analytical Chemistry*, *82*(9), 3727-3735.

[200] Liu, Y., Liu, Z., Hu, Q., Zhu, X., & Tian, S. (2010). Characterization of sulfur aromatic species in vacuum gas oil by Fourier transform ion cyclotron resonance mass spectrometry. *Shiyou Xuebao, Shiyou Jiagong*, *26*(1), 52-59.

[201] Qian, K., Edwards, K. E., Mennito, A. S., Walters, C. C., & Kushnerick, J. D. (2010). Enrichment, resolution, and identification of nickel porphyrins in petroleum asphaltene by cyclograph separation and atmospheric pressure photoionization Fourier transform ion cyclotron resonance mass spectrometry. *Analytical Chemistry*, *82*, 413-419.

[202] Hur, M., Yeo, I., Park, E., Kim, Y. H., Yoo, J., Kim, E., et al. (2010). Combination of statistical methods and Fourier transform ion cyclotron resonance mass spectrometry for more comprehensive, molecular-level interpretations of petroleum samples. *Analytical Chemistry*, *82*, 211-218.

[203] McKenna, A. M., Purcell, J. M., Rodgers, R. P., & Marshall, A. G. (2010). Heavy petroleum composition. 1. Exhaustive compositional analysis of Athabasca bitumen HVGO distillates by Fourier transform ion cyclotron resonance mass spectrometry: A definitive test of the Boduszynski model. *Energy & Fuels*, *24*, 2929-2938.

[204] Bae, E., Na, J.-G., Chung, S. H., Kim, H. S., & Kim, S. (2010). Identification of about 30 000 chemical components in shale oils by electrospray ionization (ESI) and atmospheric pressure photoionization (APPI) coupled with 15T Fourier transform ion cyclotron resonance

mass spectrometry (FT-ICR MS) and a comparison to conventional oil . *Energy & Fuels*, *24*, 2563-2569.

[205] Kima, E., Noa, M.-han, Koha, J., & Kim, S. (2011). Compositional characterization of petroleum heavy oils generated from vacuum distillation and catalytic cracking by positive-mode APPI FT-ICR mass spectrometry. *Mass Spectrometry Letters*, *2*(2), 41-44.

[206] Rodgers, R. P., McKenna, A. M., Robbins, W. K., Hsu, C. S., Lu, J., & Marshall, A. G. (2011). Structural characterization of petroleum derived materials by preparative liquid chromatography and HPLC-2 followed by FT-ICR MS analysis. *Proceedings of the 242nd ACS National Meeting & Exposition, Denver, CO, United States, Aug 28-Sept 1*.

[207] McKenna, A. M., Mapolelo, M. M., Robbins, W. K., Rodgers, R. P., & Marshall, A. G. (2011). Molecular characterization of chromatographic fractions of deasphalted crude oils by FT-ICR mass spectrometry. *Proceedings of the 241st ACS National Meeting & Exposition, Anaheim, CA, March 27-31*.

[208] Tachon, N., Jahouh, F., Delmas, M., & Banoub, J. H. (2011). Structural determination by atmospheric pressure photoionization tandem mass spectrometry of some compounds isolated from the SARA fractions obtained from bitumen. *Rapid Communications in Mass Spectrometry*, *25*(Jun), 2657-2671.

[209] Stahnke, H., Kittlaus, S., Kempe, G., Hemmerlingd, C., & Aldera, L. (2012). The influence of electrospray ion source design on matrix effects. *Journal of mass spectrometry*, *47*, 875-884.

[210] Cho, Y., Na, J.-geol, Nho, N.-sun, Kim, Sunghong, & Kim, Sunghwan. (2012). Application of saturates, aromatics, resins, and asphaltenes crude oil fractionation for detailed chemical characterization of heavy crude oils by Fourier Transform ion cyclotron resonance mass spectrometry equipped with atmospheric pressure photoionization. *Energy & Fuels*, *12*, 2558-2565.

[211] Kuki, A., Nagy, L., Zsuga, M., & Keki, S. (46AD). Atmospheric pressure photoionization mass spectrometry (APPI-MS) of nonpolar polymers. *Muanyag es Gumi*, *12*, 456-458.

[212] Kéki, S., Török, J., Nagy, L., & Zsuga, M. (2008). Atmospheric pressure photoionization mass spectrometry of polyisobutylene derivatives. *Journal of the American Society for Mass Spectrometry*, *19*, 656-665.

[213] Keki, S., Nagy, L., Kuki, A., & Zsuga, M. (2008). A new method for mass spectrometry of polyethylene waxes: The chloride ion attachment technique by atmospheric pressure photoionization. *macromolecules*, *41*, 3772-3774.

[214] Nagy, L., Pálfi, V., Narmandakh, M., Kuki, Á., Nyíri, A., Iván, B., et al. (2009). Dopant-assisted atmospheric pressure photoionization mass spectrometry of polyisobutylene derivatives initiated by mono- and bifunctional initiators. *Journal of the American Society for Mass Spectrometry*, *20*, 2342-2351.

[215] Himmelsbach, M., Buchberger, W., & Reingruber, E. (2009). Determination of polymer additives by liquid chromatography coupled with mass spectrometry. A comparison of atmospheric pressure photoionization (APPI), atmospheric pressure chemical ionization

(APCI), and electrospray ionization (ESI). *Polymer Degradation and Stability*, *94*, 1213-1219.

[216] Reingruber, E., Himmelsbach, M., Sauer, C., & Buchberger, W. (2010). Identification of degradation products of antioxidants in polyolefins by liquid chromatography combined with atmospheric pressure photoionisation mass spectrometry. *Polymer Degradation and Stability*, *95*, 740-745.

[217] Terrier, P., Desmazieres, B., Tortajada, J., & Buchmann, W. (2011). APCI/APPI for synthetic polymer analysis. *Mass Spectrometry Reviews*, *30*, 854- 874.

[218] Michel, D. (2011). Elucidation of the complex molecular structure of pine tree lignin polymer by atmospheric pressure photoionization quadrupole time-of-flight tandem mass spectrometry. *Proceedings of the 241st ACS National Meeting & Exposition, Anaheim, CA, March 27-31*.

[219] Kania, M., Skorupinska-Tudek, K., Swiezewska, E., & Danikiewicz, W. (2012). Atmospheric pressure photoionization mass spectrometry as a valuable method for the identification of polyisoprenoid alcohols. *Rapid Communications in Mass Spectrometry*, *26*, 1705-1710.

[220] Murty, M. R. V. S., Chary, N. S., Prabhakar, S., Raju, N. P., & Vairamani, M. (2009). Simultaneous quantitative determination of Sudan dyes using liquid chromatography–atmospheric pressure photoionization–tandem mass spectrometry. *Food Chemistry*, *115*, 1556-1562.

[221] March, R. E., Papanastasiou, M., McMahon, W., & Allen, N. S. (2011). An investigation of paint from a mural in the church of Sainte Madeleine, Manas, France. *Journal of mass spectrometry*, *46*, 816-820.

[222] Rivera, S., Vilaró, F., & Canela, R. (2011). Determination of carotenoids by liquid chromatography/mass spectrometry: effect of several dopants. *Analytical and Bioanalytical Chemistry*, *400*, 1339-1346.

[223] Papanastasiou, M., Allen, N. S., Mcmahon, A., Naegel, L. C. A., Edge, M., & Protopappas, S. (2012). Analysis of indigo-type compounds in natural dyes by negative ion atmospheric pressure photoionization mass spectrometry. *Dyes and Pigments*, *92*, 1192-1198.

[224] Song, L., & Bartmess, J. E. (2009). Liquid chromatography/negative ion atmospheric pressure photoionization mass spectrometry: a highly sensitive method for the analysis of organic explosives. *Rapid Communications in Mass Spectrometry*, *23*, 77-84.

[225] Bagag, A., Laprévote, O., Hirsch, J., & Kovácik, V. (2008). Atmospheric pressure photoionization mass spectrometry of per-O-methylated oligosaccharides related to D-xylans. *Carbohydrate Research*, *343*, 2813-2818.

[226] Andrilli, J. D., Dittmar, T., Koch, B. P., Purcell, J. M., Marshall, A. G., & Cooper, W. T. (2010). Comprehensive characterization of marine dissolved organic matter by Fourier transform ion cyclotron resonance mass spectrometry with electrospray and atmospheric pressure photoionization. *Rapid Communications in Mass Spectrometry*, *24*, 643-650.

[227] Podgorski, D. C., McKenna, A. M., Rodgers, R. P., Marshall, A. G., & Cooper, W. T. (2012). Selective ionization of dissolved organic nitrogen by positive ion atmospheric pressure

photoionization coupled with Fourier transform ion cyclotron resonance mass spectrometry. *Analytical Chemistry*, *84*, 5085-5090.

[228] Bagag, A., Giuliani, A., & Laprévote, O. (2008). Atmospheric pressure photoionization mass spectrometry of oligodeoxyribonucleotides. *European journal of mass spectrometry*, *14*(2), 71-80.

[229] Bagag, A., Giuliani, A., & Laprévote, O. (2011). International Journal of Mass Spectrometry Atmospheric pressure photoionization of peptides. *International Journal of Mass Spectrometry*, *299*, 1-4.

[230] Carroll, D. I., Dzidic, I., Stillwell, R. N., Horning, M. G., & Horning, E. C. (1974). Subpicogram detection system for gas phase analysis based upon atmospheric pressure ionization (API) mass spectrometry. *Analytical chemistry*, *46*(6), 706-710.

[231] McDaniel, E. W. (1964). *Collision phenomena in ionized gases*. Wiley, New York.

[232] Siegel, M. W., & Fite, W. L. (1976). Terminal ions in weak atmospheric pressure plasmas. Applications of atmospheric pressure ionization to Trace Impurity Analysis in Gases. *Journal of Physical Chemistry*, *80*(26), 2871-2881.

[233] Lin, B., & Sunner, J. (1994). Ion transport by viscous gas flow through capillaries. *Journal of the American Society for Mass Spectrometry*, *5*, 873-885.

[234] Busch, K. (2004). Space charge in mass spectrometry. *Spectroscopy*, *19*, 35-38.

[235] March, R. E., & Todd, J. F. J. (2005). *Quadrupole ion trap mass spectrometry, 2nd edition*. John Wiley & Sons, Inc. New Jersey

[236] Zook, D. R., & Bruins, A. P. (1997). On cluster ions, ion transmission, and linear dynamic range limitations in electrospray (ionspray) mass spectrometry. *International Journal of Mass Spectrometry and Ion Processes*, *162*, 129-147.

[237] Robb, D. B., Smith, D. R., & Blades, M. W. (2008). Investigation of substituted-benzene dopants for charge exchange ionization of nonpolar compounds by atmospheric pressure photoionization. *Journal of the American Society for Mass Spectrometry*, *19*(7), 955-63.

[238] Robb, D. B., & Blades, M. W. (2006). Atmospheric pressure photoionization for ionization of both polar and nonpolar compounds in reversed-phase LC/MS. *Analytical chemistry*, *78*, 8162-8164.

[239] Dorgan, J. F., Fears, T. R., McMahon, R. P., Aronson-Friedman, L., Patterson, B. H., & Greenhut, S. F. (2002). Measurement of steroid sex hormones in serum: a comparison of radioimmunoassay and mass spectrometry. *Steroids*, *67*, 151-158.

[240] Hsing, A. W., Stanczyk, F. Z., Bélanger, A., Schroeder, P., Chang, L., Falk, R. T., et al. (2007). Reproducibility of serum sex steroid assays in men by RIA and mass spectrometry. *Cancer epidemiology, biomarkers & prevention*, *16*, 1004-1008.

[241] Schioler, V., & Thode, J. (1988). Six direct radioimmunoassays of estradiol evaluated. *Clinical Chemistry*, *34*, 949-952.

[242] Hadef, Y., Kaloustian, J., Portugal, H., & Nicolay, A. (2008). Multivariate optimization of a derivatisation procedure for the simultaneous determination of nine anabolic steroids by gas chromatography coupled with mass spectrometry. *Journal of Chromatography A*, *1190*, 278-285.

[243] Choi, M. H., Kim, K.-R., Hong, J. K., Park, S. J., & Chung, B. C. (2002). Determination of non-steroidal estrogens in breast milk, plasma, urine and hair by gas chromatography/mass spectrometry. *Rapid Communications in Mass Spectrometry*, *16*, 2221-2228.

[244] Homma, K., Hasegawa, T., Masumoto, M., Takeshita, E., Watanabe, K., Chiba, H., et al. (2003). Reference values for urinary steroids in Japanese newborn infants: Gas chromatography/mass spectrometry in selected ion monitoring. *Endocrine Journal*, *50*, 783-792.

[245] Bowden, J. A., Colosi, D. M., Mora-Montero, D. C., Garrett, T. J., & Yost, R. A. (2009). Enhancement of chemical derivatization of steroids by gas chromatography/mass spectrometry (GC/MS). *Journal of Chromatography B*, *877*, 3237-3242.

[246] Wolthers, B. G., & Kraan, G. P. (1999). Clinical applications of gas chromatography and gas chromatography-mass spectrometry of steroids. *Journal of chromatography. A*, *843*(1-2), 247-74.

[247] Shimada, K., Mitamura, K., & Higashi, T. (2001). Gas chromatography and high-performance liquid chromatography of natural steroids. *Journal of chromatography. A*, *935*, 141-172.

[248] Annesley, T. M. (2003). Ion suppression in mass spectrometry. *Clinical chemistry*, *49*, 1041-1044.

[249] Schlusener, M. P., & Bester, K. (2005). Determination of steroid hormones, hormone conjugates and macrolide antibiotics in influents and effluents of sewage treatment plants utilising high-performance liquid chromatography/tandem mass spectrometry with electrospray and atmospheric pressure chem. *Rapid Communications in Mass Spectrometry*, *19*, 3269-3278.

[250] King, R., Bonfiglio, R., Fernandez-Metzler, C., Miller-Stein, C., & Olah, T. (2000). Mechanistic investigation of ionization suppression in electrospray ionization. *American Society for Mass Spectrometry*, *11*, 942-950.

[251] Hanold, K. A., Fischer, S. M., Cormia, P. H., Miller, C. E., & Syage, J. A. (2004). Atmospheric pressure photoionization. 1. General properties for LC/MS. *Analytical chemistry*, *76*, 2842-2851.

[252] Haddad, J. G., & Hahn, T. J. (1973). Natural and synthetic sources of circulating 25-hydroxyvitamin D in man. *Nature*, *244*, 515-517.

[253] Clemens, T. L., Adams, J. S., Nolan, J. M., & Holick, M. F. (1982). Measurement of circulating vitamin D in man. *Clinica Chimica Acta*, *121*, 301-308.

[254] Horst, R. L., Reinhardt, T. A., Beltz, D. C., & Littledike, E. T. (1981). A senstive competitive protein binding assay for vitamin D in plasma. *Steroids*, *37*, 581-591.

[255] Holils, B. W., & Napoll, J. L. (1985). Improved radioimmunoassay for vitamin D and its use in assessing vitamin D status. *Clinical Chemistry*, *31*, 1815-1819.

[256] Hollis, B. W., Kamerud, J. Q., Selvaag, S. R., Lorenz, J. D., & Napoli, J. L. (1993). Determination of vitamin D status by radioimmunoassay with an 125I-labeled tracer, *39*, 529-533.

[257] Lind, C., Chen, J., & Byrjalsen, I. (1997). Enzyme immunoassay for measuring 25-hydroxyvitamin D3 in serum. *Clinical Chemistry*, *43*, 943-949.

[258] Snellman, G., Melhus, H., Gedeborg, R., Byberg, L., Berglund, L., Wernroth, L., et al. (2010). Determining vitamin D status: A comparison between commercially available assays. *PLoS ONE*, *5*, 1-7.

[259] Jones, G. (1978). Assay of vitamins D2 and D3, and 25-Hydroxyvitamins D2 and D3 in human plasma by high-performance liquid chromatography. *Clinical Chemistry*, *24*, 287-298.

[260] Hymøller, L., & Jensen, S. K. (2011). Vitamin D analysis in plasma by high performance liquid chromatography (HPLC) with C30 reversed phase column and UV detection – Easy and acetonitrile-free. *Journal of Chromatography A*, *1218*, 1835-1841.

[261] Sibum, M. (2010). Determination of 25-mono-hydroxy-vitamin D2 and D3 in human plasma using a symbiosis pico system : ACN free on-line SPE-LC-MS-MS. *LC-GC Europe*, March.

[262] Byrdwell, W. C. (2010). Dual parallel mass spectrometry for lipid and vitamin D analysis. *Journal of Chromatography A*, *1217*, 3992-4003.

[263] Couchman, L., Benton, C. M., & Moniz, C. F. (2012). Variability in the analysis of 25-hydroxyvitamin D by liquid chromatography–tandem mass spectrometry: The devil is in the detail. *Clinica Chimica Acta*, *413*, 1239-1243.

[264] Højskov, C. S., Heickendorff, L., & Møller, H. J. (2010). High-throughput liquid–liquid extraction and LCMSMS assay for determination of circulating 25 (OH) vitamin D3 and D2 in the routine clinical laboratory. *Clinica Chimica Acta*, *411*, 114-116.

[265] Guo, T., Taylor, R. L., Singh, R. J., & Soldin, S. J. (2006). Simultaneous determination of 12 steroids by isotope dilution liquid chromatography-photospray ionization tandem mass spectrometry. *Clinica Chimica Acta*, *372*, 76-82.

[266] Herrmann, M., Harwood, T., Gaston-Parry, O., Kouzios, D., Wong, T., Lih, A., et al. (2010). A new quantitative LC tandem mass spectrometry assay for serum 25-hydroxy vitamin D. *Steroids*, *75*, 1106-1112.

[267] Agency for Toxic Substances and Disease Registry, (2011), www.atsdr.cdc.gov/csem/pah/docs/pah.pdf

[268] Toriba, A., Kuramae, Y., Chetiyanukornkul, T., Kizu, R., Makino, T., Nakazawa, H., et al. (2003). Quantification of polycyclic aromatic hydrocarbons (PAHs) in human hair by HPLC with fluorescence detection: a biological monitoring method to evaluate the exposure to PAHs. *Biomedical Chromatography*, *17*, 126-132.

[269] Wang, Y., Zhang, J., Ding, Y., Zhou, J., Ni, L., & Sun, C. (2009). Quantitative determination of 16 polycyclic aromatic hydrocarbons in soil samples using solid-phase microextraction. *Journal of Separation Science*, *32*, 3951-3957.

[270] Dong, C.-D., Chen, C.-F., & Chen, C.-W. (2012). Determination of polycyclic aromatic hydrocarbons in industrial harbor sediments by GC-MS. *International Journal of Environmental Research and Public Health*, *9*, 2175-2188.

[271] Lien, G.-W., Chen, C.-Y., & Wu, C.-F. (2007). Analysis of polycyclic aromatic hydrocarbons by liquid chromatography/tandem mass spectrometry using atmospheric pressure chemical ionization or electrospray ionization with tropylium post-column derivatization. *Rapid Communications in Mass Spectrometry*, *21*, 3694-3700.

[272] Blanchard, J. (1981). Evaluation of the relative efficacy of various techniques for deproteinixing plasma samples prior to high-performance liquid chromatographic analysis. *Journal of Chromatography*, *226*, 455-460.

[273] Marchi, I., Rudaz, S., Selman, M., & Veuthey, J.-L. (2007). Evaluation of the influence of protein precipitation prior to on-line SPE-LC-API/MS procedures using multivariate data analysis. *Journal of chromatography. B*, *845*, 244-52.

[274] Harwood, D. T., & Handelsman, D. J. (2009). Development and validation of a sensitive liquid chromatography–tandem mass spectrometry assay to simultaneously measure androgens and estrogens in serum without derivatization. *Clinica Chimica Acta*, *409*, 78-84.

[275] Moors, M., Massart, D. L., & McDowall, R. D. (1994). Analyte isolation by solid phase extraction (SPE) on silica-bonded phases. Classification and recommended practices. *Pure and Applied Chemistry*, *66*, 277-304.

[276] Ceglarek, U., Kortz, L., Leichtle, A., Fiedler, G. M., Kratzsch, J., & Thiery, J. (2009). Rapid quantification of steroid patterns in human serum by on-line solid phase extraction combined with liquid chromatography-triple quadrupole linear ion trap mass spectrometry. *Clinica Chimica Acta*, *401*, 114-118.

[277] Yang, X.-li, Shen, D.-qun, Fu, D.-F., Li, G.-ping, & Song, H.-liang. (2010). Optimization of solid phase extraction for determining steroid estrogens in wastewater by high-performance liquid chromatography. *2nd Conference on Environmental Science and Information Application Technology*. 663-666.

[278] Ho, E. N. M., Leung, D. K. K., Wan, T. S. M., & Yu, N. H. (2006). Comprehensive screening of anabolic steroids, corticosteroids, and acidic drugs in horse urine by solid-phase extraction and liquid chromatography–mass spectrometry. *Journal of Chromatography A*, *1120*, 38-53.

[279] Higashi, T., & Shimada, K. (2004). Derivatization of neutral steroids to enhance their detection characteristics in liquid chromatography-mass spectrometry. *Analytical and Bioanalytical Chemistry*, *378*, 875-882.

[280] Santa, T., Al-Dirbashi, O. Y., & Fukushima, T. (2007). Derivatization reagents in liquid chromatography/electrospray ionization tandem mass spectrometry for biomedical analysis. *Drug Discoveries and Therapeutics*, *1*, 108-118.

[281] Nishio, T., Higashi, T., Funaishi, A., Tanaka, J., & Shimada, K. (2007). Development and application of electrospray-active derivatization reagents for hydroxysteroids. *Journal of Pharmaceutical and Biomedical Analysis*, *44*, 786-795.

[282] Liu, G., Snapp, H. M., Ji, Q. C., & Arnold, M. E. (2009). Strategy of accelerated method development for high-throughput bioanalytical assays using ultra high-performance liquid chromatography coupled with mass spectrometry. *Analytical Chemistry*, *81*, 9225-9232.

[283] Guillarme, D., Ruta, J., Rudaz, S., & Veuthey, J.-L. (2010). New trends in fast and high-resolution liquid chromatography: a critical comparison of existing approaches. *Analytical and Bioanalytical Chemistry*, *397*, 1069-1082.

[284] Tai, S. S.-C., & Welch, M. J. (2005). Development and evaluation of a reference measurement procedure for the determination of estradiol-17beta in human serum using isotope-dilution liquid chromatography-tandem mass spectrometry. *Analytical Chemistry*, *77*, 6359-6363.

[285] Iribarne, J. V., & Thomson, B. A. (1976). On the evaporation of small ions from charged droplets. *Journal of Chemical Physics*, *64*, 2287-2294.

[286] Modhave, Y. (2012). Matrix effect in bioanalysis: An overview. *International Journal of Pharmaceutical and Phytopharmacological Research*, *1*, 403-405.

[287] Tang, K., Page, J. S., & Smith, R. D. (2004). Charge competition and the linear dynamic range of detection in electrospray ionization mass spectrometry. *Journal of the American Society for Mass Spectrometry*, *15*, 1416-1423.

[288] Matuszewski, B. K., Constanzer, M. L., & Chavez-Eng, C. M. (2003). Strategies for the assessment of matrix effect in quantitative bioanalytical methods based on HPLC-MS/MS. *Analytical Chemistry*, *75*, 3019-3030.

[289] Takino, M., Daishima, S., & Nakahara, T. (2003). Determination of perfluorooctane sulfonate in river water by liquid chromatography/atmospheric pressure photoionization mass spectrometry by automated on-line extraction using turbulent flow chromatography. *Rapid communications in mass spectrometry : RCM*, *17*(5), 383-90.

[290] Takino, M., Daishima, S., & Nakahara, T. (2003). Liquid chromatography/mass spectrometric determination of patulin in apple juice using atmospheric pressure photoionization. *Rapid communications in mass spectrometry : RCM*, *17*(17), 1965-72.

[291] Takino, M., Tanaka, T., Yamaguchi, K., & Nakahara, T. (2004). Atmospheric pressure photo-ionization liquid chromatography/mass spectrometric determination of aflatoxins in food. *Food additives and contaminants*, *21*(1), 76-84.

[292] Takino, M., Yamaguchi, K., & Nakahara, T. (2004). Determination of carbamate pesticide residues in vegetables and fruits by liquid chromatography-atmospheric pressure photoionization-mass spectrometry and atmospheric pressure chemical ionization-mass spectrometry. *Journal of agricultural and food chemistry*, *52*(4), 727-35.

[293] Guidance for industry: Bioanalytical method validation, FDA. (2001). *http://www.fda.gov/cder/guidance/index.htm*.

[294] Bonfiglio, R., King, R. C., Olah, T. V., & Merkle, K. (1999). The effects of sample preparation methods on the variability of the electrospray ionization response for model drug compounds. *Rapid Communications in Mass Spectrometry*, *1185*, 1175-1185.

[295] Taylor, P. J. (2005). Matrix effects: the Achilles heel of quantitative high-performance liquid chromatography-electrospray-tandem mass spectrometry. *Clinical Biochemistry*, *38*, 328-334.

[296] Matuszewski, B. K., Constanzer, M. L., & Chavez-Eng, C. M. (2003). Strategies for the assessment of matrix effect in quantitative bioanalytical methods based on HPLC-MS/MS. *Analytical Chemistry*, *75*, 3019-3030.

[297] Miller, J. C., & Miller, J. N. (1993). *Statistics for analytical chemistry* (3rd ed.). West Sussex, England: Ellis Horwood Limited.

[298] Hartmann, C., Vankeerberghen, P., & Massart, D. L. (1997). Robust orthogonal regression for the outlier detection when comparing two series of measurement results. *Analytica Chimica Acta*, *2670*(97).

[299] Nguyen, H. P., Li, L., Nethrapalli, I. S., Guo, N., Toran-Allerand, D. C., Harrison, D. E., Astle, M. C.,Schug, K. A. (2011). Evaluation of matrix effects in analysis of estrogen using liquid chromatography–tandem mass spectrometry. *Journal of Separation Science*, *34*, 1781-1787.

[300] Van Eeckhaut, A., Lanckmans, K., Sarre, S., Smolders, I., & Michotte, Y. (2009). Validation of bioanalytical LC–MS/MS assays: Evaluation of matrix effects. *Journal of Chromatography B*, *877*, 2198-2207.

[301] Liang, H. R., Foltz, R. L., Meng, M., & Bennett, P. (2003). Ionization enhancement in atmospheric pressure chemical ionization and suppression in electrospray ionization between target drugs and stable-isotope-labeled internal standards in quantitative liquid chromatography/tandem mass spectrometry. *Rapid communications in mass spectrometry : RCM*, *17*(24), 2815-21.

[302] Zhao, X., & Metcalfe, C. D. (2008). Characterizing and compensating for matrix effects using atmospheric pressure chemical ionization liquid chromatography-tandem mass spectrometry: analysis of neutral pharmaceuticals in municipal wastewater. *Analytical Chemistry*, *80*, 2010-2017.

[303] Strassnig, S., & Lankmayr, E. P. (1999). Elimination of matrix effects for static headspace analysis of ethanol. *Journal of Chromatography A*, *849*, 629-636.

[304] Gosetti, F., Mazzucco, E., Zampieri, D., & Gennaro, M. C. (2010). Signal suppression/enhancement in high-performance liquid chromatography tandem mass spectrometry. *Journal of Chromatography A*, *1217*, 3929-3937.

[305] Holcapek, M., Volna, K., Jandera, P., Kolarova, L., Lemr, K., Exner, M., et al. (2004). Effects of ion-pairing reagents on the electrospray signal suppression of sulphonated dyes and intermediates. *Journal of mass spectrometry*, *39*, 43-50.

[306] Kauppila, T. J., Kostiainen, R., & Bruins, A. P. (2004). Anisole, a new dopant for atmospheric pressure photoionization mass spectrometry of low proton affinity, low ionization energy compounds. *Rapid Communications in Mass Spectrometry*, *18*, 808-815.

# Appendices

## Appendix A. Parameters Affecting Charge Exchange Ionization in Field-free Atmospheric Pressure Photoionization Sources

Fluoranthene is a non-polar polycyclic aromatic hydrocarbon, stabilized through a fused structure of aromatic rings containing no appreciable basic functionalities. As a consequence, fluoranthene, alongside most PAHs, tends to be inefficiently ionized through the proton transfer mechanism. Instead, many non-polar compounds like fluoranthene may adopt a charge more readily through the charge exchange mechanism. The ability to efficiently ionize a wide range of non-polar compounds through CE supports APPI as the most universal LC-MS ion source.

In chapter 2, we identified that a loss in sensitivity was experienced with increased flight tube length for the analysis of fluoranthene standards ionized through charge exchange (see figure 2-11). The observed decrease in sensitivity was consistent and reproducible, yet inverse to the trend observed for analytes ionized through the proton transfer ionization mechanism; basic analytes tend to exhibit increased sensitivity with extended field-free reaction time. We attribute the observed loss in sensitivity for fluoranthene to be related to dopant selection. Toluene has been shown to react (often to completion) with reverse phase solvents leading to the formation of a stable population of protonated solvent clusters. Solvent clusters conveniently provide a source of acidic reagent ions suitable for proton transfer ionization, however, their formation results in a significantly depletion in the population of dopant reagent ions ($D^{+\bullet}$) available for CE. According to theory, analyte sensitivity will increase with flight tube length, but only if the available concentration of reagent ions remains in excess. Upon consumption of the stable CE reagent ion supply, we expect the effects of charge recombination to dominate the equilibrium between analyte ion formation and

loss processes. This will ultimately lead to a net reduction in both total ion current (TIC) and analyte ion yield with increased transit length and reaction time. Robb et al. reported that methods utilizing toluene as a dopant typically optimize toward higher temperatures, presumably due to a decrease in the size of solvent clusters formed and in-turn the consumption of toluene photoions may be impeded.[238] Thus, higher source temperatures may lead to improved charge exchange efficiency with increased transit length, provided the population toluene dopant reagent ions is in stable excess. Otherwise, the selection of an alternative dopant candidate, which does not react completely with reverse phase solvents, should also produce a stable population of CE reagent ions. Popular alternative charge exchange dopant candidates include anisole, fluorinated anisoles, chlorobenzene and bromobenzene.

Anisole was first identified as a potential CE dopant candidate for LC-APPI-MS applications by Kauppila et al. in 2004.[306] Anisole was demonstrated to be suitable for the analysis of compounds with low proton affinity – specifically analytes not amenable to ionization through proton transfer. Anisole may be used to provide a stable population of reagent ions as it does not react to completion in the presence of methanol or acetonitrile. As a result, anisole has been shown to provide enhanced performance for CE-APPI methods compared to toluene, at times providing sensitivity improvements over several orders-of-magnitude. In order to be an effective CE dopant, however, the ionizing reagent compound must have an ionization energy significantly above that of the analyte. The effectiveness of anisole is limited by its relatively low IE (8.2 eV), restricting the range of potential analytes. Consequently alternative dopant candidates have been sought. The result of an exhaustive study, Robb et al. identified a number of potential CE dopants capable of broadening the range of compounds ionizeable through CE.[237] Chloro- and bromobenzene emerged as the candidates with the most considerable promise, and have since garnered the widest acceptance.

In this experimental appendix we will explore the use of chlorobenzene as an alternative dopant to toluene for the analysis of a variety of non-polar compounds. The aim was to demonstrate that sensitivity will improve with transit length for compounds ionized through charge exchange, provided a suitable dopant is employed. The effects of temperature and mobile phase composition will also to evaluated, leading to a better understanding of the reagent ion chemistry at play within field-free APPI sources.

Methods and Materials:

Instrumentation, experimental conditions, chemicals and sample preparation was identical to that employed within chapter 2. See the associated methods and materials section for all relevant experimental details.

Results and discussion:

Figure A-1a presents XIC signal intensities obtained for the flow injection of fluoranthene standards as a function of flight tube length, at various source temperatures. Chlorobenzene was employed as a dopant, which has been shown to provide a stable population of dopant radical cations ($D^{+\bullet}$), even in the presence of a high organic mobile phase concentration. As expected, signal intensities were found to increase steadily with increased field-free transit length, for the range of flight tubes surveyed. This indicates that under suitable conditions, *the efficiency of analyte ionization through CE can increase with extended field-free transit length, provided a stable population of reagent ions is maintained in excess*. However, the results under these conditions were not found to be universally applicable to all non-polar PAHs. Figure A-1b provides signal intensities for the flow injection of naphthalene standards, also obtained as a function of flight tube length and source temperature. The results demonstrate that at low temperatures naphthalene conforms to the expected trend, resulting in increased signal with elongated transit length. At high temperatures, however,

the results deviate from the trend, providing diminishing returns with increased reaction time. To explain these results a closer look at the reagent species present in the source is necessary.

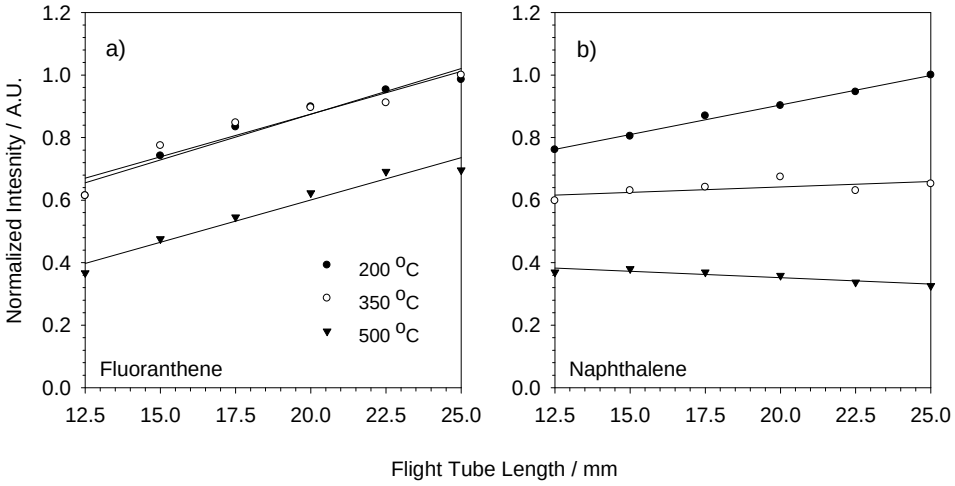


**Figure A-1. a) Fluoranthene and b) naphthalene XIC response by flow injection as a function of flight tube length, using chlorobenzene as a dopant.**

Figure A-2 provides full scan spectra obtained as an average of 10 scans. The spectrum in panel (a) was obtained for the infusion of chlorobenzene dopant only at 5 μL/min. Peaks at m/z 112 and 114 correspond to $D^{+\bullet}$ photoions produced in the absence of any reverse phase solvents. No other significant ions were observed as a result of ionized impurities introduced with the dopant supply. Panel (b) shows a spectrum under identical conditions, however, with the additional infusion of methanol at 50 μL/min. The peaks at 112 and 114 m/z have now significantly decreased in intensity and several additional peaks have emerged. The small peak at m/z 65 corresponds to a methanol solvent cluster comprised ($2S + H^+$), indicating that this primary reagent ion loss process still persists for chlorobenzene, even though a stable $D^{+\bullet}$ population is also retained. The most notable new peak appears at m/z 108 belonging to anisole, presumed to be produced through a methoxy substitution reaction between the dopant photoions and the mobile phase.[237] This reaction may be described by:

$$C_6H_5Cl^+ + CH_3OH \rightarrow C_6H_5OCH_3^+ + HCl \qquad (19)$$

Panel (c) provides a spectrum obtained with the infusion of fully substituted D4-methanol, infused at 50 μL/min. The anisole peak was observed to shift 3 mass units to m/z 111, while maintaining the same overall intensity, confirming that the presence of anisole is likely a product of the in-source substitution mechanism and not the result of carryover or the ionization of a trace impurity. (Interestingly, the solvent cluster ion appears to shift from m/z 65 to 71 and not 73 as should be expected, indicating some degree of Hydrogen-Deuterium scrambling between the chlorobenzene and D4-methanol may be evident).

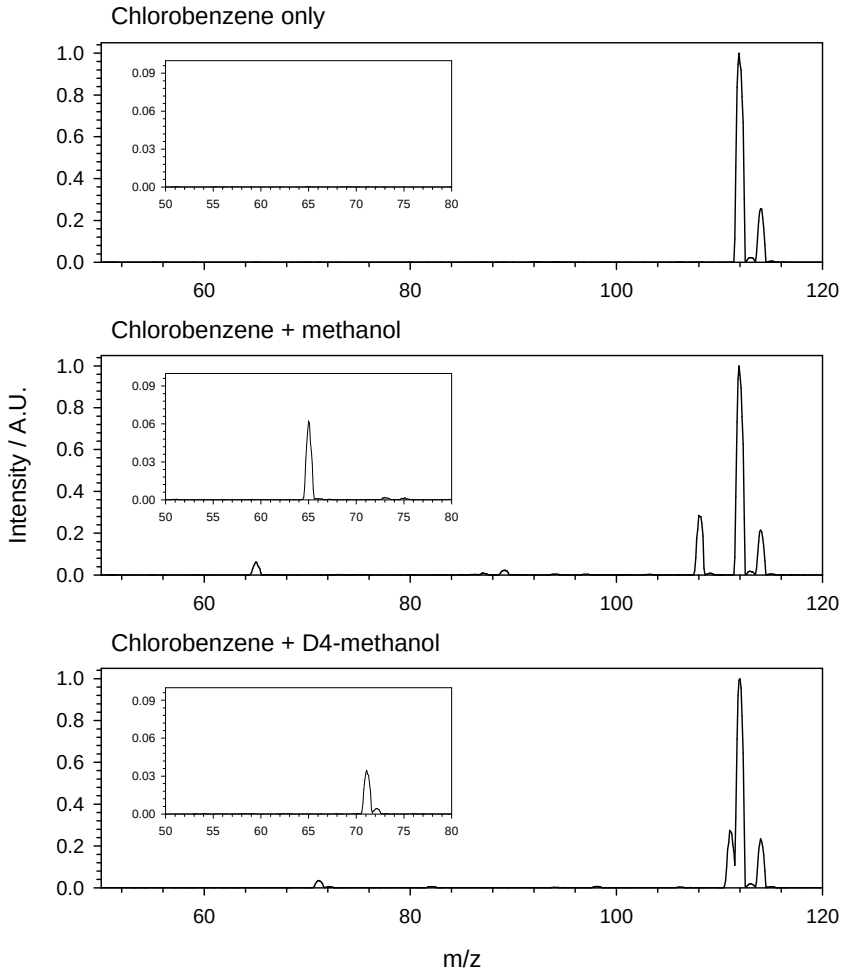


**Figure A-2. Full scan spectra for chlorobenzene at 5 μL/min a) only, b) including the additional infusion of methanol at 50 μL/min and c) including the additional infusion of D4-methanol at 50 μL/min.**

Both anisole and chlorobenzene are capable of maintaining a stable population of reagent cations under common reverse phase conditions. Likewise, both are capable of acting as CE reagent ions for many analytes possessing a lower IE than the electron recombination energy of their respective radical cations ($D^{+\bullet}$). In this regard, chlorobenzene has been identified as a superior candidate to anisole for its ability to ionize a broader range of compounds. However, this advantage could be lost if the population of chlorobenzene reagent ions is depleted due to the formation of anisole cations. Figure A-3 demonstrates the effect of source temperature on the relative concentrations of anisole and chlorobenzene reagent ions available for charge exchange under common LC-MS conditions.

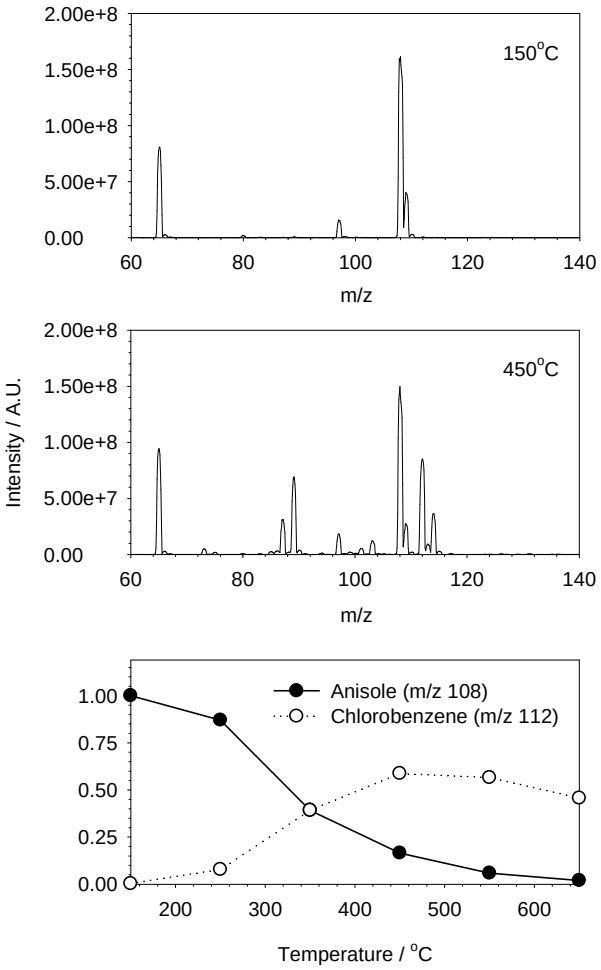


**Figure A-3. MCA full scan spectra for chlorobenzene introduced at 20 µL/min including the additional infusion of methanol at 200 µL/min a) at 150°C and b) 450°C. c) Normalized MRM signal intensities for anisole (m/z 108) and chlorobenzene (m/z 112) ions at a range of vapourizer temperatures.**

At lower source temperatures (figure A-3a) reaction 19 proceeds virtually to completion, converting nearly all chlorobenzene dopant radical cations into anisole ions. We expect the methoxy substitution reaction to proceed quickly given that both reactants are present in excess and the rate of the reaction will be governed by a very high collision frequency at atmospheric pressure. At higher temperatures (figure A-3b) the equilibrium swings heavily in favour of the reactants, resulting in limited anisole ion formation, while preserving the population of chlorobenzene reagent ions. For completeness, figure A-3c fully characterizes the effect of vapourization temperature upon the relative contributions of anisole and chlorobenzene reagent ion species.

Figure A-4 describes the influence of source temperature on the XIC signal intensities obtained for the flow injection of 1 μM fluoranthene, naphthalene and 1,3,5-trimethylbenzene single component standards, utilizing both chlorobenzene and toluene as dopants. Relevant relative ionization energies are provided for reference in table A-1.

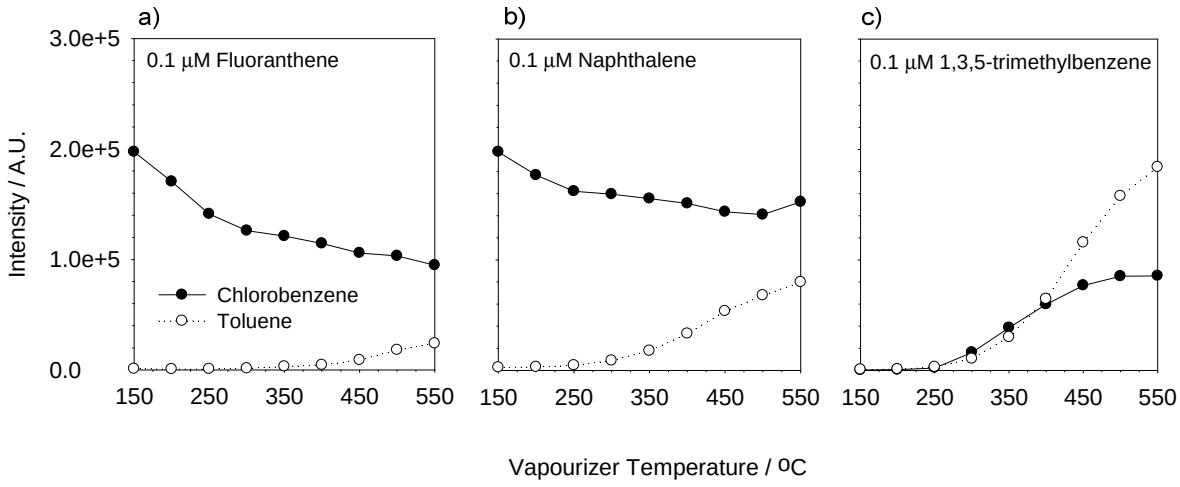


**Figure A-4. Effect of source temperature on the XIC intensities obtained for a) fluoranthene, b) naphthalene and c) 1,3,5-trimethylbenzene. Results provided using both toluene and chlorobenzene as dopants.**

**Table A-1. Ionization energies of various dopants and non-polar analytes**

| Compound | MW (g/mol) | IE (eV) |
|---|---|---|
| Chlorobenzene | 112.6 | 9.07 |
| Bromobenzene | 157.0 | 9.00 |
| Toluene | 92.1 | 8.83 |
| Phenyl acetate | 136.2 | 8.72 |
| Mesitylene | 120.2 | 8.40 |
| Anisole | 108.1 | 8.20 |
| Naphthalene | 128.2 | 8.14 |
| Fluoranthene | 202.3 | 7.90 |

Panel (a) presents results for fluoranthene. As suggested previously, fluoranthene response appears to optimize toward high temperatures when toluene is used as a dopant. The results obtained while using chlorobenzene, however, exhibit the opposite trend, demonstrating a steady decrease in response at higher source temperatures. Fluoranthene has an ionization energy of 7.9 eV, well below both anisole and chlorobenzene, meaning it should be effectively ionized using either dopant. The results suggest that fluoranthene ionizes more efficiently at low temperatures through interaction with anisole reagent ions, rather than with chlorobenzene radical cations at high temperatures. Panel (b) provides the results obtained for naphthalene. A similar trend is obtained, however, with a reduced bias toward lower temperatures and the presence of anisole. The separation in ionization energies between naphthalene (IE 8.14 eV) and anisole (IE 8.20 eV) is much smaller, suggesting that the ionization efficiency through interaction with anisole may be impeded. Panel (c) presents results obtained for 1,3,5-trimethylbenzene, with an IE of 8.40 eV, well above that of anisole yet below chlorobenzene (9.07 eV). Here, analyte ionization is observed only toward high source temperatures where an excess population of chlorobenzene reagent ions is maintained. No significant CE was observed at low temperatures, presumably because the anisole cation is insufficiently electron withdrawing to abstract an electron from the analyte. Curiously, the ionization efficiency of 1,3,5-trimethylbenzene was found to be

better using simply toluene rather than chlorobenzene despite the extensive depletion of toluene reagent ions with the formation of protonated solvent clusters.

Referring back to the results presented for naphthalene in figure A-1b, we can draw the conclusion that at low source temperatures, sensitivity for naphthalene steadily improves as the field-free reaction zone is lengthened, suggesting that an excess supply of reagent ions (presumably anisole) is maintained. However, as the temperature is increased the slope of the trend regresses, ultimately exhibiting a loss of analyte ion yield with increased field-free reaction time. This result suggests that at high vapourizer temperatures, the reagent ion population has potentially been exhausted. This may be an indication that CE ionization under conditions utilizing chlorobenzene as a dopant may in fact rely heavily upon a mechanism involving the anisole intermediate, rather than the primary reagent photoions themselves. To illustrate this further, figure A-5 presents spectra obtained for the analysis of a new 10 μM D8-naphthalene standard. Panel A-5a was obtained for the dopant only case, displaying only the expected chlorobenzene reagent ions. Panel A-5b was obtained for the infusion of chlorobenzene and pure methanol mobile phase only, with at vapourizer temperature set to 300$^{o}$C. Stable reagent ion species are clearly present for both chlorobenzene (m/z 112 and 114) and the anisole by-product (108). The last panel in figure A-5 shows the same spectrum, however, now including the additional infusion of the D8-fluoranthene standard. A new strong $M^{+\bullet}$ signal is observed for D8-naphthalene at m/z 136. At the same time the signal for the anisole reagent ion species has diminished by roughly a corresponding amount, while the chlorobenzene signal remained largely unaffected. We take this as evidence that the charge exchange from the anisole reagent species to the analyte is the dominant ionization channel under the given conditions. In any event, careful optimization of reagent composition and source temperature should be performed for all analytes as APPI methods are still far from turnkey assays.

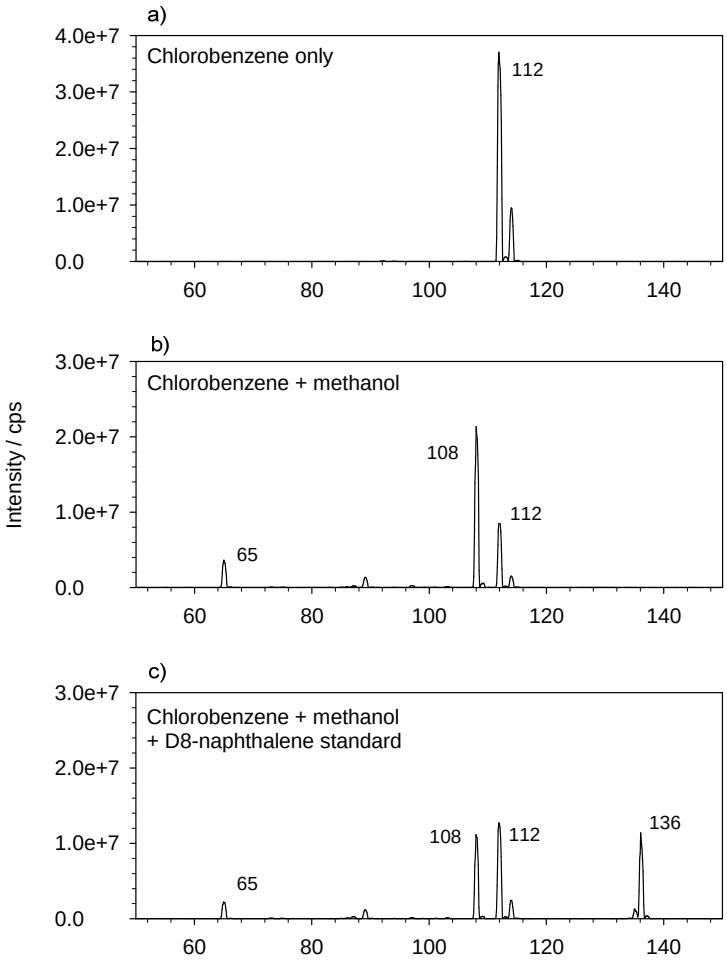


**Figure A-5. MCA full scan spectra for chlorobenzene a) only, b) with methanol effluent flow and c) methanol plus D8-naphthalene (m/z 136) standards infused at 5 µL/min.**

## Conclusions

Most importantly, for the field-free APPI source, analyte sensitivity by charge exchange will improve with field-free reaction length provided a population of suitable dopant reagent ions is maintained in excess. This implies that increasing the length of the flight tube further will ultimately lead to improved sensitivity, at least until the reagent ion population has been consumed. This presents a geometric parameter through which source design may be optimized in the future.

Additionally, chlorobenzene (and presumably bromobenzene) may react with methanol to produce anisole through a methoxy- substitution reaction pathway. Other reactions may be expected to occur for alternative reverse phase solvents (i.e. acetonitrile), however, this has yet to be studied. The formation of anisole represents a potential reagent ion loss process, which could ultimately limit the effectiveness of these dopant candidates. Anisole cations generated in-source may still participate in subsequent ion-molecule reactions with non-polar compounds provided the analyte has an ionization energy below 8.2 eV. Our results also suggest this may represent the preferred ionization pathway for non-polar analytes with an IE below that of anisole.

## Appendix B. Design and Evaluation of a Pneumatic Dopant Delivery Device for LC-APPI-MS Applications

The use of chemical dopants is now considered standard practice for the modern LC-APPI-MS workflow. The stable, continuous delivery of a dopant to the APPI source, however, can be considered an existing technical limitation of the technique. Typically, a dopant is introduced to the ion source independently from the LC sample stream by means of either a syringe infusion pump or a dedicated chromatographic solvent pump. Syringe pumps, although reasonably reliable and cost effective have a restricted volume limit. As the syringe volume is increased to improve capacity the pump delivery step rate must in-turn decrease, ultimately leading to flow pulsations, adversely impacting signal stability. In practice, pulse-free operation is only possible for a few hours before the dopant supply is exhausted at flow rates associated with APPI applications. Additionally, the use of glass syringes may be prohibitive for systems exhibiting significant backpressure. Glass syringes have a propensity for developing leaks or plugs and have even been known to shatter without warning. A dedicated chromatographic pump may be used to provide a continuous dopant flow over extended periods; however, this requires the addition of costly instrumentation to an already expensive MS workflow. LC pumps have been shown to be generally more effective and robust than syringe pumps, though they may be viewed as excessive for dedicated APPI dopant delivery.

In this appendix we describe a simple, inexpensive device designed to pneumatically deliver dopant for LC-APPI-MS applications. We have included a detailed parts list and assembly instructions to enable others to reproduce this device, facilitating inexpensive, high capacity dopant delivery. Pneumatic solvent delivery is by no means a novel concept. A number of pressure driven pump designs have been described and even commercialized in the past. Most of these, however, still rely upon mechanical piston mechanisms opening the

potential for moving parts to fail, or valves and seals to degrade over time. The Dionex PC10 Post column delivery system is an example of a commercially available pressure driven solvent pump that operates in the absence of moving parts, valves or seals. The PC10 is intended for the automated delivery of chemical reagents required for ion chromatography applications. Since the device is specifically designed as a post-column utility, it can be inferred that it is only suitable for operation under low backpressure conditions. The largest drawbacks to a device of this kind for dopant delivery may only be the initial instrument cost associated with a commercial product and perhaps a lack of user control for systems not equipped to run its specialized software.

The device introduced here contains no moving parts or pistons and requires no input electrical power to provide stable, pulse-free isocratic dopant flow, demonstrated for flow rates ranging from 1 to over 100 μL/min. This flow rate range lends the device ideally, however, not exclusively to dopant delivery for APPI applications. As designed, this device is not suitable for LC mobile phase solvent delivery as it is not capable of meeting column pressure requirements. All device components identified here are readily obtainable from common scientific parts suppliers, requiring no rigorous machining, cutting or bending of materials. A functional device can be built and calibrated for use in under an hour.

In an effort to quickly demonstrate relative device performance, a number of experiments were devised comparing the capabilities of the pneumatic device to a standard syringe infusion pump. Factors such as spectral background complexity, stability and assay reproducibility were assessed for both systems using dopant only experiments. Furthermore, a sample mixture of three polycyclic aromatic hydrocarbons was analyzed utilizing both dopant delivery methods while performing a routine LC-APPI-MS 13-minute gradient method. PAHs are now adopted as somewhat of a de facto standard analyte for APPI analyses,[54,55,135] given their relatively low ionization energies, range of polarity and environmental relevance.

**Method and Materials:**

A schematic representation of the pneumatic dopant delivery device is presented in figure B-6. A continuous, regulated 100-psi supply of clean lab gas (i.e. air, helium or nitrogen) is used to pressurize a stainless steel sample cylinder containing the dopant. As the headspace is pressurized the dopant is forced from the cylinder through a fixed length of PEEK tubing at a flow rate directly proportional to the input gas pressure. Modifying the internal diameter of the outlet PEEK tube alters the effective backpressure and subsequently the tunable range of available flow rates. This allows the user to tailor the apparatus to meet experimental flow rate requirements. The consumption of gas in this design is negligible since the system is sealed from loses apart from small volume of eluted dopant effluent.

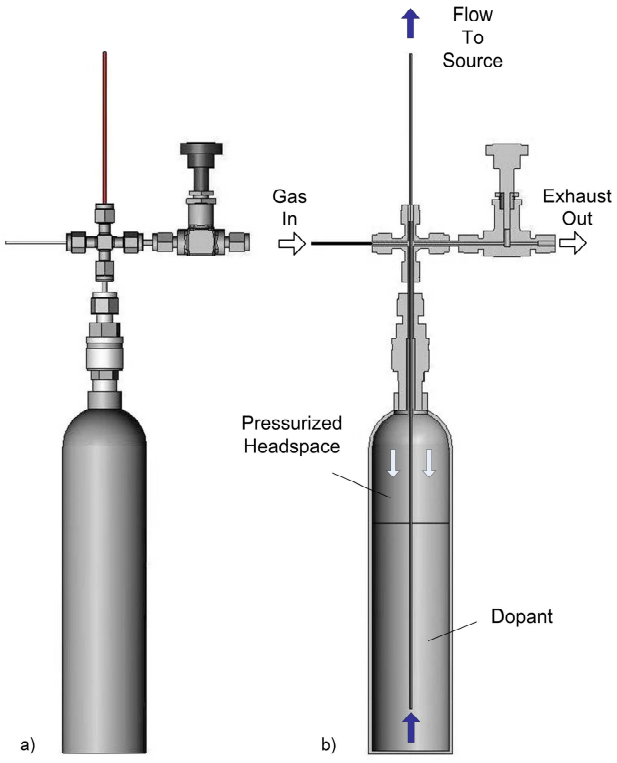


**Figure B-6. Diagrams for a) the assembled pneumatic dopant delivery device and b) the schematic representation demonstrating functionality and parts configuration.**

All required device components with applicable part numbers have been included in Table B-2 for the benefit of any who wish to reproduce its fabrication. Most required parts are simply stainless steel Swagelok fittings, ferrules, unions and vessels, thus no machining or modification is required. Figure B-6a and b are provided to illustrate the basic configuration of parts. A stainless steel sample vessel was fitted with a two-piece quick-connect union for rapid dopant refilling, thus no tools are required during day-to-day operation. On top of the quick-connect fitting a 4-way branched T-union with suitable fittings, ferrules and unions was mounted. A source of clean regulated lab gas was introduced through one horizontal arm of the branched union. A 1/4 turn stainless steel plug valve was attached to the opposite arm of the union, providing a mechanism for releasing the gas headspace, thereby reducing or halting the flow of dopant. Through the remaining top-most connection of the branch T-union a 40 cm length of PEEK tubing was secured utilizing a Vespel 1/8” to 1/16” reducing ferrule. When the reservoir is filled with solvent the end of PEEK tubing is submerged providing a flow outlet for the dopant when headspace pressure is applied. Finally, a 24” length of red PEEK tubing (0.005” ID) was utilized to connect the outlet of the pneumatic device to the APPI source dopant nebulizer using a zero-dead-volume union. The length and diameter of the PEEK tubing must kept constant, as dopant flow rate is calibrated based upon the amount of backpressure produced by the outlet restriction.

**Table B-2. Suggested part list for the pneumatic dopant delivery device**

| Supplier | Part Number | Quantity | Description |
|---|---|---|---|
| Swagelok | 304L-05SF4-300 | 1 | Sample Cylinder, 300 mL S/S |
| Swagelok | SS-QF4-B-400 | 1 | Quick-Connect Body, Female, 1/4" S/S |
| Swagelok | SS-QF4-S-4PM | 1 | Quick-Connect Body, Male, 1/4" S/S |
| Swagelok | SS-201-PC | 1 | Tube Fitting, Port Connector, 1/8" OD S/S |
| Swagelok | SS-2P4T | 1 | 1/4-Turn Instrument Plug Valve, 1/8" S/S |
| Swagelok | SS-400-R-2 | 1 | Reducer, 1/4" x 1/8" OD S/S |
| Swagelok | SS-200-4 | 1 | Union Cross, 1/8" OD S/S |
| Swagelok | SS-401-PC-2 | 1 | Reducing Port Connector, 1/4" x 1/8" OD S/S |
| Fisher Sci | AT200100VG1 | 2 | Vespel/Graphite Reducing Ferrule 1/8" to 1/16" OD |
| Upchurch | U-152 | 1 | Tube, 1/16" OD x 0.005" ID x 5 cm S/S |
| Upchurch | 1535 | [a]1 | 1/16" OD x 0.005" ID PEEK Tubing, 5' length |

[a] Substitute Upchurch p/n 1560, Natural PEEK tubing 1/16" x 0.0025" ID, 30 cm length for low flow rate applications

The completed device must be calibrated for flow rate. As a pressure driven device, calibration is complicated by any additional sources of backpressure (liquid or gas) that may affect the dopant flow rate. For instance, orthogonal AB/Sciex Photospray sources utilize an auxiliary dopant nebulizing system, operated independently of the heated nebulizer that is used to vapourize the analytical solvent flow. The dopant nebulizer gas (GS1) is supplied at pressures ranging from 20 psi to potentially more than 90 psi, creating a supply of gas containing dopant vapour. This gas flow is subsequently used to assist the vapourization of the analytical solvent flow within the heated nebulizer. The amount of gas pressure (GS1) that is ultimately supplied to the heated nebulizer must be exceeded in order to overcome the force of backpressure applied upon the liquid dopant flow. As an example, when disconnected from the ion source the pneumatic dopant delivery device was calibrated to provide 20 μL/min of toluene flow at an applied pressure of 30 psi. Connected to the Photospray source, however, the nebulizer (GS1) pressure must then be accounted for. If the nebulizer gas is set to 40 psi then the pneumatic dopant delivery device must be pressurized to 70 psi in order to overcome the applied backpressure and supply toluene at the desired 20 μL/min flow rate. Our device was tested exclusively upon an orthogonal geometry AB/Sciex Photospray source, including the auxiliary nebulizer for independent dopant introduction. If the device is utilized for introducing dopant through a post-column t-union (combining the liquid dopant and the LC solvent streams), flow rate calibration would be affected. Post column solvent flows represent additional sources of backpressure and can be accounted for through modified calibration (method not discussed). Combining the dopant and analytical solvent flows is not recommended as this method does not consider solvent immiscibility issues which may impair signal stability.

A straightforward method of calibrating the device involves simply measuring the volume of dopant delivered per unit time at a variety of applied gas pressures. When pressure is applied to the vessel, flow of dopant is established which may

then be collected using a small graduated cylinder. Timing the flow of dopant, while measuring the volume delivered allows for the reasonably accurate determination of absolute flow rate. Figure B-7 provides a sample calibration plot derived for the pneumatic delivery system demonstrating a linear flow rate response to applied gas pressure over the range of values tested. Regression lines with reported linear equations (useful for flow calibration) are shown for two different configurations utilizing alternative diameters of PEEK outlet tubing (0.005” ID, red and 0.0025” ID, natural). Higher flow ranges can be adapted by simply utilizing an even larger internal diameter PEEK tubing – further reducing outlet backpressure. Selecting a suitable PEEK outlet tube diameter enables the operator to select an optimal flow rate range for a desired application. As discussed previously, additional backpressure sources will have an additive property and must be accounted for when utilizing the calibration plot.

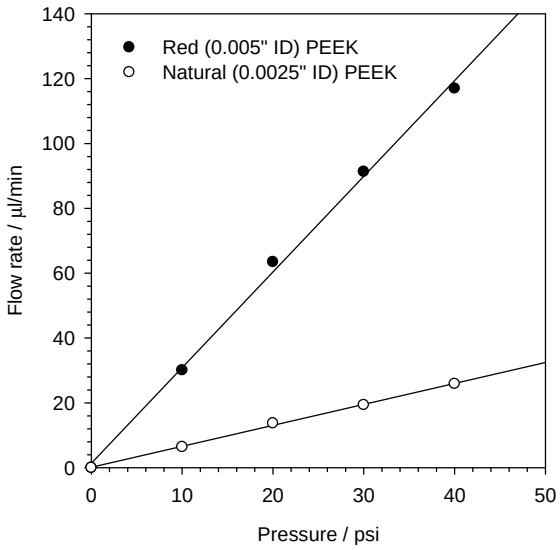


**Figure B-7. Sample flow calibration plot for the pneumatic dopant delivery deice utilizing both red (0.005” ID), and natural (0.0025” ID) PEEK tubing outlets.**

Chemicals:

HPLC grade methanol, acetonitrile and toluene were obtained from Fisher Scientific (Ottawa, ON, Canada). Deionized water was obtained using an in-house generator. A stock standard polycyclic aromatic hydrocarbon sample was

produced containing naphthalene (20 μg/mL), acenaphthylene (40 μg/mL) and acenaphthene (20 μg/mL), diluted in HPLC grade methanol. All three PAHs were obtained from Sigma Aldrich (St. Louis, MO) as dry solids at the highest available purity (> 99%). The stock sample was diluted 10-fold in pure mobile phase to match LC starting conditions.

Instrumentation:

The performance of the pneumatic dopant introduction device was evaluated upon an AB/Sciex API 3200 (Concord, Ontario, Canada) triple-quadrupole mass spectrometer, operated in selected ion mode. A prototype Photospray source, functionally identical to commercially available ion sources was utilized for all experiments. Most infusion tests were performed using a stepper motor driven infusion pump integrated within the MS. Tests requiring an additional pump for solvent delivery made use of a second external Harvard Apparatus (Holliston, MA) syringe infusion pump. The APPI source heated nebulizer was operated at 400 $^{o}$C with the transfer voltage set to 750 Volts. Nebulizer and lamp gases were set to 60 and 30 psi respectively. All gases were supplied from a high purity liquid nitrogen boil-off source. Spectral background comparison experiments were performed at dopant flows range 0.5 to 100 μL/min. Some full scan spectra were obtained with an additional flow of methanol at 95 μL/min. Flow stability analyses were performed with the infusion of toluene dopant only at 5 μL/min.

Chromatographic separations were performed using an 1100 series Hewlett Packard (Santa Clara, CA) HPLC system. A GL Sciences Inc. (Torrance, CA) Inertsil ODS-P reversed-phase, 250 mm x 2.1 mm ID, 5 μm column was utilized for sample separations. The column was placed in-line with a single 0.5 μm pre-column filter from Upchurch Scientific (Oak Harbor, WA) situated between the injection valve and the column. A short 13-minute chromatographic method was employed using methanol:water (90:10 v/v) (solvent A) and acetonitrile (solvent B) in a one step gradient elution. Solvent A was held at 100% for 3-minutes

followed by a linear increase of solvent B to 100% over a 7-minute period. This composition was maintained for 3-minutes, followed by a return to initial conditions for column re-equilibration. The combined solvent flow rate was kept maintained at 200 μL/min. 10 μL sample volumes were injected on-column through the microfilter using the injection valve integrated within the mass spectrometer.

**Results and Discussion:**

The relative performance of the pneumatic dopant delivery device was characterized through several basic infusion tests comparing relative flow stability and spectral background differences. Figure B-8 presents spectra acquired for the infusion of toluene at 5 μL/min with an additional methanol effluent flow at 95 μL/min. Spectra obtained using both dopant introduction methods were dominated by characteristic methanol and background product ions at m/z 65, 73 and 87 and 101. Both methods provided roughly equivalent relative intensities for each signal, with no evidence of extraneous contamination displayed in either spectrum. Due to the relatively high methanol component there was no evidence of a toluene peak at m/z 92 present in the spectrum. The complete loss of toluene reagent ion species ($D^{+\bullet}$) is a direct result of the formation of protonated solvent clusters – a process typical of LC-APPI-MS experiments under reversed-phase solvent conditions.[53,58] This makes toluene a less than ideal dopant candidate for the analysis of highly non-polar analytes through charge exchange as the requisite reagent ion ($D^{+\bullet}$) population is entirely consumed, limiting analyte ionization efficiency.

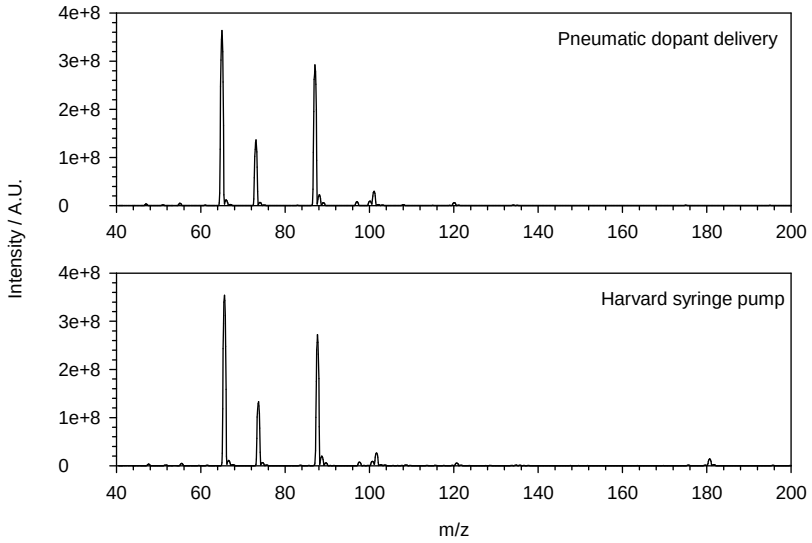


**Figure B-8. Spectra obtained using the pneumatic dopant delivery device (top) and a standard Harvard syringe pump (bottom). Toluene dopant was provided at 5 μL/min. Methanol mobile phase was infused at 95 μL/min.**

Flow stability was accessed under the same infusion conditions described above, however, without the additional methanol solvent flow. XIC scans were performed at m/z 92 and compared for the simple infusion of toluene dopant at 1 μL/min using both the pneumatic and syringe pump introduction methods (data not shown). The XIC was monitored for 30-minute intervals and the standard deviation was calculated. It was demonstrated that signal and thus flow stability for both systems was in excellent agreement over the range of flow rates tested, yielding indistinguishable results.

APPI is of course usually used as an ion source for LC/MS workflows. The potential of the pneumatic dopant delivery system is realized when the device is used to extend the operating time available for LC/MS applications without exhausting the dopant supply. A full 300 mL reservoir may last for more than 10 days of continuous operation at a common APPI flow rate of 20 μL/min. Syringe based infusion pumps utilizing a 5-mL syringe volume (permitting adequate flow stability and flow rate accuracy) may only be capable of continuous operation for slightly over 4 hours before the dopant supply is exhausted. When extended

overnight analyses are required, reliance on syringe pump dopant infusion may not be possible and thus an expensive isocratic LC pump is typically used.

To demonstrate that the pneumatic delivery device is suitable for practical LC-APPI-MS applications, a short reversed-phase gradient method was created for the analysis of a standard PAH mixture. The results presented in Figure B-9 show TIC chromatograms obtained for the analysis of the PAH panel containing (i) naphthalene, (m/z 128), (ii) acenaphthylene (m/z 152) and (iii) acenaphthene (m/z 154). Toluene was delivered to the source via the dopant nebulizer at 20 μL/min using both the pneumatic delivery device (operated at 70 psi, with GS1 set to 40 psi) and a standard syringe pump. All three analytes were fully resolved with retention times ranging between 5 and 8 minutes. Relative peak intensities were found to be in excellent agreement between both dopant delivery methods. We take these results to indicate that high quality LC/MS data is attainable with the pneumatically driven dopant delivery device.

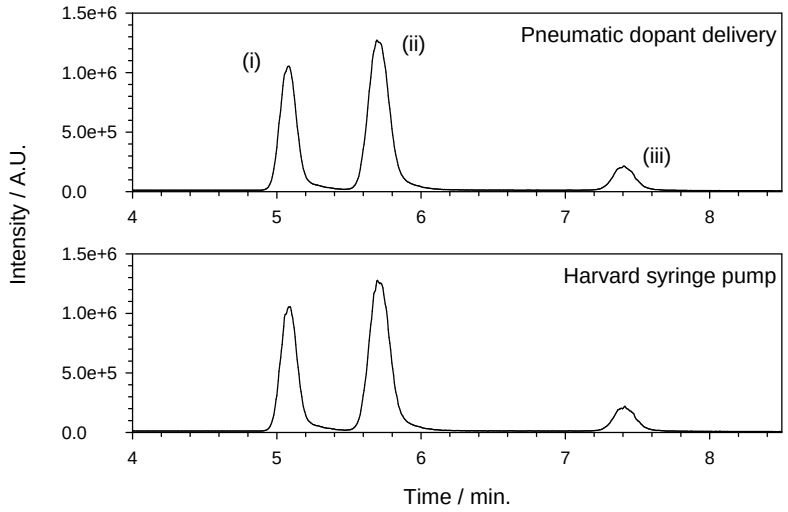


**Figure B-9. TIC chromatograms obtained for the analysis of a simple PAH panel containing (i) naphthalene, (ii) acenaphthylene and (iii) acenaphthene using a) the pneumatic dopant delivery device and b) a standard Harvard syringe pump to supply toluene dopant.**

**Conclusions:**

The construction and characterization of a pneumatically driven dopant delivery device was demonstrated. The device was capable of delivering stable, pulse-free, isocratic dopant flow for APPI applications with analytical results directly comparable to that of conventional solvent delivery instrumentation. The 300 mL dopant capacity lends the pneumatic device ideally toward lengthy, overnight analyses, eliminating the need to monitor and frequently replenish the dopant supply. The device was shown to be simple, robust, cost effective and practical for real-world applications through practical implementation within a plausible LC-APPI-MS workflow. A detailed list of part numbers was included to allow others to replicate device fabrication for their own experimental needs.

Future work could include the implementation of simple enhancements to improve device control and serviceability. The device could potentially utilize a glass reservoir in order to monitor dopant levels more closely. This was opted against during the development process due to concerns regarding operational safety at high-pressures. It has been envisioned that a similar pneumatic device could be easily engineered and provided with commercially available APPI instruments with the aim of improving practicality and ease of use.

## Appendix C. A Modified Heated Nebulizer Probe for Isolated Dopant Introduction

This appendix will describe a modified heated nebulizer probe, intended to overcome some technical limitations associated with dopant delivery in orthogonal geometry Photospray sources. This device was utilized for the experiments described in chapters three and four, to introduction both the dopant and LC effluent flows simultaneously, yet independently, to the field-free APPI source. A standard unmodified APCI probe was used for all experiments involving the commercial, open-geometry Photospray source.

There are several methods for introducing dopant to APPI sources. Syagen built sources for example, provide no explicit mechanism for independently vapourizing a chemical dopant into the nebulizer gas stream. (This is a holdover technical limitation that pre-dates a cross licensing agreement allowing them to officially endorse dopant use within Photomate sources.) Instead, for Photomate sources, a dopant must be added directly to the analytical solvent flow, either as a pre-mixed component of the mobile phases, or as a secondary flow combined through a T-union prior to entering the ion source. As discussed previously, solvent immiscibility issues may lead to erratic background levels that may in-turn negatively affect detection limits.

Conversely, first-generation Photospray sources were equipped with a dedicated means for introducing a dopant flow to the source through a stainless steel spray capillary, inserted directly into the heated nebulizer region. In this way, dopant may be efficiently vapourized into the heated gas stream within a controlled, high-temperature environment. Second-generation, orthogonal geometry Photospray sources, however, turned away from this method of dopant introduction in favour of an auxiliary dopant nebulizer. Here, dopant is vapourized at ambient temperature into a wide diameter stainless steel tube,

coiled around the outside of the heated nebulizer tower. Although some heat is inevitably transferred from the tower to the dopant transfer tubing, measured temperatures tend to be far below the boiling point of most dopant candidates. Additionally, the volume of the transfer tubing is prohibitively large, presenting a large surface area to facilitate carryover should modification of the dopant composition be required.

We have developed a customized sample probe for APPI applications, intended to overcome the limitations associated with the current methods of dopant introduction. Figure C-10 illustrates the modified probe design. Similar to first-generation sources, the modified probe utilizes two isolated flow paths to introduce the LC effluent and dopant streams to the source independently, eliminating concerns regarding solvent miscibility. Both liquid flows are delivered to the heated nebulizer probe through stainless steel hypodermic capillaries – passing directly through the thermally controlled, high temperature region. Dopant flow is introduced through a short capillary, terminating within the heated probe (typically operated at minimum 250$^{o}$C) where it is vapourized into the nebulizer gas (GS1) stream. Mobile phases are introduced through a second longer capillary terminating 0.5 to 1.0-mm beyond the end of the probe assembly, analogous to the unmodified APCI design. The high-speed nebulizer gas, partially comprised of dopant vapour, is used to pneumatically assist vapourization of the LC effluent flow. A stainless steel bracket was required to mount and secure the hypodermic capillaries, external to probe assembly. Analytical results obtained using the modified APCI probe were identical those obtained using the standard probe design, however, without the potential for signal instability attributed to solvent mixing incompatibility.

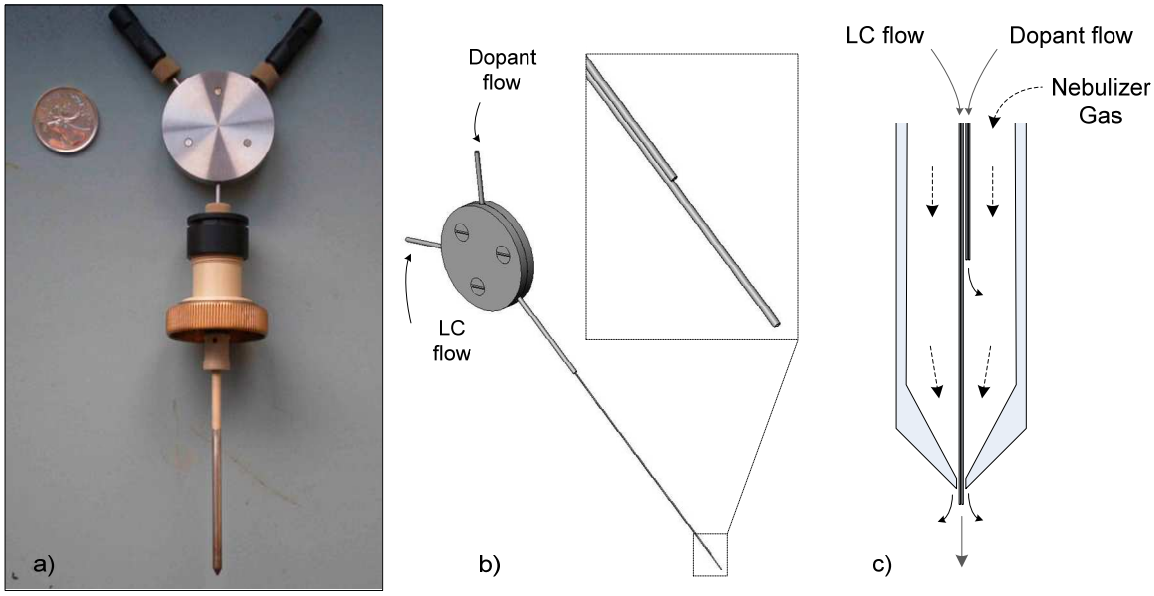


**Figure C-10. Illustrations describing the modified dopant introduction probe. a) Photo of the assembled, modified APCI probe, b) a representation of the custom capillary system, c) a functional schematic diagram.**

The device was rigorously put to test, as it was utilized for dopant introduction for all field-free APPI experiments described in chapters three and four. Recognized drawbacks to the present design include robustness and serviceability. The flow path of the modified probe contains two soldered connections, joining 1/16” OD (0.005” ID) transfer tubing to 0.015” OD (0.005” ID) hypodermic capillaries. These connections should be ideally welded as opposed to soldered given the high temperature environment and potentially corrosive solvent conditions present within APPI sources. Miniature welding facilities were not immediately available to us, however, thus soldering was selected as a temporary, adequate alternative. These connections required infrequent repair as leaks or plugs were detected. The design was overall functional, however, not elegant. Fragile capillaries and connections do not lend the device ideally to use by novice operators. A future design should be easily serviceable by any operator, similar to modern ESI and APCI probe assemblies. That being said, the modified probe was found to be suitable for routine dopant introduction, while addressing the limitations associated with modern dopant introduction methods.